FLORIDA INTERNATIONAL UNIVERSITY

Miami, Florida

INVESTIGATION OF THE EFFECT OF STRUCTURE ON REACTIVITY IN THE TITANIUM DIOXIDE MEDIATED PHOTODECOMPOSITION OF PHENOLS AND HALOETHERS WHEN IRRADIATED AT 350 NM IN AN AQUEOUS MEDIUM.

A thesis submitted in partial satisfaction of the requirements for the degree of

MASTER OF SCIENCE

IN

CHEMISTRY

by

Claudia Cardona

1994

To: Dean Arthur W. Herriot
College of Arts and Sciences

This thesis, written by Claudia Cardona, and entitled "Investigation of the effect of structure on reactivity in the TiO_2 mediated photodecomposition of phenols and haloethers when irradiated at 350 nm in an aqueous media", having been approved in respect to style and intellectual content, is referred to you for judgment.
We have read this thesis and recommend that it be approved.

Martin Quirke

William J. Cooper

Ramon Lopez de la Vega

Kevin E. O'Shea, Major Professor

Date of Defense: November, 2, 1994.

The thesis of Claudia Cardona is approved.

Dean Arthur W. Herriott
College of Arts and Sciences

Dr. Richard L. Campbell
Dean Of Graduate Studies

Florida International University, 1994

ACKNOWLEDGEMENTS

All thanks to God!

I am extremely grateful to Dr. Kevin E. O'Shea, my mentor, for his advise, support, guidance, and especially his patience. I wish to thank the members of my committee, Dr. Martin Quirke, Dr. William Cooper, and in particular, Dr. Ramon Lopez de la Vega for their insight and helpful comments.

A special thanks must go to Rose Ann Slifker and the staff at the Drinking Water Research Center (FIU) for their instructive training. I also want to thank Ms. Zaida Morales-Martinez, for her encouragement to enter the MS program and her guidance throughout; Dr. John Landrum and all the professors in the FIU Chemistry Department, for their motivation; Judy Whitt, for her valuable help, as well as Mirtha and Mayra; Lilia San Miguel, John Walton, Gina Alume, Fabius Foti, and Stephan Jannach, for their assistance and friendship; and my parents, John and Dolly Cirillo, whose moral and financial support was fundamental in accomplishing this degree.

Thanks to the FIU-ACS-SA (Chem Club) and the Graduate Student Association (FIU) for travel funds and financial support for this research by the Petroleum Research Fund and the National Science Foundation (R.I.M.I. program) is greatly acknowledged.

ABSTRACT OF THE THESIS

INVESTIGATION OF THE EFFECT OF STRUCTURE ON REACTIVITY IN THE TITANIUM DIOXIDE MEDIATED PHOTODECOMPOSITION OF PHENOLS AND HALOETHERS WHEN IRRADIATED AT 350 NM IN AN AQUEOUS MEDIA.

by

Claudia Cardona

Florida International University, 1994

Miami, Florida

Professor Kevin E. O'Shea, Major Professor

Three studies were performed to obtain fundamental mechanistic information on the TiO_2 catalyzed photooxidations of organic substrates irradiated at 350 nm in dilute aqueous solutions under oxygenated conditions: (a) The photodecomposition of three haloethers, 2-chloroethyl ether, 4-chlorophenyl phenyl ether, and 4-bromophenyl phenyl ether, was investigated in an aqueous media at pH 7.0. (b) A comparative study of structure-reactivity was conducted on *para*-substituted phenols whose substituents range from electron-withdrawing to electron-donating in an aqueous media at pH 3.0. (c) The initial rates of the TiO_2 catalyzed photodegratation of phenol were studied in an aqueous media at pH 1.0, 3.0, 5.0, 7.0, 9.0, 11.0, and 13.7 and a pH effect profile was obtained and compared to the removal efficiency after four hours of irradiation. Controls were

carried out throughout the three studies in the absence of light and under anoxic conditions, as well as without the semiconductor to evaluate the role of photolysis. The Langmuir-Hinshelwood model was employed in an attempt to characterize and evaluate differences in reactivity.

TABLE OF CONTENTS

LIST OF TABLES PAGE

LIST OF FIGURES PAGE

LIST OF APPENDIXES PAGE

1. INTRODUCTION.

1.1 WATER DECONTAMINATION - THE LATEST TECHNOLOGIES.

Over the past decade, researches have focused on an array of water decontamination processes, including the Advance Oxidation Processes (AOP) which apply catalytic and photochemical oxidative degradation to organic pollutants ideally leading to complete mineralization.[1] Upon direct irradiation of the organic substrate, or by reaction with hydroxyl radical or other reactive species produced by AOP's, organic radicals are formed which, combined with solvated molecular oxygen, can be oxidized to innocuous mineral acids and carbon dioxide.

A variety of AOPs, including H_2O_2/UV, O_3/UV, O_3/ H_2O_2/UV, involve the production of hydroxyl radical and have been extensively studied.[1] In the evaluation of these processes, efficiency, effectiveness, and economics must be considered. Semiconductor catalyzed photooxidation, another AOP, has created substantial interest for the treatment of a variety of organic pollutants since it is inexpensive in comparison to other AOPs and it has proven effective in the degradation of pollutants.[2] However, the mechanistic details of the TiO_2 catalyzed degradation process is poorly understood and more data is needed to develop this technique into an applicable method of potable water decontamination.

1.2 SEMICONDUCTOR-SOLUTION THEORY.

In crystalline solids, the atoms are arranged in a three-dimensional pattern, or lattice, at equilibrium inter-atomic distances with the electrons in discrete energy levels. The location of electrons around the nucleus has been described as an electron cloud and the density of this cloud at any point is a measure of the probability of finding an electron at that point.

In a crystal, electron clouds overlap and valence electrons interact with all the atoms in the lattice. Subsequently, each energy state of each atom making up the lattice splits into upper and lower energy levels; these levels are so closely spaced that they are considered as a continuous band of allowed energies. Therefore, the discrete energy states of the atoms are replaced by bands in the lattice crystal structure.[3]

Semiconductors are characterized by this band structure. The valence band (VB), which contains electrons, and the conduction band (CB), which is unfilled, are separated by an energy gap (Eg) that is small enough for electrons to overcome with thermal or photochemical excitation. When an electron is excited from the VB into the CB, an unoccupied energy state or hole (h^+) is left behind; these holes are considered positively charged since electrons tend to recombine with to them to produce the unexcited species.

When a semiconductor is immersed in a liquid electrolyte solution, this ionic solution exerts an electrical field on the holes and electrons (e^-) of the semiconductor causing the h^+'s and e^-'s to migrate in different directions. This migration produces unequal charge distribution and a variation in potential in this space-charge region near the semiconductor surface. An electron in this space-charge region will interact with the electric field exerted by the solution and its energy will vary, causing bending in the energy bands near the surface. Charge injection in this region of band bend will drive electrons in the opposite direction from holes which increases the lifetime of the charge separation.[3,4,5,6]

1.3 KINETICS.

When the semiconductor absorbs light of energy equal or greater than E_g, an electron-hole pair is produced which is followed by the migration of these charge carriers to the surface of the semiconductor.

A reducible, adsorbed compound can capture the photogenerated electron while an adsorbed, oxidazible compound can donate electrons into the hole. The oxidation potential of the donor must be less positive than the valence band and the acceptor reduction potential more positive than the conduction

band of the semiconductor.[4] The valence band of most common metal oxide semiconductors lies more positive than the oxidation potential of most organic compounds with nonbonding or π-electrons, thus presenting a thermodynamically favorable situation for electron transfer from the organic substrate to the photogenerated h^+.[6]

Metal oxides such as TiO_2, $SrTiO_2$, or ZnO are very active and efficient as photooxidative catalyst with relatively large E_g values which require mid-to-long wavelength UV light for excitation. Small band gap energy semiconductors, such as CdS, allow excitation with visible light which potentially makes them very effective in the decontamination of waters using solar excitation. Unfortunately, CdS is susceptible to corrosion under continuous irradiation. Despite the relatively large E_g of TiO_2, 3.0 V, excitation with light in the 300-380 nm range has proven very effective for the oxidative degradation of organic pollutants. TiO_2 is non-toxic, inexpensive, and stable to continuous irradiation.[7]

In aqueous media, strong evidence supports the production of the hydroxyl radicals, •OH, at the surface of the semiconductor. The hydroxyl radical is believed to be the primary oxidizing species in semiconductor mediated photodegradation.[8,9] This radical appears to be formed by the reaction of adsorbed hydroxyl ions, or water molecules, and the hole of the excited semiconductor as shown in equation 1 and 2.

$$^{-}OH + h^{+} \longrightarrow \bullet OH + (h^{+}/\ e^{-}) \qquad (1)$$

$$H_2O + h^{+} \longrightarrow \bullet OH + H^{+} + (h^{+}/\ e^{-}) \qquad (2)$$

Similar initial disappearance rates of a variety of substrates suggest the rate-limiting step of the process is the formation of the hydroxyl radical or the relatively uniform rate that •OH reacts with many organics.

There is also evidence[10] supporting the direct reaction of the adsorbed substrate with the h^{+} to form a radical cation which undergoes oxygenation, Eq. 3, to products which are similar to those formed in the reaction of the substrate with •OH, as shown in Eq. 4. Both oxidative pathways can give similar product distribution and ultimately lead to complete mineralization.

$$S_{ads} + h^{+} \longrightarrow S^{+\bullet} \xrightarrow{O_2 \text{ or } H_2O} S_{oxid} \qquad (3)$$

$$S_{ads} + \bullet OH \longrightarrow\longrightarrow \xrightarrow{O_2} S_{oxid} \qquad (4)$$

Surface effects of the semiconductor and adsorption equilibrium of the substrate will significantly influence the course of the photochemical transformations at or near the liquid-solid interface. The Langmuir-Hinshelwood model (L-H) has been used to describe the photochemical transformations catalyzed by a semiconductor. The L-H model assumes the reaction occurs on the

surface of the semiconductor between adsorbed species and there is homogeneous coverage of the TiO_2 surface by the substrate. Another model commonly employed to describe such processes is the Eley-Rideal (E-R) which assumes the reaction occurs between a desorbed reactant and a surface bound species.[4,8,11,12]

In the L-H model, the rate is defined as Eq. 5,

$$\text{rate} = k\Theta_S \qquad (5)$$

where k is the reactivity constant and Θ_S represents the homogeneous surface coverage of the substrate. The surface coverage is defined by Eq. 6,

$$\Theta_S = K_S[S]/(1 + K_S[S]) \qquad (6)$$

where K_S is the adsorption constant and [S] is the substrate concentration;

$$[S] \underset{k_{des}}{\overset{k_{ads}}{\rightleftharpoons}} [S]_{ads}$$

k_{ads} is the rate constant for adsorption, k_{des} is the rate constant for desorption of the substrate with the surface of the semiconductor, and then $K_S = k_{ads}/ k_{des}$.

Eq. 7 is obtained by substituting Eq. 6 into Eq. 5,

$$\text{rate} = kK_S[S]/(1 + K_S[S]) \qquad (7)$$

Although the L-H rate equation simulates the degradation kinetics observed for many organic compounds, it has been suggested that its parameters may not represent those defined by the original model since several diffusion limited processes, such as those shown in Eqs. 8 to 11, yield similar rate expressions[2,8]

$$\bullet OH_{ads} + S_{ads} \longrightarrow \text{products} \qquad (8)$$

$$\bullet OH_{ads} + S \longrightarrow \text{products} \qquad (9)$$

$$\bullet OH + S_{ads} \longrightarrow \text{products} \qquad (10)$$

$$\bullet OH + S \longrightarrow \text{products} \qquad (11)$$

Reaction 8 represents the original L-H model while reactions 9 and 10 describe the rate limiting steps of the E-R model. Notice that if both interacting species react near the surface following desorption, as represented by Eq. 11, the rate equation, Eq. 7, will still represent the degradation of the substrate.

The role of oxygen is also fundamental in the photocatalyzed oxidation reaction.[13,14] Molecular oxygen can trap the electron in the conduction band of the excited semiconductor, inhibiting recombination of the electron-hole pair while forming superoxide, $\bullet O_2^-$, which can produce hydroxyl radical (Eq. 12) upon reaction

with hydrogen peroxide, formed in low quantities as a by-product of the reaction of two hydroxyl radical.

$$\bullet O_2^- + H_2O_2 \longrightarrow \bullet OH + OH^- + O_2 \qquad (12)$$

The rate of photodegradation is dependent on the concentration of oxygen in solution. Adsorption of O_2 molecules is expected at the Ti^{III} sites of the semiconductor lattice while the hydroxyl radicals are formed by adsorption of OH^-/H_2O molecules at the Ti^{IV} and lattice oxygen sites.[15,16] Therefore, oxygen and OH^-/H_2O do not compete for the same adsorption sites and thus, the process is enhanced by extension of the h^+/e^- pair lifetime. The reaction rate can be expressed in Eq. 13 as

$$\text{rate} = k''\Theta_{O_2}\Theta_S \qquad (13)$$

where k'' is the surface second order rate constant, Θ_{O_2} is the fractional site coverage by oxygen, and Θ_S is the fractional site coverage of the substrate as described above (6).

Θ_{O_2} is defined by Eq. 14 as[17]

$$\Theta_{O_2} = K_{O_2}\ p_{O_2}/\ (1 + K_{O_2}\ p_{O_2}) \qquad (14)$$

where K_{O_2}, k_{ads}/ k_{des}, is the adsorption constant of molecular oxygen onto the surface of the semiconductor. The rate equation (Eq. 15) then becomes

$$\text{rate} = k'' \{K_{O_2} p_{O_2}/ (1 + K_{O_2} p_{O_2})\} \{K_S[S]/ (1 + K_S[S])\} \quad (15)$$

By-products and intermediate molecules formed near or at the semiconductor surface are expected to compete with the original substrate for active sites. These intermediate products are decomposed by subsequent oxidation processes leading to complete mineralization. Since it is not feasible to account for all intermediate products in the degradation model, the most frequently employed version of the L-H model takes into account only the initial rates and initial concentration of the studied substrate at a constant concentration of dissolved oxygen yielding the simple form shown in Eq. 16,

$$\text{rate}_0 = kK[S]_0/ (1 + K[S]_0) \quad (16)$$

Ollis and Turchi argue that k does not actually represent the reactivity constant of a particular substrate as depicted in the original model, but it is related to the generation of •OH and depends on the catalyst properties and the reaction conditions, and it is independent of the particular organic reactant. They also suggest that K represents the adsorptivity constant of the

substrate and/or is proportional to a second-order reaction rate constant of the two reacting species, the •OH and the substrate.[8] The L-H parameters are therefore considered "apparent kinetic parameters" and not absolute constants.

These apparent parameters are obtained from a plot of $1/rate_0$ vs $1/[S]_0$, the reciprocal relationship of Eq. 16,

$$1/rate_0 = 1/kK[S]_0 + 1/k \qquad (17)$$

where $rate_0$ is the initial rate of disappearance of the substrate and $[S]_0$ its initial concentration. The values of k and K can be deduced from the intercept and slope obtained experimentally.

1.4. EFFECTS OF STRUCTURE ON REACTIVITY.

The reactivity of organic compounds can be drastically affected by the electronic characteristics of their substituents. Hammett constants represent the electrical, resonance, and field effects that different substituents have on the electronic character of a given molecule. Correlation of these Hammett constants with different reaction parameters have been used to obtain fundamental information about reaction intermediates and mechanisms.[18]

Although Hammett correlations have been used primarily for reactions occurring in homogeneous solutions, successful applications on heterogeneous systems have also been reported. A correlation between the relative rates of TiO_2 mediated photooxidation of aromatic olefins and Hammett constants has been interpreted as evidence for hole catalyzed reactions in nonaqueous media.[19]

The Hammett equation is a linear free energy relationship that describes the susceptibility of a reaction on the electronical effects of the substituents on the reactants. The total free energy change of a reaction affected by a particular substituent (Eq.18) can be obtained by adding the free energy change of the reaction of unsubstituted reactant, $\Delta G_0°$, plus an increment due to the substituent, $\Delta\Delta G°$,[20]

$$\Delta G° = \Delta G_0° + \Delta\Delta G° \qquad (18)$$

A Hammett constant, σ, has been defined for each substituent in terms of the free energy change as

$$\Delta\Delta G° = -2.303\ RT\ \sigma \qquad (19)$$

The relationship between free energy and equilibrium, Eq. 20,

$$\Delta G^\circ = -2.303\ RT\ \log K \qquad (20)$$

can be substituted with Eq. 19 into Eq. 18 to obtain

$$\log K = \log K_0 + \sigma$$

or

$$\log\ (K/K_0) = \sigma \qquad (21)$$

Hammett derived Equation 21 initially for the dissociation of substituted benzoic acids to evaluate and quantify the substituent effects.[20,21] For a different reaction, the change in free energy due to a substituent, -2.303 RT σ, must be multiplied by a ρ factor which characterizes the sensitivity of this new reaction to electronic effects. The free energy change of this new reaction can be written as

$$-\Delta G^{\circ\prime} = -\Delta G_0^{\circ\prime} + 2.303\ RT\ \rho\sigma \qquad (22)$$

which treated as above produces

$$\log\ (K/K_0) = \rho\sigma \qquad (23)$$

Eq. 23 is known as the Hammett equation also expressed as

$$\log\ (k/k_0) = \rho\sigma \qquad (24)$$

which correlates the rates of the reaction with the effects of the substituents and is derived by using the free energies of activation instead of the changes in ground-state free energies.

Linear free energy relationships, such as Eq. 23 and 24, can provide mechanistic information of a given reaction. If the substituent effect, σ, is directly proportional to the reactivity rates for a given class of compounds, a linear relationship is observed between log (k/k_0) and σ, suggesting a similar reaction mechanism among the class of compounds, and a constant sensitivity, ρ, of this reaction to electronic effects is expected. Small changes in the slope, ρ, producing a smooth curve relationship indicates a gradual variation in the mechanism while a pair of intercepting straight lines indicate an abrupt change in the mechanism occurring as substituents and their electron demand varies.[20,22]

The ρ value can also provide information on the charge character of the transition state or intermediate of the reaction. A large negative or positive value of ρ indicates the development of defined charge, carbocation or carbanion respectively, in the transition state of the reaction. When the reaction proceeds through radical transition states or intermediates, the sensitivity of these reactions towards the effect of substituents is expected to be smaller ($\rho \leq \pm 1.5$) since their character is less polar.[19,22]

1.5. pH EFFECTS.

The effect of pH on semiconductor-catalyzed photooxidation has been studied on an assorted number of substrates under different experimental conditions.[23-32]

While reaction rates appear to depend slightly on pH and changes of one order of magnitude have been observed, the mechanistic details and overall dependence are not well understood. Several important factors must be considered when studying the effects of pH on the initial and overall rates of photooxidation such as surface charge of the semiconductor which can significantly influence the oxidation process. The isoelectric point of TiO_2 occurs at approximately pH 6.0 and the surface is expected to be positively charged at lower pH and negatively charged at higher pH values.

Since adsorption plays a critical role, the rates of the photooxidation reactions can be affected by the electrostatic interaction between the semiconductor surface, the solvent, the polar substrate, and the charged radicals formed throughout the reaction process.[5,31] In an aqueous media, the acidity or basicity of the substrate must be considered since repulsive or attractive interactions with the semiconductor surface can be affected by the development of charge on the substrate. Competition for adsorption sites between the substrate and the $H_2O/^-OH$ species at

different pH values is expected to cause an increase or decrease in the photodecomposition.[26,29]

Another factor to be considered is the oxidative power of the photogenerated holes with relation to the oxidation/reduction potential of the substrate at different pH values. The location of the valence band is critical in these photooxidation reactions.[28,29] The semiconductor band potentials are functions of pH with TiO_2 VB lying at about +2.6 V (vs NHE) at neutral pH and varying by 0.059 V/pH, the same change as the redox potential for oxidation and reduction of water. Thus, the oxidation potential for the formation of •OH from ^-OH and/or H_2O remains above VB and it is therefore thermodynamically favored throughout the pH range.[2,27]

2. PHOTOCATALYZED DEGRADATION OF HALO-ETHERS.

2.1. INTRODUCTORY REMARKS.

A number of haloethers, included on the EPA list of 129 priority pollutants, are suspected carcinogens and have been detected in raw and finished drinking water, as well as effluents.[33] This class of organic compounds is commonly used for a variety of industrial processes, i.e., 2-chloroethyl ether is used as a pesticide emulsifier and a textile scouring agent.[34] Surprisingly, very little research has been done on their degradation in aqueous media.[24] The TiO_2 catalyzed photooxidation of 4-chlorophenyl phenyl ether (4-chlorodiphenyl ether), 4-bromophenyl phenyl ether (4-bromodiphenyl ether), and 2-chloroethyl ether (bis(2-chloroethyl)) ether) when irradiated at 350 nm in a neutral aqueous mixture are reported herein.

Since these haloethers do not appreciably absorb light in the near UV/visible region, direct photodegradation by solar irradiation is very ineffective. In addition, oxidation in aqueous environments with naturally occurring hydroxyl radicals, and other oxidative processes, is too slow to yield significant decontamination.[35]

As Table I shows, the water solubility of the aliphatic halo-ether, 2-chloroethyl ether, $7.132X10^{-3}$ M,[36] and its log octanol/water partition coefficient (log K_{OW}), 1.58,[37] suggest a low probability for bioaccumulation and minimal adsorption onto

suspended organic matter or clays. With a vapor pressure of 0.71 torr at 20 °C,[36] evaporation will be limited and hydrolytic cleavage of the carbon-chlorine bond may have a half-life of six months to several years as it is observed with other chloro-aliphatic compounds.[38]

TABLE I. Summary of the Studied Haloethers and Their Physical Characteristics.

Haloether	Aqueous Solubility (M) X 10^5	log K_{OW}	VaporPressure (torr) X 10^2
2-Chloroethyl ether $ClCH_2CH_2OCH_2CH_2Cl$	713.2 [36]	1.58 [37]	71(20°C) [36]
4-Chlorodiphenyl ether 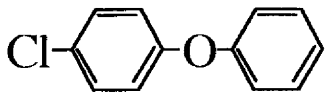	1.450	4.08 [39]	0.27(25°C) [39]
4-Bromodiphenyl ether 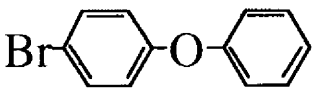	1.428	4.28 [37,40]	0.15(20°C) [41]

The aromatic halo-ethers, 4-chlorodiphenyl ether and 4-bromodiphenyl ether, are very hydrophobic. Due to their limited aqueous solubilities, the maximum obtainable concentration for the stock solutions was approximately 15 μM prepared at pH 7.0

and 22 °C. The log K_{OW} for 4-chlorodiphenyl ether, 4.08,[39] and its vapor pressure, 0.0027 torr at 25 °C,[39] suggest this compound will undergo significant bioaccumulation and adsorb strongly onto organic particles and clays. Similar characteristics and behavior are expected of the 4-bromodiphenyl ether with a calculated $\log K_{OW}$ = 4.28,[37,40] and a vapor pressure of 0.0015 torr at 20 °C.[41]

These aromatic halo-ethers appear to be very stable under normal conditions encountered in the environment. Even irradiation of 4-chlorodiphenyl ether with light of 250-300 nm produces only partial degradation to 4-hydroxydiphenyl ether, which in turn is not further degraded.[42]

2.2 EXPERIMENTAL SECTION.

2.21 Materials.

2-Chloroethyl ether, 4-chlorodiphenyl ether, and 4-bromodiphenyl ether, were obtained from Aldrich (99% purity). The internal standards employed were 1,2-dichlorobenzene HPLC grade (Sigma-Aldrich, 99%) and Toluene Optima (Fisher, Residue and Pesticide Analysis). Deionized water was used throughout these investigations. The pH was adjusted to 7.0 with 0.1 N NaOH as required. The extracting solvent was Hexane Optima (Fisher, Residue and Pesticide Analysis) and chloroform (Fisher Scientific, Certified A.C.S.) was the solvent used in the preparation of the

toluene internal standard solution. The photocatalyst used was TiO_2, Degussa P25 lot# RV2186 (surface area 50 m^2/g, avg. primary particle size 30 nm, X-Ray structure primarily anatase).

2.22 Procedure.

A 100 mL aliquot of an aqueous stock solution of the halo-ether and 10 mg of TiO_2 (0.1 g/L) were placed in a cylindrical, round bottom, pyrex tube fitted with a screwed, teflon cap. The mixture was magnetically stirred (8X13 mm teflon stirring bar) for 5 min to obtain a homogeneous suspension followed by purging with O_2 for 1 min before sampling (t = 0 min) for analysis.

The reaction mixture was irradiated for the desired time intervals in a Rayonet Photochemical Chamber (reactor model RPR-100 from Southern New England Ultraviolet Company) fitted with sixteen low pressure mercury lamps blazed at 350 nm, a Rayonet Merry-Go-Round (model RMA-500), and a cooling fan. The intensity of the incident light, 1.6 X 10^{16} photons/sec cm^3 (Appendix I), was measured by means of potassium ferrioxilate actinometer.[43,44] No corrections were made for the light scattered by the semiconductor. The mixtures were magnetically stirred throughout irradiation by placing a magnetic stirrer inside the reactor. The operating temperature inside the reactor was 40 °C ± 2 °C. Prior to irradiation, each mixture was equilibrated to this temperature and cooled down to 22 °C for sampling purposes.

A specific volume of the mixture was removed from the reaction vessel and placed into a 42 mL extracting vial (Borosilicate, clear glass with open top phenolic caps and PTFE septa). Deionized water pH 3.0 was added until a total volume of 25.0 mL was obtained. The internal standard was then injected into the extracting vial and the resulting solution was extracted with hexane which was analyzed by gas chromatography.

Since the aromatic halo-ether aqueous solutions were only one order of magnitude more concentrated than the minimum detection limit, 15 mL aliquots of the mixture were removed and extracted with 3 mL aliquot of hexane to increase the concentration for analysis. On the other hand, only 5.0 mL aliquots of the aliphatic halo-ether aqueous mixture were sampled and extracted with 5.0 mL of hexane after its volume was diluted to 25.0 mL and the internal standard injected.

10 μL of a 0.01777 M solution of 1,2-dichlorobenzene in hexane was used as the internal standard for each sample of 4-bromodiphenyl ether. 20 μL of 1,2-dichlorodiphenyl (0.1777 M) solution in hexane was employed for the 2-chlorodiphenyl samples; and 20 μL of a 0.09407 M solution of toluene in $CHCl_3$ were used with 4-chlorodiphenyl ether samples.

The extracting vials were then shaken for 10 min at 300 rpm in an Orbit Shaker (Lab-Line Instruments) and the hexane layer was transferred with a disposable pipette into amber

autosampler vials which were sealed and analyzed by gas chromatography.

Control reactions were carried out to evaluate the effect of the presence or absence of O_2 by purging with N_2, direct photolysis of the substrate by running the reaction without TiO_2, and adsorption in the dark by avoiding any light exposure while keeping all other experimental conditions constant.

2.23 Analysis.

The disappearance of the 4-bromodiphenyl ether was monitored by a HP 5890 Gas Chromatograph equipped with an ECD detector and a J&W Scientific DB-608 (30 m X 0.32 mm, 0.5 microns) column. The temperature program started at 100 °C for 2 min and increased at 20 °/min to 250 °C with a final time of 20 min. The temperatures of the injector and detector were 250 and 280 °C respectively. The head pressure was set at 12 psi, the He (carrier) at 40 psi, and the N_2 (auxiliary and anode purge) at 35 psi. The purge valve was off at 0 min and on at 1.5 min.

FID detection was more effective for 4-chlorodiphenyl ether and 2-chloroethyl ether. These were analyzed with a J&W Scientific DB-1 (30 m X 0.25 mm, 0.25 microns) column. The initial temperature was 40 °C for 5 min increasing at 20 °/min to 220 ° with a final time of 10 min; the FID detector was set at 250 °C and the injector at 220 °C. The column head pressure was set at 12 psi;

the gas flows were 375 mL/min for air, 30 mL/min for N_2 + He (carrier), and 30 mL/min for H_2.

The amounts of ether extracted with the hexane were quantified with standardization curves (Appendix II) obtained as follows: working standard solutions of the ethers were prepared in hexane, 0.005712 M 4-bromodiphenyl ether, 0.005820 M 4-chlorodiphenyl ether, and 0.1706 M 2-chlorodiphenyl ether. Specific volumes of these working standards (i.e., 1.0, 5.0, 10.0, 15.0, 20.0, 30.0, and 40.0 μL) were injected to extracting vials containing 25.0 mL deionized water pH 3.0, and the same internal standard as well as the hexane volume employed in the sampling procedure for the specific ether. The extracting vials were then shaken and the hexane layer was analyzed as described above.

2.3 RESULTS AND DISCUSSION.

The aromatic halo-ethers presented a serious analytical challenge due to their strong hydrophobic character when a TiO_2 catalyzed photooxidation kinetic study at pH 7.0 was attempted. Only very dilute aqueous solutions could be prepared, about 15 μM, after sonicating for 5 min and letting stir overnight. Their minimum limit of detection is approximately $1x10^{-6}$ M under the conditions describe above.

The analytical procedure for the aromatic ethers was modified to maximize the recoveries obtained at 0 min irradiation. Initially, sonication and stirring had been used to disperse the semiconductor before irradiation and the sample was filtered with a 0.45 μm PTFE acrodisc to remove the TiO_2 before the extraction procedure. These steps, however, appear to lower the recoveries significantly and procedural modifications were made to improve the analytical method. For example, approximately 50% of the 4-bromodiphenyl ether was not recovered at t = 0 min due to dark adsorption. This ether adheres onto the glassware, the acrodisc surface, and TiO_2.

When the slurry was stirred for 5 min, without sonication, and the filtration step was bypassed, the recovery was increased to approximately 90%. The TiO_2-aqueous mixture was shaken with the extracting solvent, Hexane Optima, after irradiation and the organic layer was pipetted into autosampler vials to be analyzed by GC. Since the semiconductor surface is completely hydroxylated (polar) at pH 3.0, it remains in the aqueous layer and the hexane layer can be injected in the GC without filtration.

The aliphatic ether, 2-chloroethyl ether, was relatively simple to analyze because of its hydrophilicity. Recoveries greater than 90% were obtained and eight concentrations were studied for the kinetic analysis (Figure 1). The initial rates were measured at 3 min of irradiation, about 10-20% of disappearance, as depicted

in Figure II. A summary of the initial degradation rates as a function of concentration are shown in Table II.

Table II. The Initial Rates ($Rate_0$) of Degradation of the Halocthers Studied in the TiO_2 Catalyzed Photooxidation Reaction. The Aqueous Mixtures (pH 7.0) were irradiated at 350 nm. % Recoveries Before Irradiation (t = 0 min) are also reported.

SUBSTRATE (S)	$[S]_0$ (M)	$RATE_0$ (10^5 M/min)	%RECOVERY
4-Bromophenyl phenyl ether	9.242×10^{-6}	--- [a]	85
4-Chlorophebyl phenyl ether	1.146×10^{-5}	--- [a]	88
2-Chloroethyl ether	2.900×10^{-3}	4.92	94
	1.005×10^{-3}	3.77	98
	9.487×10^{-4}	3.82	93
	7.541×10^{-4}	3.59	98
	7.025×10^{-4}	3.36	92
	5.041×10^{-4}	3.05	98
	2.714×10^{-4}	2.55	88
	2.529×10^{-4}	2.37	98

a - Degradation occurred too fast to measure the initial rates. Substrates were not detected after irradiation time as short as 5 min.

FIGURE I: Disappearance of 2-chloroethyl ether, after 30 min of irradiation at 350 nm, from a TiO2 aqueous mixture at pH 7.0.

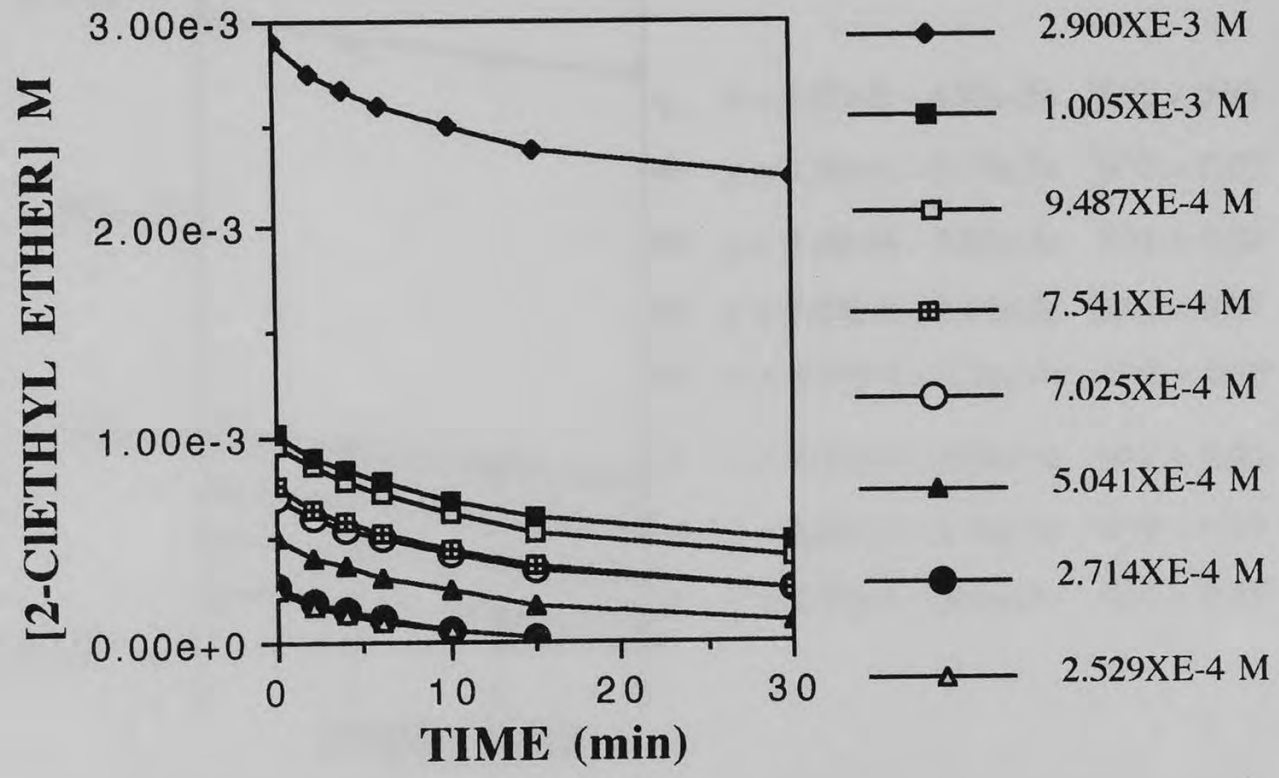

FIGURE II: Initial rates of disappearance of 2-chloroethyl ether from a TiO2 photocatalyzed (350 nm) reaction in an aqueous media at pH 7.0.

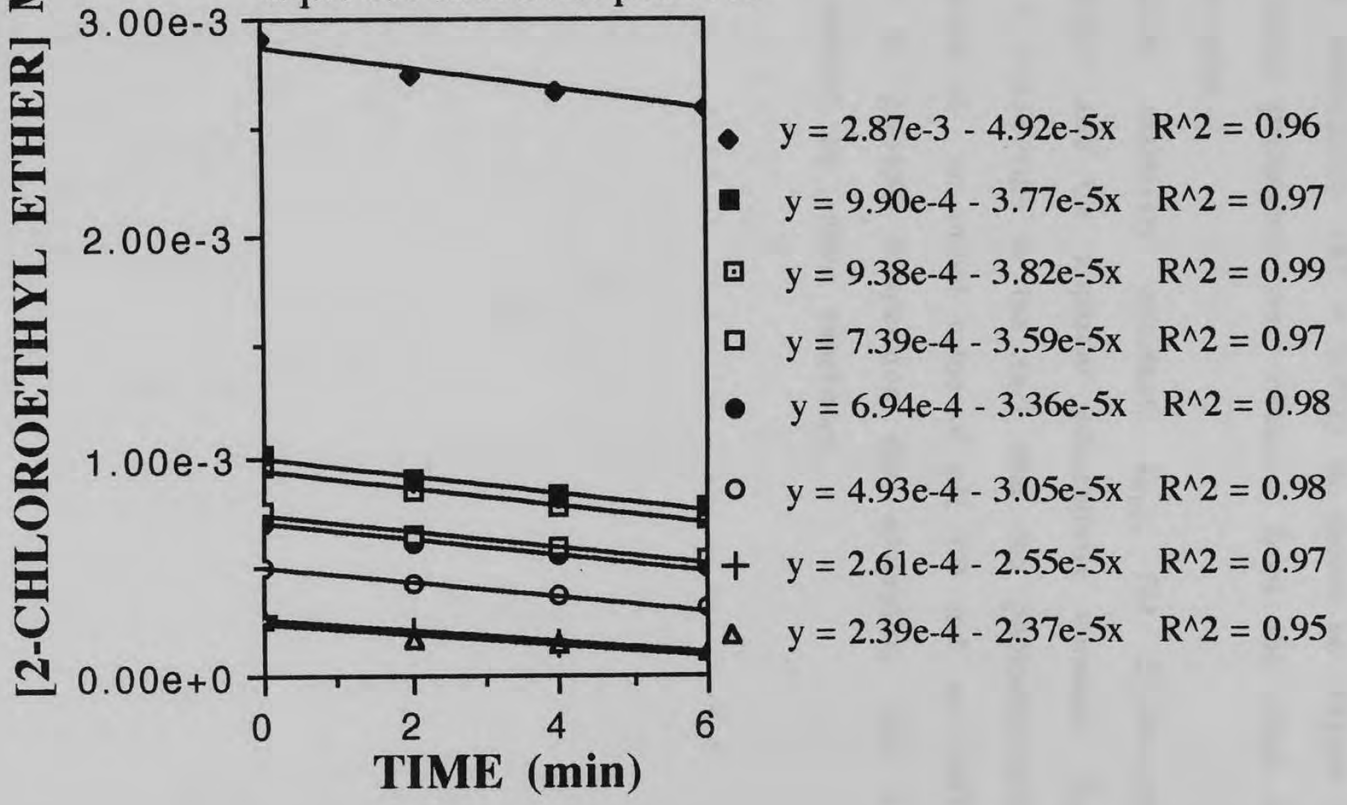

The L-H model was applied to the degradation data of 2-chloroethyl ether. The plot of $1/Rate_0$ vs 1/[2-chloroethyl ether] yields a linear relationship (R^2 = 0.971) as shown on Figure III and the L-H kinetic parameters were obtained from the slope and intercept of this plot.

The apparent reactivity constant, k_{app}, for 2-chloroethyl ether is 27.4 M/min and the apparent adsorptivity constant, K_{app}, 6.69 X 10^{-3} M^{-1}. Noteworthy is the fact that the photodegradation reaction was carried at an initial value of pH 7.0 and no buffers were employed to prevent competition for adsorption onto the semiconductor surface by other substrates.

FIGURE III: Langmuir-Hinshelwood model applied to the initial rates of disappearance of 2-chloroethyl ether when irradiated at 350 nm in a TiO2 aqueous mixture (pH 7.0).

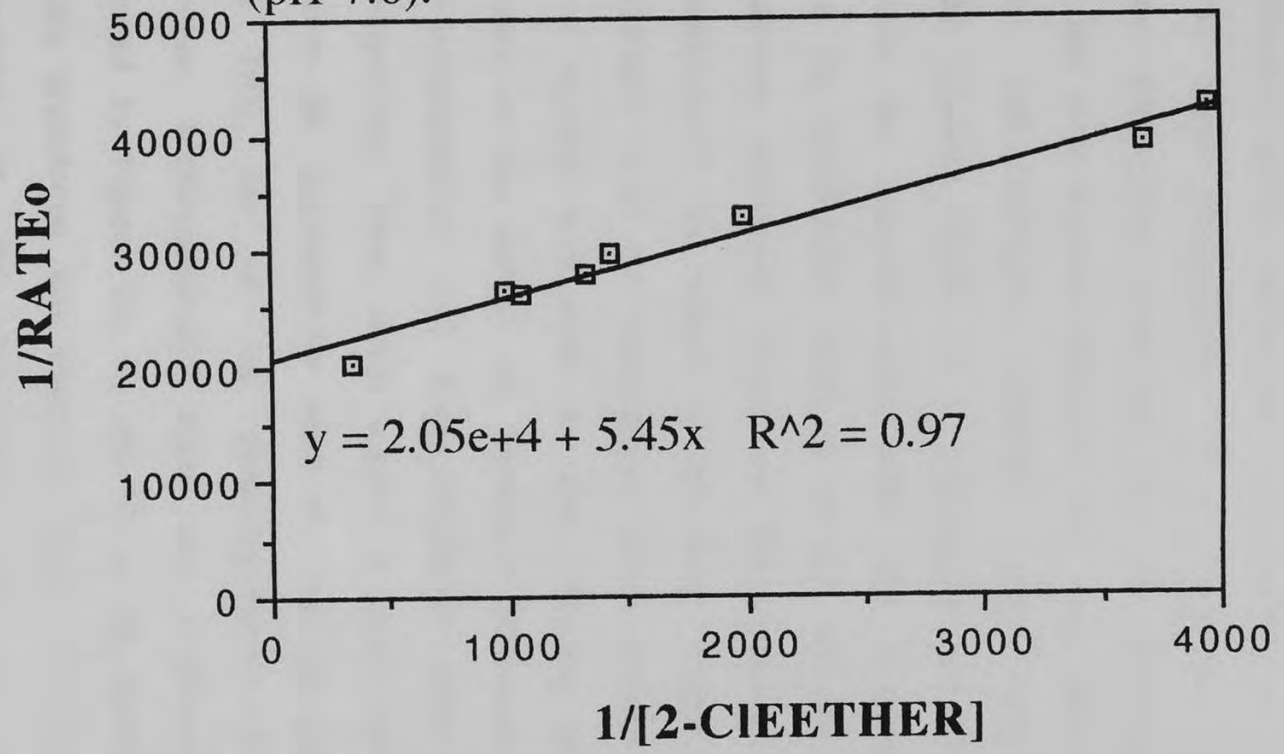

The aromatic haloethers degraded within two minutes of irradiation under our experimental conditions. Because of the limited solubility (low concentrations) and relatively fast disappearance, detailed kinetic studies are not feasible. It is not clear whether the rapid disappearance is a result of greater adsorption of these hydrophobic compounds onto the photoexcited TiO_2 or the fact that these aqueous solutions were very dilute and the semiconductor had sufficient available active sites for adsorption for the aromatic ethers, or a combination of both. A correlation between the apparent first order rate constant of disappearance and the hydrophobic character of the substrate, the octanol/water partition coefficient (K_{OW}), has been reported in a study of chlorophenols.[45] The authors of this study suggest that the closer the pollutant is to the photocatalyst active surface, the greater its rate of reaction with holes or other oxidizing species, such as •OH, formed at the surface. As mentioned previously, the log K_{OW} for 4-bromodiphenyl and 4-chlorodiphenyl ethers are 4.28 and 4.08 respectively. These values suggest a great tendency for adsorptivity onto the semiconductor when in aqueous media.

The effect TiO_2 has on the photodegradation of 4-bromodiphenyl ether, 4-chlorodiphenyl ether and 2-chloroethyl ether is demonstrated by Figures IV, V, and VI. In the absence of TiO_2 no appreciable degradation was observed. Figure VI shows a dramatic enhancement of the degradation rate of bis-2-chloroethyl ether by TiO_2 in an aqueous medium when irradiated

at 350 nm. An analogous enhancement has been reported[46] upon irradiation with a more powerful light source (an UV Hanovia Lamp). In the absence of light, negligible disappearance of the examined haloethers is observed.

FIGURE IV: Degradation of 4-bromodiphenyl ether at pH 7.0, 14.28 μM, under different experimental conditions over a 10 min period.

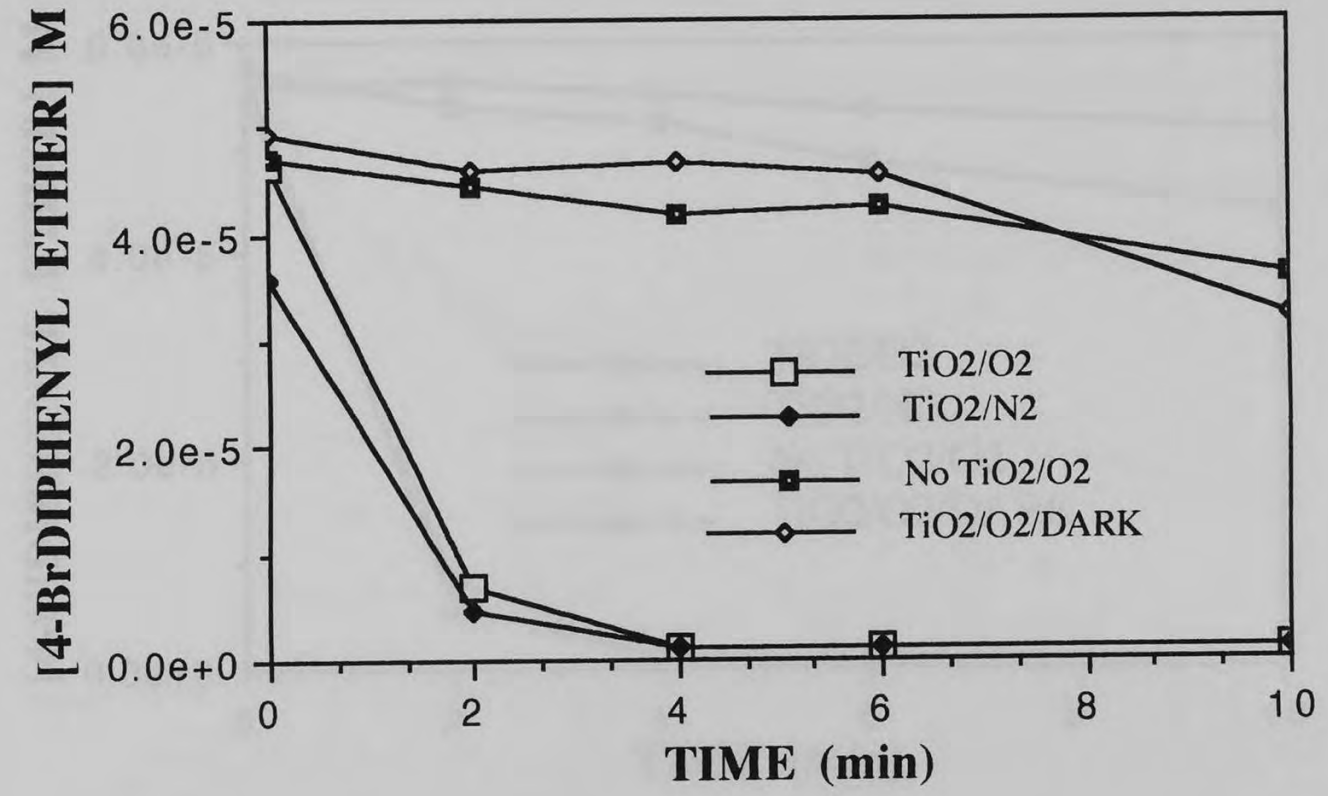

FIGURE V: Degradation of 4-chlorodiphenyl ether at pH 7.0, 14.50 μM, under different experimental conditions over a 10 min period.

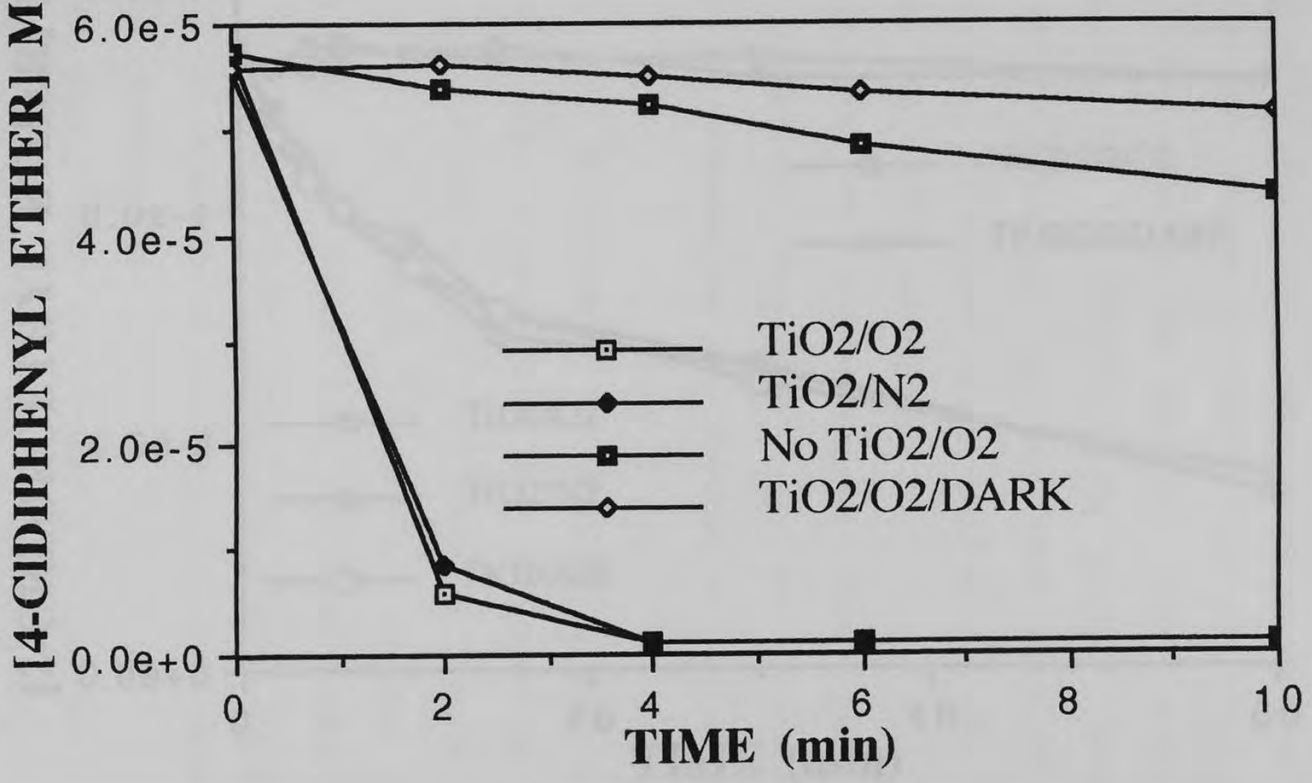

FIGURE VI: Degradation of 2-chloroethyl ether at pH 7.0, 1.024 mM, under different experimental conditions over 1 hour period.

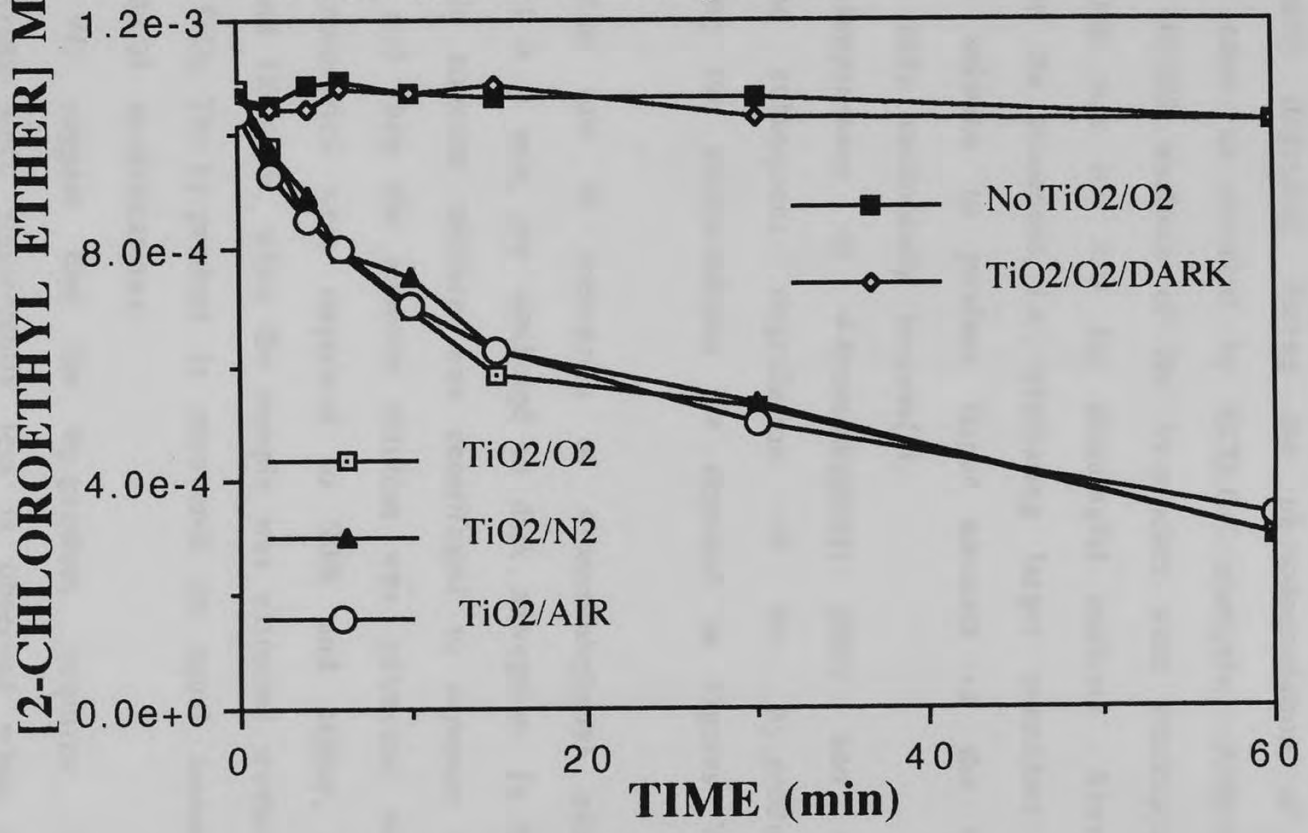

Preliminary results indicate that the haloethers are degraded from aqueous media when irradiated with 350 nm light in the presence of TiO_2. A relatively stable by-product is formed, and subsequently degraded, during the photodegradation of 4-bromodiphenyl ether as detected by ECD-GC analysis. Although isolation and GC-MS analysis of the by-product were attempted, the concentration was too low for meaningful analysis. Several modifications of the procedure, i.e., irradiating larger quantities of aqueous stock solution to produce larger amounts of the by-product, were only moderately successful.

The disappearance of 4-bromodiphenyl ether and the formation, and subsequent degradation of the by-product, observed during the photocatalysis are depicted in Figures VII, VIII, and IX.

The initial low % recoveries of 4-bromodiphenyl ether, Figure VII at t = 0 min, are attributed to dark adsorption. In this experiment, the aqueous mixture was centrifuged to separate the semiconductor and then the aqueous solution was extracted with hexane. The recoveries were improved to 90% and higher, as Figures VIII and IX show, when the sample was extracted without removing the TiO_2. The by-product is recovered in equal amounts despite procedural modifications.

Figure VII suggest that the by-product requires the presence of oxygen since significantly less is observed when the reaction was purged with nitrogen. The relatively small quantities

formed in the N_2 purged experiments may be due to adsorbed oxygen molecules on the TiO_2 surface which were not displaced completely or to direct oxidation via electron transfer from the substrate to the photogenerated hole. These three graphs also suggest that the byproduct reaches a maximum concentration at 15 min under the given experimental conditions, and then, it is decomposed.

FIGURE VII: 4-Bromodiphenyl ether vs Byproduct, relative ECD-GC detection (0 to 60 min). Irradiation at 350 nm under oxic and anoxic conditions in a TiO2 aqueous mixture at pH 7.0.

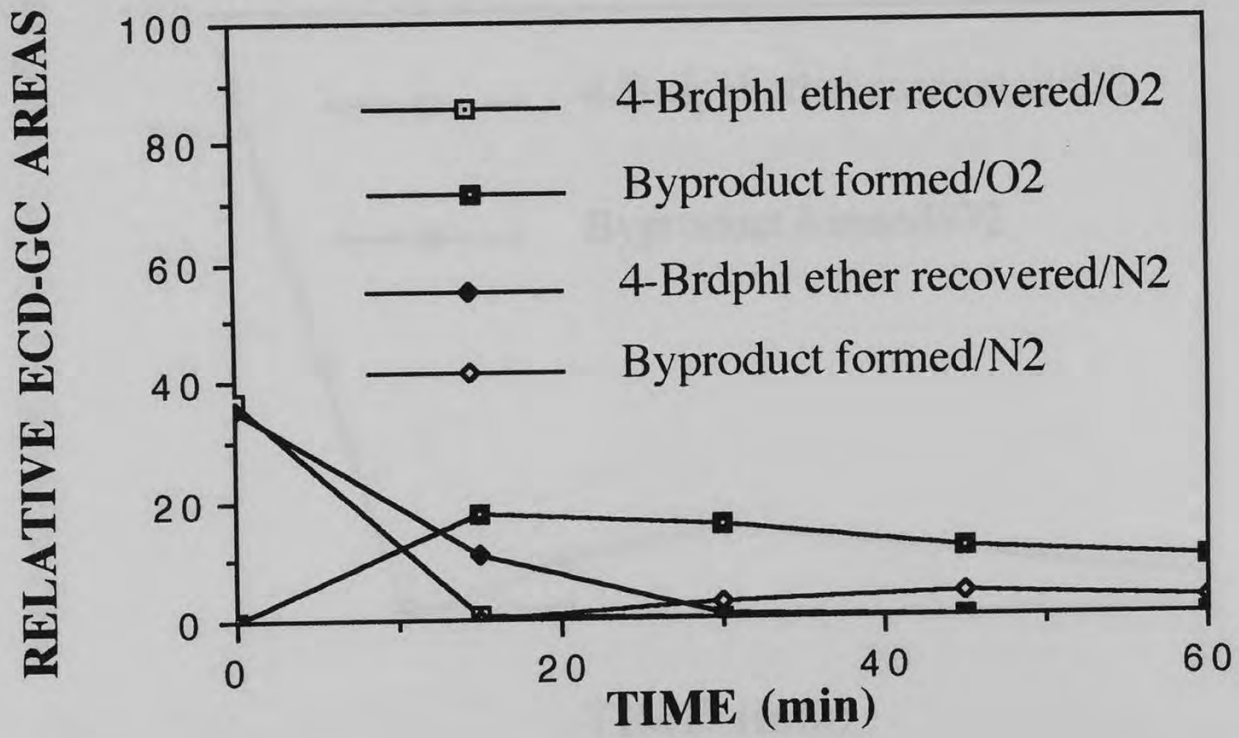

FIGURE VIII: 4-Bromodiphenyl ether vs Byproduct, relative ECD-GC detection (0 to 30 min). Irradiation at 350 nm under O2 in a TiO2 aqueous mixture at pH 7.0.

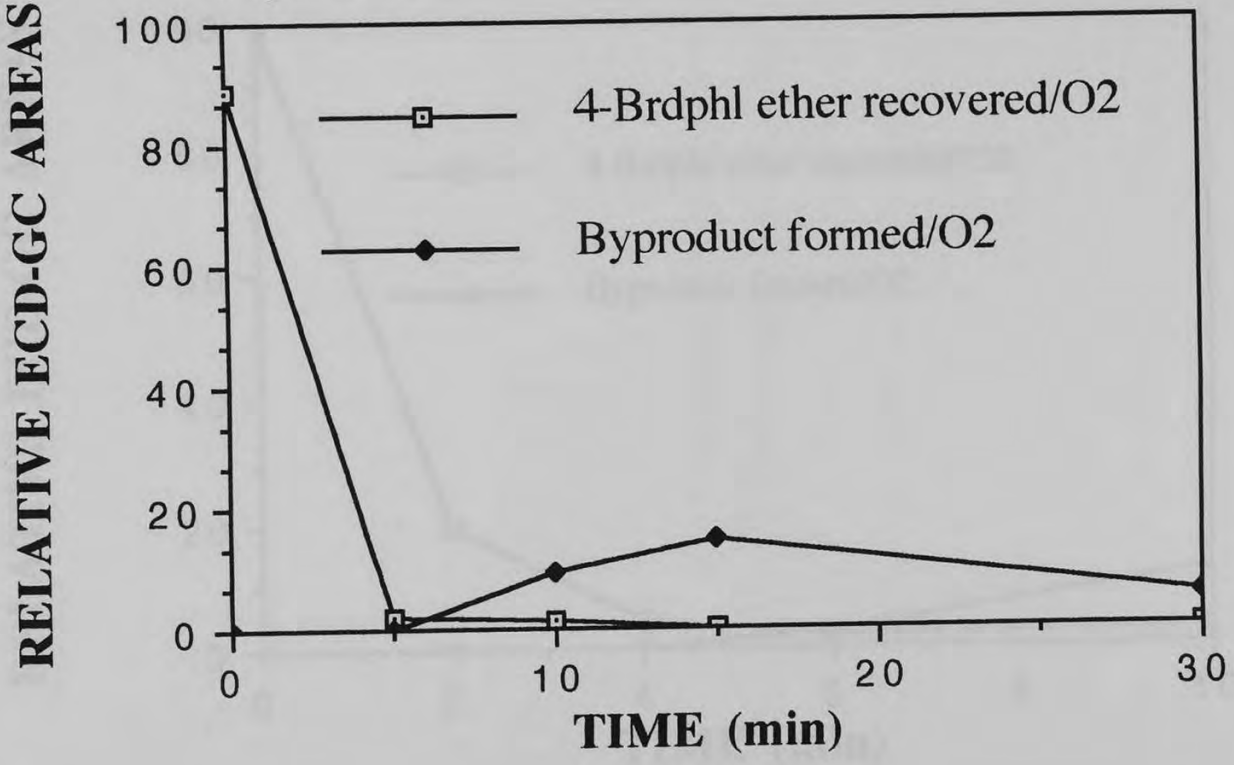

FIGURE IX: 4-Bromodiphenyl ether vs Byproduct, relative ECD-GC detection (0 to 10 min). Irradiation at 350 nm under O2 in a TiO2 aqueous mixture at pH 7.0.

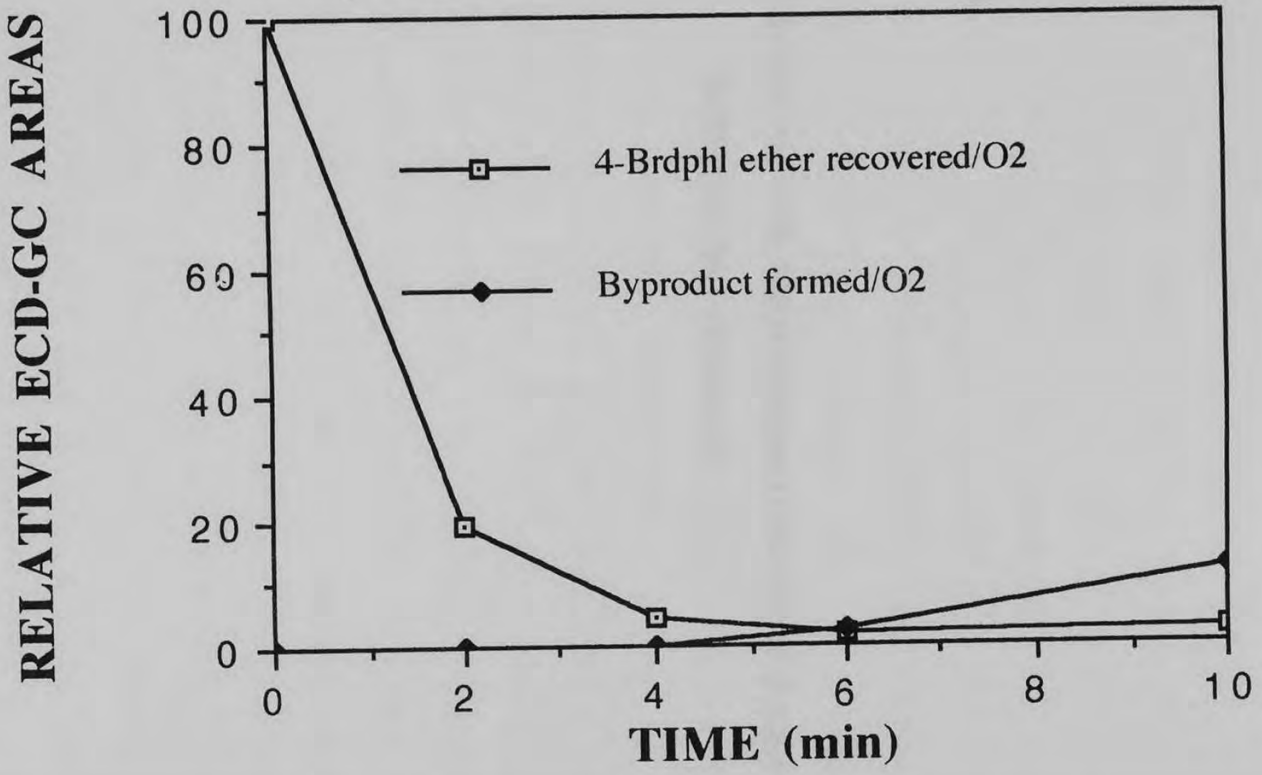

3.0 A HAMMETT STUDY OF THE PHOTODEGRADATION OF *PARA*-SUBSTITUTED PHENOLS

3.1 INTRODUCTORY REMARKS.

Phenols and phenolic compounds pose a significant threat to the environment and are commonly found as dilute contaminants in ground water and surface water. Although these compounds are also produced from natural sources, they are primarily the result of anthropogenic activity. Phenols are discharged into the environment as automobile exhaust, photooxidation byproducts, and industrial waste.[47,48]

Although TiO_2 mediated photodecomposition and complete mineralization studies have been carried out on several substituted phenols, a single study comparing this photocatalyzed degradation of monosubstituted phenols, at identical experimental conditions, has not been previously reported.[2,49]

Correlations between the rate of electron transfer,[50] as well as the rate of reaction with •OH,[51] and substituent effect on aromatic compounds have been observed. In addition, a Hammett relationship between *para*-substituted phenols and the rates of reaction with hydroxyl radical in homogeneous aqueous media has been reported[52] and, as mentioned before, hole-oxidation reactions, in a TiO_2 non-aqueous media, correlated with the effects of the substituents on the aromatic substrate.[19] Thus Hammett correlations have been independently reported for both oxidizing species, •OH and h^+, and if either of these processes dominates the

semiconductor photocatalyzed degradation of *p*-substituted phenols, a Hammett relation would be expected.

In this study, we evaluated potential Hammett relationships in the TiO_2 mediated photodegradation of nine *p*-substituted phenols in an aqueous media. The electronic properties of the substituents range from strong electron-donating to strong electron-withdrawing while phenol was the reference compound. The phenols employed in this study are shown below.

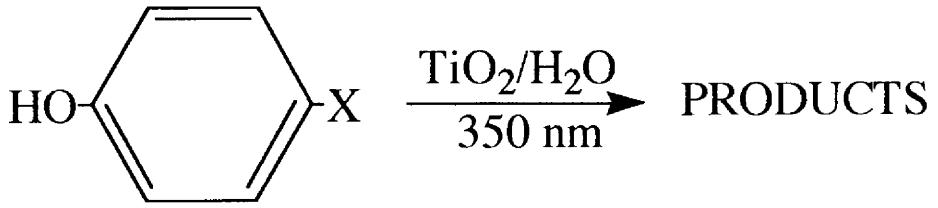

X = H, OCH_3, CH_3, F, Cl, Br, I, CF_3, $COCH_3$, and CN

3.2 EXPERIMENTAL SECTION.

The photodegradation reactions were conducted in deionized water at pH 3.0 and the phenol concentrations were measured from standardization curves devised from $CHCl_3$ extractions. The reported concentrations are not absolute but

semiconductor photocatalyzed degradation of *p*-substituted phenols, a Hammett relation would be expected.

In this study, we evaluated potential Hammett relationships in the TiO_2 mediated photodegradation of nine *p*-substituted phenols in an aqueous media. The electronic properties of the substituents range from strong electron-donating to strong electron-withdrawing while phenol was the reference compound. The phenols employed in this study are shown below.

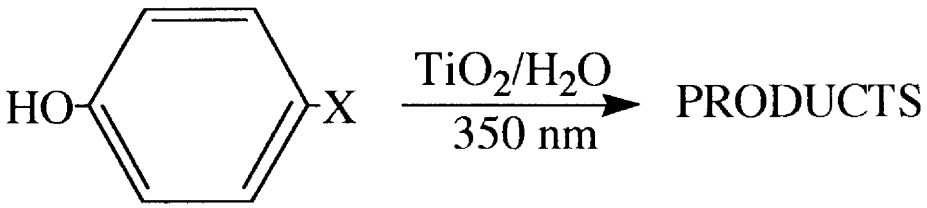

X = H, OCH_3, CH_3, F, Cl, Br, I, CF_3, $COCH_3$, and CN

3.2 EXPERIMENTAL SECTION.

The photodegradation reactions were conducted in deionized water at pH 3.0 and the phenol concentrations were measured from standardization curves devised from $CHCl_3$ extractions. The reported concentrations are not absolute but

relative to the maximum that could be extracted under our experimental conditions.

Appendix III shows these standardization curves. Moderate linear correlations were encountered with *p*-cyanophenol and 4-hydroxyacetophenone (R^2 = 0.987 and 0.990 respectively). These curves were broken into three linear relationships (R^2 = 0.999) to accurately determine concentrations over a given range. The deviation from linearity for these two compounds coincided with significant difficulty encountered when preparing the aqueous stock solution: instead of 0.1 M, 0.02 M for *p*-cyanophenol and 0.05 M for 4-hydroxyacetophenone were the concentrations used because of limited solubilities even upon sonicating and stirring overnight. The *p*-cyanophenol also presented problems dissolving in chloroform: a 0.2 M stock solution was prepared instead of 1.0 M solutions used for the other phenols because of low solubility even following sonication and stirring.

Two other compounds were slightly soluble in water: *p*-bromophenol and *p*-iodophenol. Instead of a 0.1 M aqueous stock solution, a 0.05 M and a 0.01 M had to be prepared respectively. These still require stirring overnight to completely dissolve and can not be stored in the refrigerator because precipitation will occur.

In addition, this study was further complicated by low recoveries of the phenols upon extraction from water which limit the detection because of the relatively low concentrations

obtained. Table III presents the percentage recovered in the concentration range studied after extracting and the minimum limit of detection for chloroform solutions and extracted solutions.

TABLE III. % Recoveries and Minimum Detection Limits (MDL) for *p*-substituted phenols in $CHCl_3$ and Extracted by $CHCl_3$ from Aqueous Solutions at pH 3.0

SUBSTITUENT	MDL in $CHCl_3$ X10^6 M	MDL extracted X 10^5 M	% RECOVERY
H	< 5.0	< 2.0	30
p-OCH_3	< 5.0	< 2.0	40
p-CH_3	< 5.0	< 0.7	65
p-F	< 5.0	< 2.0	30
p-Cl	< 7.0	< 1.0	56
p-Br	< 10.0	< 1.0	70
p-I	< 10.0	< 2.0	80
p-$COCH_3$	< 30.0	< 10.0	10
p-CF_3	< 10.0	< 1.0	77
p-CN	< 50.0	< 20.0	8

3.21 Materials.

Phenol was purchased from Fisher Scientific (Purified Grade) and the *p*-substituted phenols, *p*-methoxyphenol, *p*-cresol, *p*-fluorophenol, *p*-chlorophenol, *p*-bromophenol, *p*-iodophenol, 4-hydroxyacetophenone, α,α,α–trifluoro-p-cresol, and *p*-cyanophenol, were obtained from Aldrich. Deionized water pH 3.0 (pH adjusted with 0.1 N HCl) and chloroform (Fisher Scientific,

Certified A.C.S.) were the solvents used throughout this study. The photocatalyst was TiO_2, Degussa P25 lot# RV2186 (surface area 50 m^2/g, avg. primary particle size 30 nm, X-Ray structure primarily anatase).

3.22 Procedure.

A 50 mL aliquot of deionized water pH 3.0 was placed in a cylindrical, round bottom, Corex tube fitted with a screwed cap and a teflon septa. A determined volume of this water was removed and replaced with an equal volume of an aqueous stock solution (0.1 M prepared in deionized water pH 3.0) of the phenol studied. Then, 5 mg of TiO_2 (0.1 g/L) were added and the mixture was sonicated (43 kHz) for 5 min. to achieve a homogeneous suspension.

After sonicating, the mixture was cooled down to 22 °C with an ice-water bath while stirring. A 5.0 mL aliquot of the mixture was filtered, by using a 10 mL gas tight syringe and a 0.45 μm PTFE acrodisc, into a 40 mL extracting vial (Borosilicate, clear glass with open top phenolic caps and PTFE septa) followed by the filtration of two separate 5 mL aliquots of deionized water pH 3.0 to rinse the syringe and acrodisc. Then, a 10 mL aliquot of deionized water, pH 3.0, was added to the extracting vial as well as a 5.0 mL aliquot of $CHCl_3$ to bring the volume to 30.0 mL. The resulting solution was shaken in an Orbit Shaker (3 min at 300

rpm) and the $CHCl_3$ layer was pipetted into an amber autosampler vial to be chromatographed.

The rest of the mixture was purged with O_2 for 1 min, step that was repeated after every hour of irradiation. A control reaction was purged with N_2 for 5 min initially and after every hour of irradiation. After purging, the mixture was placed in a 40 °C constant temperature bath, and only when it equilibrated to this temperature, irradiation was performed for the desired time interval. The photoreactor employed was as described in section 2.22. Following irradiation, the mixture was rapidly cooled to 22 °C with an ice-water bath while stirring, and then, a 5.0 mL aliquot was removed for analysis as above.

The sampling times were 0, 5, 10, 15, and 30 min for the kinetic study carried out at different concentrations; the control reactions were usually sampled at 0, 15, 30, 60, 120, and 240 min. These control reactions were carried out and analyzed to assess the effect, if any, of irradiation in the presence of TiO_2 under O_2 or N_2; irradiation without TiO_2 (direct photolysis) under O_2; and no irradiation at all (kept in the dark at 40 °C) in the presence of TiO_2 and O_2.

The concentrations employed for the control reactions were comparable for all the phenols except for *p*-cyanophenol and 4-hydroxyacetophenone which had much lower detection limits. The least concentrated solution, that could still be detected under our analysis procedure, was irradiated without the semiconductor

because the greatest effect was expected in the most dilute solutions.

3.23 Analysis.

The degradation of the phenols was monitored with a HP 5890 GC equipped with a FID detector and a J&W Scientific DB-1 (30 m X 0.25 mm, 0.25 microns) column. The temperature program started at 40 °C for 5 min and increased at a rate of 20 °/min to 220 °C where it remained for 5 min. The temperature of the injector was 200 °C and 220 °C for the detector. The head pressure was set at 14.1 psi; The purge was on at 1.50 min and off at 0.00 min. The gas flows were 375 mL/min for air, 30 mL/min for He (carrier) + N_2, and 30 mL/min for H_2.

Under these GC conditions a standard calibration curve was obtained for each phenol by preparing a working standard $CHCl_3$ solution (0.1 M) from a stock solution (usually 1.0 M) by dilution. Then, specific volumes of the working standard (i.e., 1.0, 5.0, 10.0, 20.0, 30.0, 50.0, 100.0, and 200.0 µL) were injected to a series of eight 40 mL extracting vials which contained 25.0 mL of deionized water pH 3.0, 5.0 mL $CHCl_3$ (both measured with glass volumetric pipettes), and 10.0 µL of the internal standard solution (1.0 M toluene in $CHCl_3$). At least eight calibration points were thus attempted for each standardization curve. The extracting vials were shaken in an Orbit Shaker for 3 min at 300 rpm and the

$CHCl_3$ layers were transferred with disposable pipettes into amber autosampler vials which were, then, sealed and chromatographed.

Each time a reaction was carried out, the particular standardization curve was checked by preparing two or three calibration points as described above. The results obtained were compared against the original curve and if the concentration of these samples deviated by more than 10%, a new curve was needed.

3.3 RESULTS AND DISCUSSION.

Consistency and sound analytical procedures are fundamental to obtain meaningful data for kinetic analysis such as those performed in this study. Thus any reaction with a recovery of less than 90 % before irradiation (t = 0 min) was repeated and reevaluated.

The first 20% of the reaction occurs at about 5 min of irradiation; therefore, the initial rates were calculated from a linear plot of concentration vs. time for the first 10 min of reaction. Table IV summarizes these initial rates at the examined concentrations and Appendix IV depicts the degradation of each phenol followed for 30 min and their initial rates at 5 min of reaction.

TABLE IV. Initial Reaction Rates as a Function of Concentration of the *para*-substituted phenols irradiated at 350 nm in TiO_2 aqueous mixtures at pH 3.0.

Subst. X	Concentration (mM X10^2), [Initial Rates[a](M/min X 10^5)]
H	182.1 [2.44]; 89.54 [1.77]; 63.26 [1.73]; 53.79 [1.59]; 46.13 [1.66]; 36.43 [1.36].
p-OCH_3	178.7 [2.70]; 86.08 [2.06]; 62.11 [1.78]; 52.68 [1.38]; 45.90 [1.55]; 36.70 [1.23].
p-CH_3	180.0 [2.10]; 81.59 [1.71]; 53.81 [1.50]; 47.76 [1.32]; 38.03 [1.36]; 30.51 [1.24].
p-F	184.2 [3.83]; 183.4 [3.81]; 92.41 [3.14]; 64.78 [2.37]; 55.50 [2.49]; 45.91 [2.28]; 37.08 [1.86].
p-Cl	192.54 [2.52]; 91.10 [1.82]; 70.37 [1.54]; 62.69 [1.63]; 51.74 [1.38].
p-Br	187.6 [1.80]; 88.21 [1.32]; 61.02 [1.15]; 53.05 [1.52]; 44.57 [1.03]; 36.03 [0.966].
p-I	181.3 [1.38]; 125.0 [1.04]; 88.21 [0.879]; 75.11 [0.780]; 50.51 [0.611]; 49.67 [0.590]; 39.67 [0.497].
p-CF_3	187.8 [2.12]; 89.29 [1.65]; 56.94 [1.47]; 40.77 [1.34].
p-$COCH_3$	176.0 [1.66]; 134.8 [1.78]; 89.22 [1.65]; 60.53 [1.28]; 52.59 [1.07]; 45.87 [0.946].
p-CN	254.4 [1.64]; 173.9 [1.30]; 140.5 [1.16]; 104.3 [0.853]; 91.36 [0.717]; 81.12 [0.717].

a- Estimated error in the measurement of the initial rates is < 8% based on results from duplicate runs.

The Langmuir-Hinshelwood model (Equation 17) was applied to the data obtained for each phenol examined, graphically represented in Appendix V. The L-H models for all the phenols studied are compared in Figure X. The apparent kinetic parameters, k and K, were calculated from the slope and intercept of the plot of $1/rate_0$ vs. $1/[phenol\text{-}X]_0$ and they are summarized in Table V.

FIGURE X: L-H model applied to the initial rates of disappearance in the TiO2 photocatalyzed (350 nm) degradation of p-substituted phenols in an aqueous media at pH 3.0.

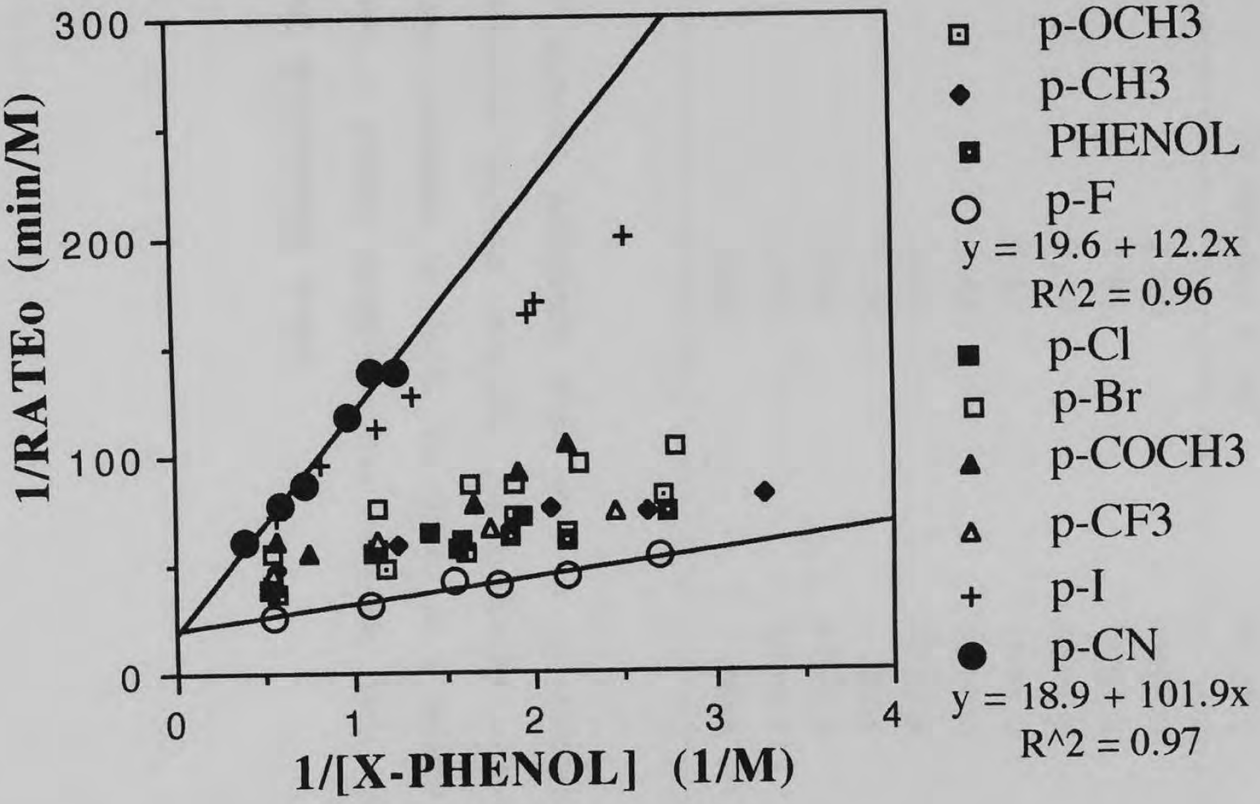

TABLE V. L-H Apparent Kinetic Parameters of the Examined Phenols.

Subst. X	k (M/min) X 10^5	K (M^{-1})
H	2.68	2904.7
p-OCH_3	3.86	1283.2
p-CH_3	2.29	3608.5
p-F	5.11	1601.2
p-Cl	3.43	1293.0
p-Br	2.05	2327.4
p-I	2.38	668.4
p-$COCH_3$	2.83	1192.2
p-CF_3	2.38	2996.1
p-CN	5.41	180.1

These L-H apparent parameters were used in an attempt to establish a correlation between structure and reactivity with the Hammett constants presented in Table VI. While in a number of cases no or only a limited correlation was observed, there were some interesting relationships found.

TABLE VI. Hammett Constants Employed in this Study.

Subst. X	σ_p[22]	σ[21]	σ^+[21]	$\sigma_{I(Hine)}$[20]	$\sigma_{I(Taft)}$[18]	$\sigma_{I(Grob)}$[18]
H	0.00	0.00	0.00	0.00	0.00	0.00
p-OCH_3	-0.28	-0.27	-0.78	0.27	0.23	0.31
p-CH_3	-0.14	-0.17	-0.31	-0.04	-0.05	0.02
p-F	0.15	0.06	-0.07	0.50	0.50	0.46
p-Cl	0.24	0.23	0.11	0.46	0.47	0.44
p-Br	0.26	0.23	0.15	0.44	0.45	0.47
p-I	0.28	0.18	0.13	0.39	0.38	0.41
p-$COCH_3$	0.47	0.50	---	---	0.27	0.29
p-CF_3	0.53	0.54	---	0.45	---	---
p-CN	0.70	0.66	0.66	0.56	0.59	0.55

There was a reasonably good relationship noted among the reactivities of the monohalogenated phenols and σ_p as well as σ^+ as depicted on Figures XI and XII. The *p*-fluorophenol reacted the fastest followed by the *p*-chlorophenol while the *p*-bromo and *p*-iodophenol had similar reactivities. These results suggest that the monohalogenated phenols follow analogous photodecomposition mechanisms. There is also a good correlation between the apparent adsorptivity constant of the *para*-substituted phenols and the inductive/field effect of the substituents. The Hammett plot of $\log(K_X/K_H)$ vs. $\sigma_{I(Grob)}$ has R^2=0.462; however, when comparing only the halogenated phenols (R^2=0.974) and the remaining phenols (R^2=0.916), as depicted on Figure XIII, good correlations are observed for the two sets of substituted phenols.

FIGURE XI: Correlation between k, the L-H apparent reactivity parameter, and σ_p for the monohalogenated p-substituted phenols.

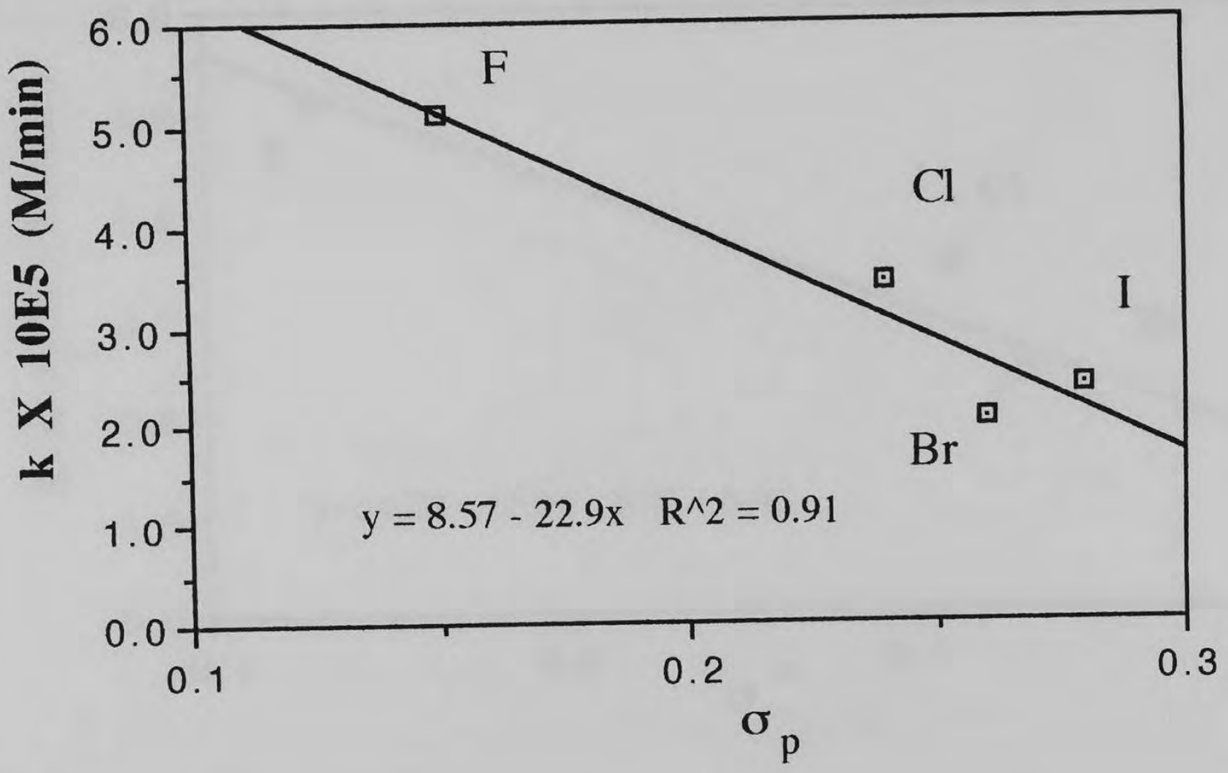

FIGURE XII: Correlation between k, the L-H apparent reactivity parameter, and σ^+ for the monohalogenated p-substituted phenols

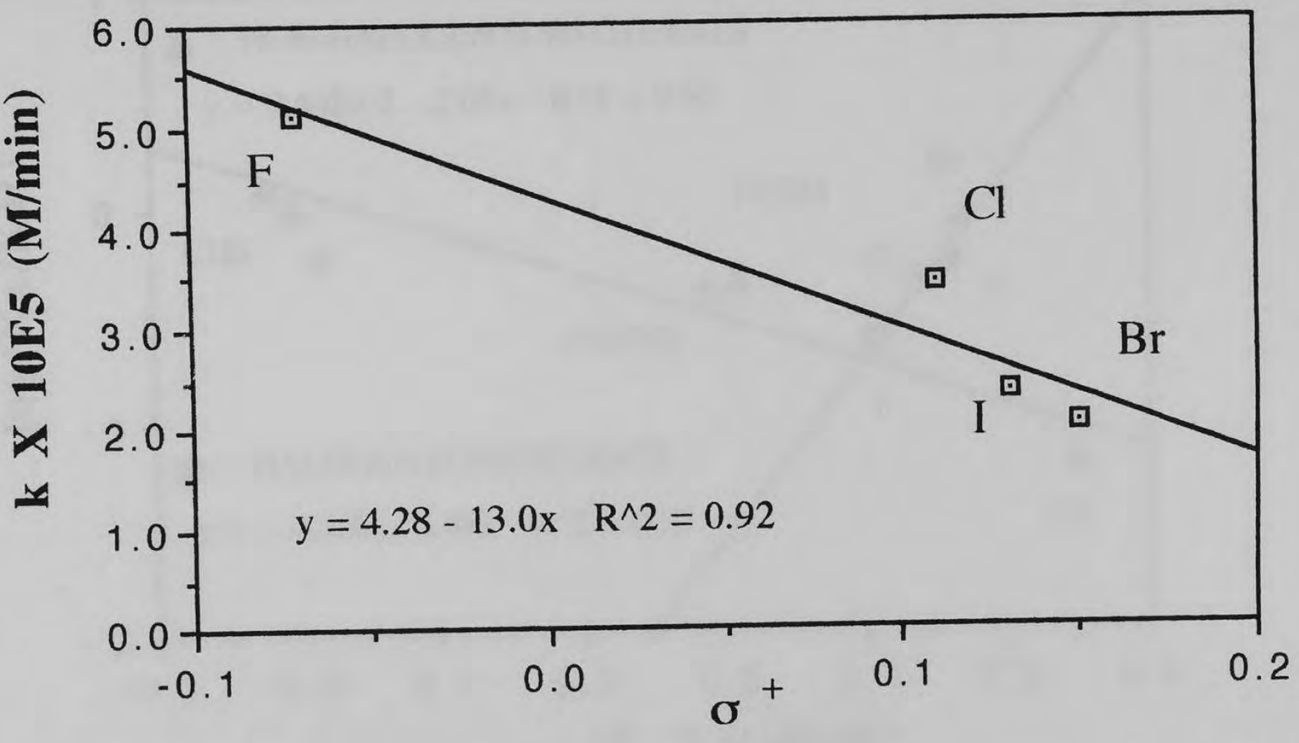

FIGURE XIII: Hammett correlation between log(Kx/KH), K is the L-H apparent adsorptivity parameter, and σI(Grob), the inductive effect of substituent X.

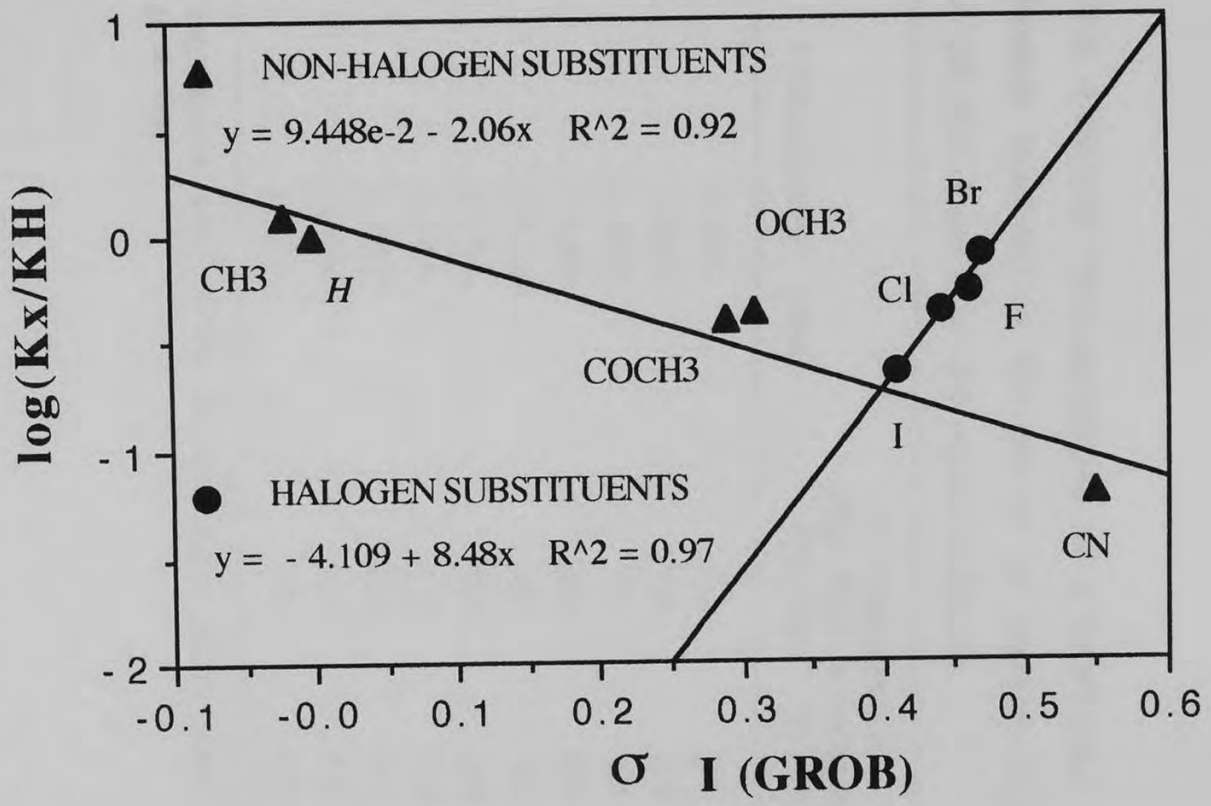

Tables VII and VIII summarize the results of the control reactions carried out with all the examined phenols (see Appendix VI for a graphical portrayal of these controls). Dark controls showed minimal (1-4%) loss of the starting material.

TABLE VII. TiO_2 Catalyzed Photodegradation of *p*-Substituted Phenols Irradiated at 350 nm in an Aqueous Media at pH 3.0 under oxic and anoxic coditions.

Subst. X	Concentration (mM)	% Degradation after 4hrs of irradiation TiO_2/O_2	TiO_2/N_2
H	1.919	91	21
p-OCH_3	1.954	86	25
p-CH_3	1.933	76	22
p-F	1.959	87[a]	87
p-Cl	1.934	88	23
p-Br	1.956	58	24
p-I	1.917	60	24
p-$COCH_3$	1.912	68	21
p-CF_3	1.902	75[a]	32
p-CN	1.961	53	16

a- Reported % degradation after 2 hrs of irradiation; below limit of detection at 4 hrs.

TABLE VIII. Photodecomposition of *p*-substituted Phenols in the Absence of TiO_2 irradiated at 350 nm (Aqueous Solutions at pH 3.0).

Subst. X	Concentration (mM X 10^2)	% Degradation/ irradiation time(hrs)
H	9.595	20[a]/ 2
p-OCH_3	9.771	17 / 4
p-CH_3	9.385	39 / 4
p-F	9.795	33 / 4
p-Cl	9.669	25 / 4
p-Br	9.780	22 / 4
p-I	9.583	15 / 4
p-$COCH_3$	47.10	18 / 4
p-CF_3	9.520	19 / 4
p-CN	78.44	4 / 4

a - Below limit of detection after 4 hrs. of irradiation.

These control reactions clearly show three results:

A.) There is no degradation of any of the phenols, in the presence of TiO_2, without irradiation; high percent recoveries were obtained for controls done in the dark at 40 °C which implies there was little dark adsorption of the phenols onto the TiO_2 surface under our experimental conditions.

B.) When irradiated in an aqueous media in the absence of the photocatalyst, TiO_2, there is slight direct photolysis which has been observed previously when irradiated at 254 and 296 nm.[53] These controls were carried out with the lowest detectable

concentration to maximize the relative contribution of these non-catalytic reactions. In all cases, only a small portion of phenol is degraded when irradiated at 350 nm without TiO_2.

C.) Moderate degradation occurs when the mixtures were purged with N_2 initially and after each hour of irradiation. This degradation may be due to not all the O_2 being displaced or to another species (i.e., the phenol itself) capturing the hole of the valence band. The *p*-fluorophenol and the α,α,α-trifluoro-*p*-cresol were the most extensively degraded, 87 and 32 % respectively, when irradiated under N_2 for 4 hours. These phenols are also degraded most extensively under oxygenated conditions when compared to the other phenols in this study.

4. pH STUDY OF THE PHOTOCATALYZED DEGRADATION OF PHENOL

4.1 INTRODUCTORY REMARKS.

In this study, the initial rates were compared in the TiO_2 catalyzed photodecomposition of phenol in aqueous media over the pH range from 1.0 to 13.7 (2 N NaOH). The relationship between these initial rates and pH was followed at three different concentrations. The degradation efficiency of phenols was also evaluated after four hours of irradiation under oxic and anoxic conditions in the presence of the semiconductor as well as in its absence and in the dark over the same pH range.

The pK_a of phenol is 9.89[54] and the isoelectric point of TiO_2 is at about pH 6.0. At higher pH values than the pK_a of phenol, electrostatic repulsion with the semiconductor surface is expected since they both are negatively charged. These coulombic interactions should be considered since the models employed to explain the semiconductor catalyzed photooxidation reaction requires the substrate to be adsorbed (L-H model) or in close proximity (E-R model) to the TiO_2 surface.

In aqueous media, the rate of substrate degradation is expected to decrease at low pH values since the TiO_2 surface is protonated and the dominant species in solution would be H_3O^+ inhibiting the formation of hydroxyl radical by reaction 2,

$$H_2O + h^+ \longrightarrow {}^\bullet OH + H^+ + (h^+/\ e^-) \qquad (2)$$

As the initial pH of the heterogeneous mixture increases, the degradation rate is believed to accelerate[26,29] due to the increase in $H_2O/^-OH$ species and a marked enhancement is expected especially in alkaline media since reaction 1 would then be favored,

$$^-OH + h^+ \longrightarrow \bullet OH + (h^+/ e^-) \qquad (1)$$

The focus of this investigation is on a range of initial solution pH values where the electrostatic repulsion and coulombic interactions are expected to have a direct effect on the degradation process. The relationship between solution pH and reactivity of phenol is evaluated in this study and compared to previous reports describing the degradation of organic substrates in a TiO_2 photocatalyzed reaction at a variety of pH values.

The L-H model (Eq. 17) was also applied to the initial rates of degradation of phenol and compared over the 1.0 to 13.7 pH range studied. The control reactions carried out in this investigation also provided fundamental information, not reported previously, on the efficiency of the semiconductor catalyzed photooxidation reaction after several hours compared to the initial rates of disappearance.

4.2 EXPERIMENTAL SECTION.

The photodegradation of phenol was carried out in deionized water at pH 1.0, 3.0, 5.0, 7.0, 9.0, 11.0, and 13.7. The initial pH of the phenol aqueous solution was adjusted to the desired value with 0.1 M HCl, 0.1 N NaOH, and conc. HCl, except for the reactions at pH 13.7 which were actually carried out in a 2 N NaOH. The pH electrode and meter (Corning) were not very sensitive for the pH measurement at this alkaline concentration. Buffers were not used to avoid competition with other ions for adsorption sites on the semiconductor surface.

The same phenol (Fisher Scientific, Purified Grade) used in section 3.0 is employed in this study without further purification and the experimental procedure followed is described in section 3.22 with slight modifications outline below. An aqueous stock solution of phenol was prepared at the pH studied (0.1237 M at pH 1.0, 0.1016 M at pH 3.0, 0.09797 M at pH 5.0, 0.09606 M at pH 7.0, 0.09786 M at pH 9.0, 0.1020 M at pH 11.0, and 0.1001 M at pH 13.7). A 50 mL aliquot of deionized water at the same pH was placed in a round- bottom, cylindrical Corex tube; a determined volume of this water was removed and replaced with an equal volume of the appropiate phenol aqueous stock solution to obtain the desired concentration. 5.0 mg of TiO_2 (100.0 mg/L) were added and the mixture was sonicated (43 kHz) for 5 min to achieve a homogeneous suspension.

After sonicating, the mixture was cooled to 22 °C in an ice-water bath while stirring and a sample was removed for analysis (t = 0 min) as follows: A 5.0 mL aliquot of the mixture was filtered through a 0.45 μm acrodisc, attached to a 10 mL gas tight syringe, into a 40 mL extracting vial. Two 5.0 mL aliquots of deionized water pH 3.0 were filtered consecutively to rinse the syringe, the acrodisc, and the TiO_2 removed from the sample. The filtrate pH was adjusted to pH 3.0 with conc. HCl when necessary (i.e., samples at pH 13.7 required 35 drops of conc. HCl). Then, the filtrate volume was brought to 30.0 mL with the addition of 10.0 mL aliquot of deionized water pH 3.0, 5.0 mL aliquot of $CHCl_3$, and 10 μL of the internal standard solution (0.9704 M toluene in $CHCl_3$). The extracting vials were shaken in an Orbit Shaker (Lab-Line Instruments) for 3 min at 300 rpm and the $CHCl_3$ layer was transferred with disposable pipettes into amber autosampler vials which were then sealed and analyzed. The remaining mixture was either purged with O_2 or N_2 prior to irradiation and after every hour of light exposure.

The photoreactor employed was as described in section 2.22, and since its operating temperature was 40 ± 2 °C, the reaction mixtures were always equilibrated to this temperature before irradiation and cooled down to 22 °C before sampling. Samples were taken at 0, 5, 10, 15, and 30 min of irradiation for the kinetic analysis and the control mixtures were sampled at 0, 15, 30, 60, 120, and 240 min. All the control reactions were carried

out for a period of 4 hours at the same concentration (2.0 mM) over the pH range studied to evaluate the effect of the presence of O_2 vs. N_2, direct photolysis of the substrate, and adsorption in the dark.

The amounts of phenol left after irradiation were quantified with a standardization curve prepared from extractions of aqueous solutions at pH 3.0 and the analytical procedure employed was as described in section 3.23.

4.3 RESULTS AND DISCUSSION.

The initial rates of phenol disappearance were obtained by plotting the remaining concentration vs. time for the first 10 min of reaction (Appendix VII). A summary of the initial degradation rates is shown in Table IX.

The L-H model (Eq. 17) was applied to this data (Appendix VIII), as depicted in Figure XIV, to obtain the apparent kinetic parameters from the slope and intercept of the plots $1/Rate_0$ vs. $1/[phenol]_0$. These L-H parameters are listed in Table X; the largest differences are observed at pH 1.0 and 11.0. It is also noteworthy that the K value (apparent adsorptivity constant) for phenol at 13.7 was the largest while it remained relatively constant at pH 3.0, 5.0, and 7.0 with a gradual increase at pH 9.0, at about the pK_a of phenol (9.89). The k, apparent reactivity

constant, remains relatively constant for most of the pH studied except at pH 1.0 and 11.0 which show a significant decrease.

TABLE IX. Initial Rates of Disappearance Obtained at the Corresponding Initial Concentration in the Photocatalyzed, TiO_2 Mediated, Decomposition of Phenol. Mixtures were Irradiated at 350 nm.

pH	$[Phenol]_0$ X 10^5 (M) {$Rate_0$ X 10^5 ($Mmin^{-1}$)}[a]
1.0	44.62{0.210}; 53.17{0.249}; 70.65{0.264};87.76{0.334}; 122.7 {0.311}; 174.4 {0.451}.
3.0	36.43 {1.36}; 46.13 {1.66}; 53.79 {1.59}; 63.26 {1.73}; 89.54 {1.77}; 182.1 {2.44}.
5.0	43.60 {1.60}; 51.14 {1.61}; 52.23 {1.66}; 70.42 {1.88}; 86.12 {2.01}; 86.90 {1.94}; 119.5 {2.15}; 122.1 {2.00}; 172.4 {2.45}; 173.3 {2.44}.
7.0	45.24 {2.01}; 55.26 {2.15}; 73.3 {2.35}; 90.71 {2.37}; 129.5 {2.72}; 182.2 {3.11}.
9.0	46.17 {1.87}; 55.34 {2.00}; 72.13 {2.05}; 91.02 {2.14}; 128.6 {2.36}; 186.1 {2.78}.
11.0	46.64 {0.707}; 54.88 {0.661}; 73.69{0.754};92.81{1.06}; 126.9 {0.0950}; 185.3 {1.25}.
13.7	60.24 {2.19}; 81.07 {2.41}; 101.3 {2.34}; 141.5 {2.7}; 202.0 {2.68}; 203.1 {2.77}.

a- Estimated error in the measurement of the initial rates of disappearance is < 7% based on results from duplicate runs.

FIGURE XIV: L-H model applied to the initial rates of disappearance of phenol in the TiO2 mediated photodecomposition (350 nm) in an aqueous media over the pH range of 1.0 to 13.7.

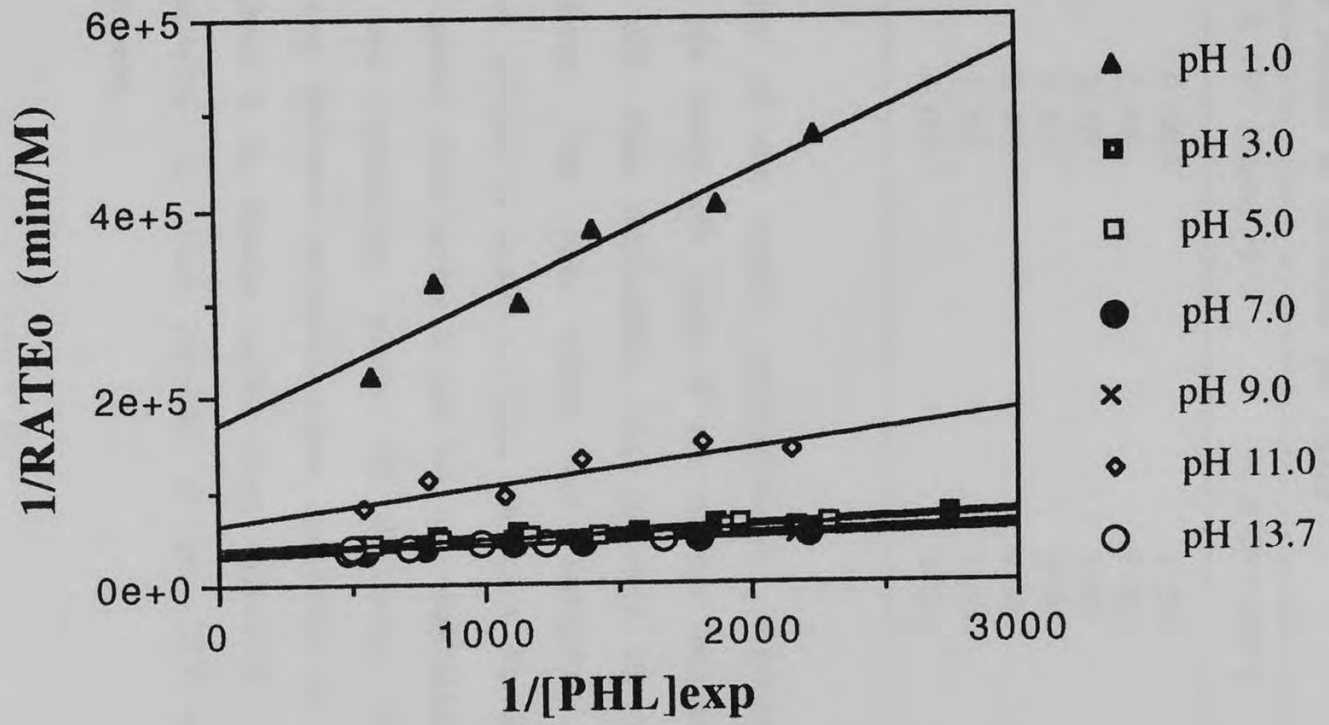

TABLE X. Apparent Kinetic Parameters Obtained from the L-H Model Applied to the Photocatalyzed Decomposition Rates of Phenol at Different pH values.

pH	k X 10^5 ($Mmin^{-1}$)	K X 10^{-3} (M^{-1})
1.0	0.584	1.29
3.0	2.68	2.90
5.0	2.80	2.83
7.0	3.47	2.93
9.0	2.95	3.59
11.0	1.52	1.62
13.7	3.05	4.21

The dependency of the initial photocatalytic degradation rate of phenol with the initial pH value of the reaction mixture is depicted in Figure XV. This relationship was followed at three different concentrations. The data points are connected by straight lines and no attempt is made to draw the best fit curve due to lack of data points. Data points at pH 5.0 were duplicated at different dates and are reproducible within 7% difference. These values proceeded from different reactions whose recoveries at t = 0 min varied by about 2 %. Similar results were observed with regards to reproducibility for runs repeated at pH 13.7 at a concentration of 2.0 mM.

FIGURE XV: Relationship between the initial rates of TiO_2 photocatalyzed (350 nm) degradation of phenol and the initial pH of the aqueous reaction mixture.

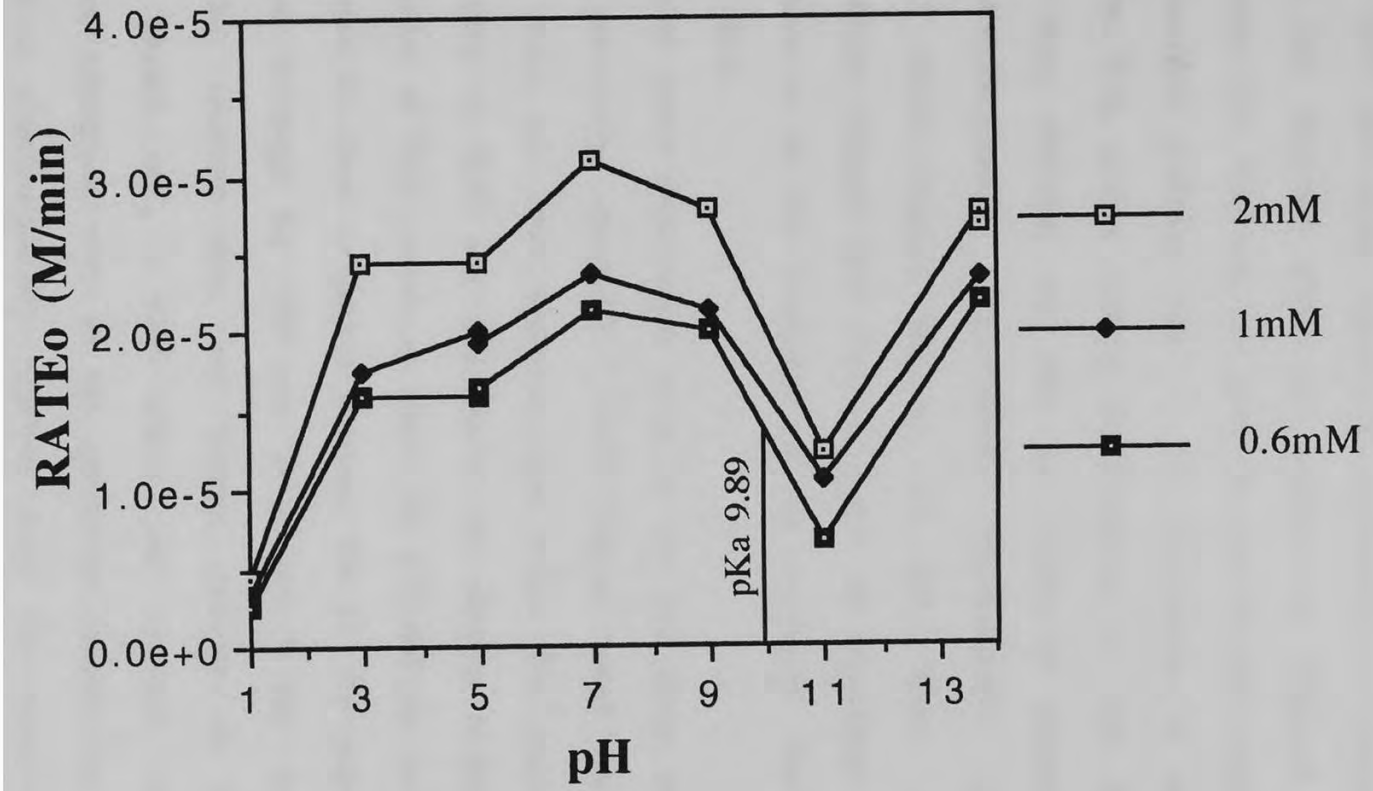

Although only moderate changes (less than an order of magnitude) are observed among the initial rates of disappearance over the 1.0 to 13.7 pH range, significant information is obtained. Common trends are detected when the reaction is followed at three concentrations, 2.0, 1.0, and 0.6 mM. At pH 1.0, the reaction seems to be retarded probably due to the protonation of most active sites on the TiO_2 surface slowing the formation of •OH. This retardation has been observed not only on studies of phenol,[29] but with 4-chlorophenol, chlorinated aliphatics,[54] and chlorobenzene[24] which suggest that at low pH values, the semiconductor surface changes and there is either an inhibition on substrate adsorption or on the formation of the oxidative species such as •OH, or both.

The observed initial degradation rates in the pH range from 3.0 to 9.0, as previously reported,[23,29] were similar which seems to indicate that there are other processes that affect the reaction besides the variation of H_3O^+ and ^-OH ions in the starting solution. The isoelectric point of TiO_2 occurs at about pH 6.0 and the initial rates were expected to show a marked increase due to the greater extent of surface coverage by ^-OH ions at pH 9.0. It has been propose that this increase does not happen because of the dissociation of phenol (pK_a = 9.89) which can compete with hydroxyl ions for adsorption sites as the phenoxide species but at the same time it is electrostatically repelled from the negatively charged semiconductor surface.[29] Nevertheless, previous studies

with chlorobenzene[24] also show a constant degradation rate in the pH range from 6.0 to 11.0 where the TiO_2 surface should be covered with ^-OH ions. In this case, there is no special competition with the substrate for adsorption sites and since the chlorobenzene does not develop a charge in this alkaline media, no electrostatic repulsion occurs from the negatively charged semiconductor surface.

The surprising results occurred in the 2 N NaOH (pH 13.7) media where the initial rate of phenol disappearance was observed to increase in comparison to that at pH 11.0.

The control reactions (Appendix IX) carried for 4 hours over the pH range studied also show some unexpected results. Figure XVI depicts the % of phenol that disappeared after following the reaction for four hours at the pH studied. Those reactions irradiated under N_2, in the presence of TiO_2, show a significant decrease in the efficiency of phenol removal after irradiation at 350 nm for a period of four hours. About 20-30 % of the initial phenol concentration is degraded across the pH range studied. No reaction was expected to occur in a N_2 saturated environment since O_2 is generally required for appreciable photooxidation to occur;[13,14,55] however, strongly adsorbed oxygen molecules on the semiconductor surface may have remained even after the 5 min N_2 purging or direct oxidation of the phenol by the photoexcited semiconductor can explain the decrease in phenol concentration.

No color developed in these controls and the least efficient removal occurred at pH 1.0 ($\sim$ 7 %).

There was a decrease of 20 % of the initial phenol concentration under oxygen at pH 1.0 in the absence of the semiconductor which was comparable to the decrease in its presence as Figure XVI shows. Both reactions developed a strong yellow color which suggest that the phenol did not photodegrade by TiO_2 mediated catalysis but in fact, there was direct absorption and probable formation of colored oligomers which has been previously observed when phenols were irradiated at 254 and 296 nm in a homogeneous aqueous media.[53]

FIGURE XVI: Removal efficiency of phenol after 4 hrs. of reaction in an aqueous media under different experimental conditions over the 1.0 to 13.7 pH range.

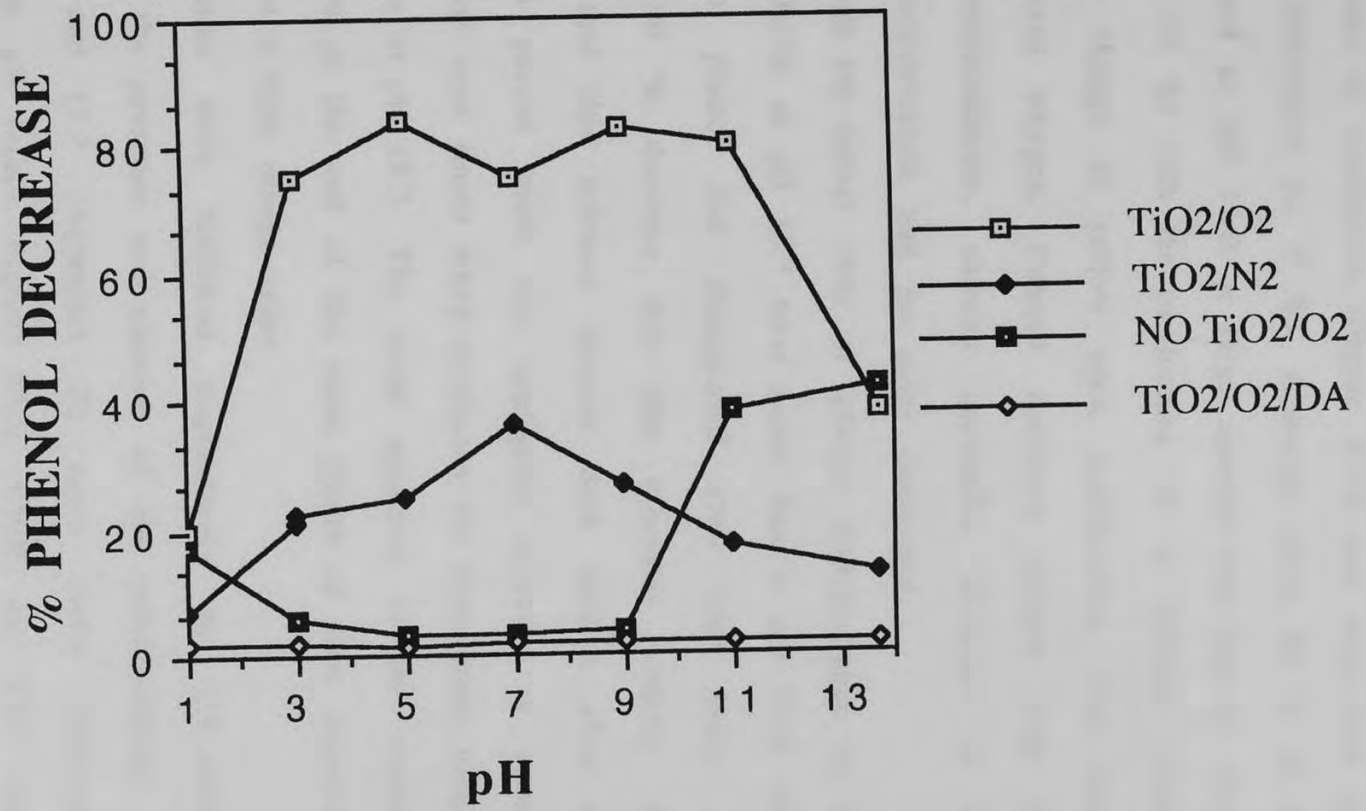

The reactions in the presence of TiO_2 and O_2 showed a similar % removal efficiency over the pH range of 3.0 to 9.0 ($\sim$ 80 %) after four hours of irradiation (Figure XVI) and very little was due to direct photolysis ($\sim$ 5 %). Although about 80 % of the phenol disappeared at pH 11.0, a large amount was due to direct photolysis ($\sim$ 40 %) with the production of a reddish colored solutions which change to yellow upon acidification. This direct photolysis required oxygen. Control reactions purged with N_2, without the semiconductor, showed negligible decrease of the initial phenol concentration and no color developed.

Even though the initial rates of phenol disappearance in the presence of TiO_2/O_2 at pH 13.7 were faster than at pH 11.0, only 40 % of the phenol had disappeared after four hours of irradiation. A 40 % decrease was also observed without the semiconductor and this solution became dark reddish after the same irradiation period under O_2; negligible decrease of phenol and lack of color were found when irradiated for four hours under N_2 without TiO_2 at pH 13.7. The color appeared in the reaction with TiO_2/O_2, but at the end of the same length of time exposure, it had faded into a light orange color.

The reactions were followed qualitatively by UV-visible spectroscopy in the presence and absence of the semiconductor at pH 1.0, 11.0, and 13.7 (Appendix X) since direct photolysis occurred at these pH values. Figures XVII, XVIII, and XIX verify that the disappearance of phenol in the presence of TiO_2 was due

to a degradation process other than just photolysis and clearly the organic substrate is completely mineralized while in the absence of the semiconductor, highly colored oligomers remained after long irradiation periods.

FIGURE XVII: UV-visible degradation of phenol at pH 1.0 in the presence and absence of TiO2 when irradiated at 350 nm.

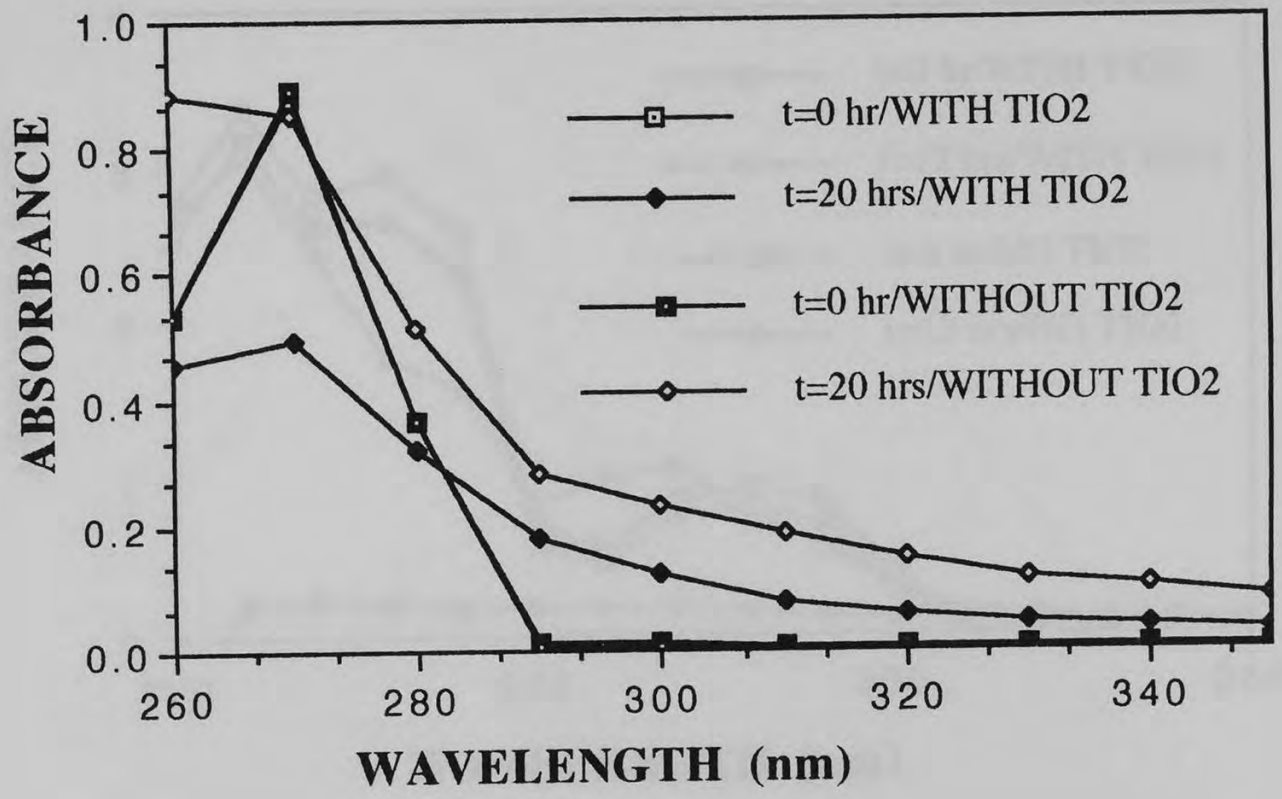

FIGURE XVIII: UV-visible degradation of phenol at pH 11.0 in the presence and absence of TiO2 when irradiated at 350 nm.

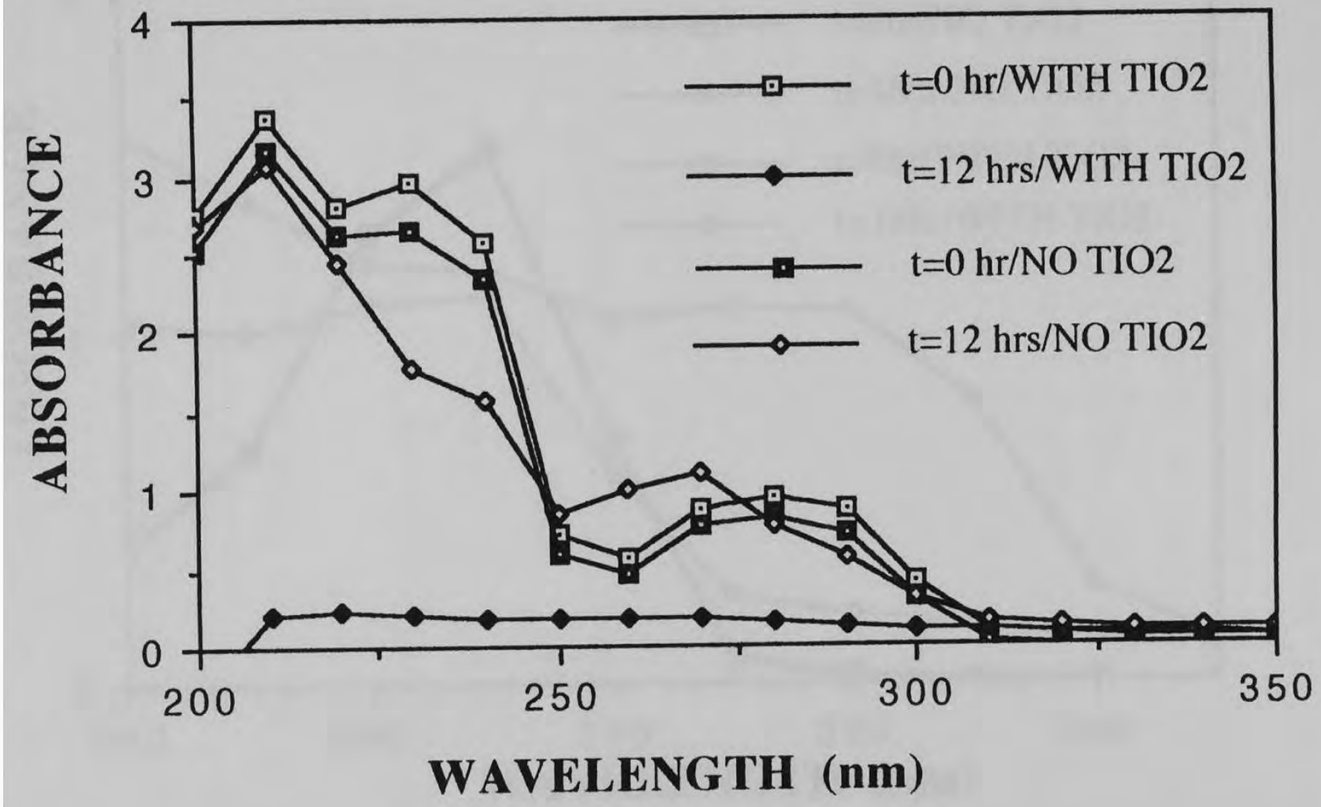

FIGURE XIX: UV-visible degradation of phenol at pH 13.7 in the presence and absence of TiO2 when irradiated at 350 nm.

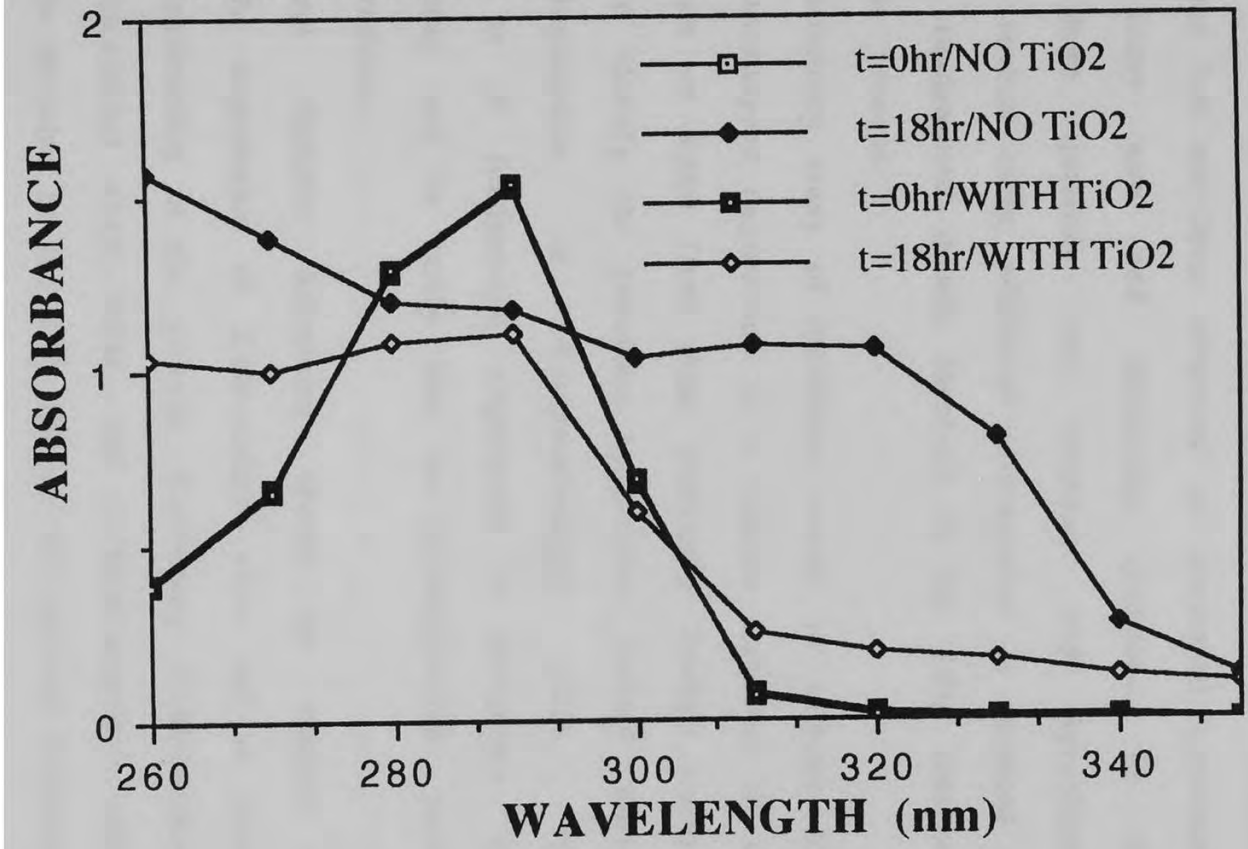

5. CONCLUSIONS.

In the three studies presented in this thesis, the role of TiO_2, in the photooxidative degradation of pollutants in an aqueous media, has been explored. These investigations also procured information that had not been observed or presented previously and raised many new and interesting questions. In this conclusion, these questions are carefully and specifically addressed. In several cases, additional investigation is required to elucidate the fundamental details involved in the TiO_2 catalyzed photooxidation process.

The preliminary study of haloethers seems to indicate that the TiO_2 photocatalyzed degradation is a feasible technique in the decontamination of water from these pollutants. Further research is required to identify the persistant by-product formed during the photodegradation of 4-bromodiphenyl ether. This identification is of fundamental importance to determine the reaction pathway and to verify that the decomposition yields innocuous products.

Additional aliphatic haloethers should be studied to compare to the degradation of 2-chloroethyl ether and to assess the general applicability of the process. Examining 2-chloroethoxy methane, 2-chloroethyl vinyl ether, and 2-chloroisopropyl ether, which are also included in the EPA list of 129 priority pollutants, is of great interest. Table XI shows the Octanol/Water Partition

Coefficient, K_{OW}, of these aliphatic ethers; establishing a correlation between these values and the initial rates of degradation would provide a measure of the significance of adsorption in the degradation process. A comparison between the Langmuir-Hinshelwood apparent kinetic parameters, k and K, and the K_{OW} of these compounds may provide insight as to the actual meaning of these parameters and be a useful tool for predicting the degradation rates of other pollutants by extrapolation.

TABLE XI. Aliphatic Haloethers Physical Constants.

Ether	H_2O Solubility (g/L)	K_{OW}	VaporPressure (torr at 20 °C)
2-chloroethoxy methane $(ClCH_2CH_2O)_2CH_2$	81.0 [56]	18.2 [37]	< 0.1 [41]
2-chloroethyl vinyl ether $ClCH_2CH_2OCH{=}CH_2$	15.0 [56]	19.0 [37]	26.75 [41]
2-chloroethyl ether $(ClCH_2CH_2)_2O$	10.2 [36]	38.0 [37]	0.71 [36]
2-chloroisopropyl ether $(ClCH_2(CH_3)CH)_2O$	1.70 [36]	380.2 [37]	0.85 [36]

In the study of substituent effects on the TiO_2 mediated photooxidation of ten different phenols, the data shows that the decay kinetics is consistent with the Langmuir-Hinshelwood (L-H) model. The compounds studied were phenol, *p*-methoxyphenol, *p*-

cresol, *p*-fluorophenol, *p*-chlorophenol, *p*-bromophenol, *p*-iodophenol, 4-hydroxyacetophenone, α,α,α-trifluoro-*p*-cresol, and *p*-cyanophenol. The relationship between Hammett constants and the apparent kinetic parameters strongly suggest that a number of competing reaction pathways are involved in the TiO_2 catalyzed photodegradation of *para*-substituted phenols. The correlation found among the halogenated phenols indicates that these compounds follow a similar reaction path which seems to be confirmed by the relationship found among their apparent adsorptivity constants, K, and the inductive effect of the substituent, $\sigma_{I(Grob)}$, as depicted in Figure XIII. This Hammett correlation appears as two intercepting lines indicating an abrupt change in mechanism, as discussed in the introduction. The non-halogenated appear to follow a different adsorption/reaction mechanism than the halophenols with respect to the inductive effect of their substituents.

Although a variety of substituents were employed, the changes in the L-H kinetic parameters, k and K, are surprisingly small. The y-intercept of the L-H plots, 1/k, and therefore, the apparent reactivity constants for the studied phenols, appear to be independent of the electronic influence of the substituent. The similarity among these parameters seems to support Turchi and Ollis claims that, for a given reactor, these disappearance rate constants are similar despite the different substrates studied.[8] While they suggest that k should be dependent on the type of

TiO_2 employed, comparison of their studies with our investigations using different TiO_2 showed similar y-intercepts (1/k), Figure X. This may be coincidental or suggest an independence of the degradation rate on the physical and electronic properties of the semiconductor.[8]

Ollis and Turchi have also suggested that the apparent adsorptivity constant, K, should be proportional to a second order homogeneous reaction rate constant ($k_{\bullet OH}$) for the two reacting species, the •OH and the organic substrate, and thus, a correlation between log $k_{\bullet OH}$ and log kK would be expected. On the other hand, K would reflect the adsorptivity properties of the substrate if it were adsorbed onto the semiconductor surface when it reacts with the hydroxyl radical.

Only a limited number of absolute rate constants, $k_{\bullet OH}$, were found in the literature (Table XII) for the reaction of hydroxyl radical with *para*-substituted phenols in a homogeneous aqueous media.

TABLE XII. Comparison of the Second Order Rate Constant, $k_{\bullet OH}$ (for the Reaction of •OH with Phenols in a Homogeneous Aqueous Media), the Experimentally Obtained L-H Kinetic Parameters (log kK), and Substituent Effects (σ) for *para*-Substituted Phenols.

Subst. X	$k_{\bullet OH}$ X 10^{-10} ($M^{-1}sec$)	log kK	σ [21]
H	1.8 [57]	-1.108	0.00
p-OCH_3	2.6 [58]	-1.305	-0.27
p-CH_3	1.2 [59]	-1.082	-0.17
p-Cl	7.6 [60]	-1.353	+0.23

Although a good correlation (R = 0.91)[52] between the relative rates of *para*-substituted phenols with •OH and σ has been reported, the limited correlation observed in Figure XX (R^2 = 0.52, R = 0.72) may be due to the fact that these $k_{\bullet OH}$ values were measured by different groups under different experimental conditions. Considering these factors, the correlation between the L-H kinetic parameter K, as log kK, and the second order hydroxyl radical rate constant, $k_{\bullet OH}$, appears quite good (R^2 = 0.79, R = 0.89) in Figure XXI.

FIGURE XX: Hammett correlation of the relative rate constants of the reaction of •OH with p-substituted phenols and the substituent effect in a homogeneous aqueous media.

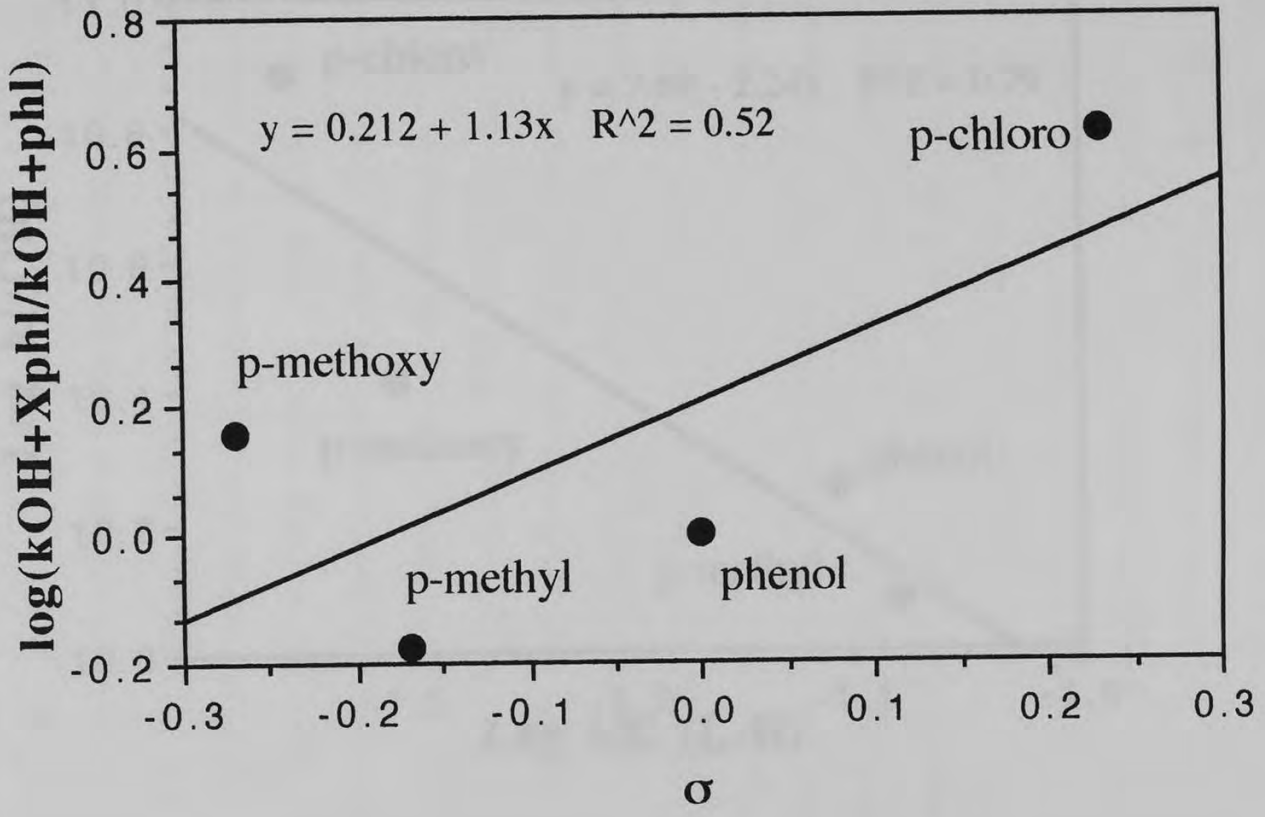

FIGURE XXI: Correlation between log k•OH (the absolute rate constant for the reaction of •OH with the corresponding phenol) and the experimentally obtained L-H kinetic parameters, log kK.

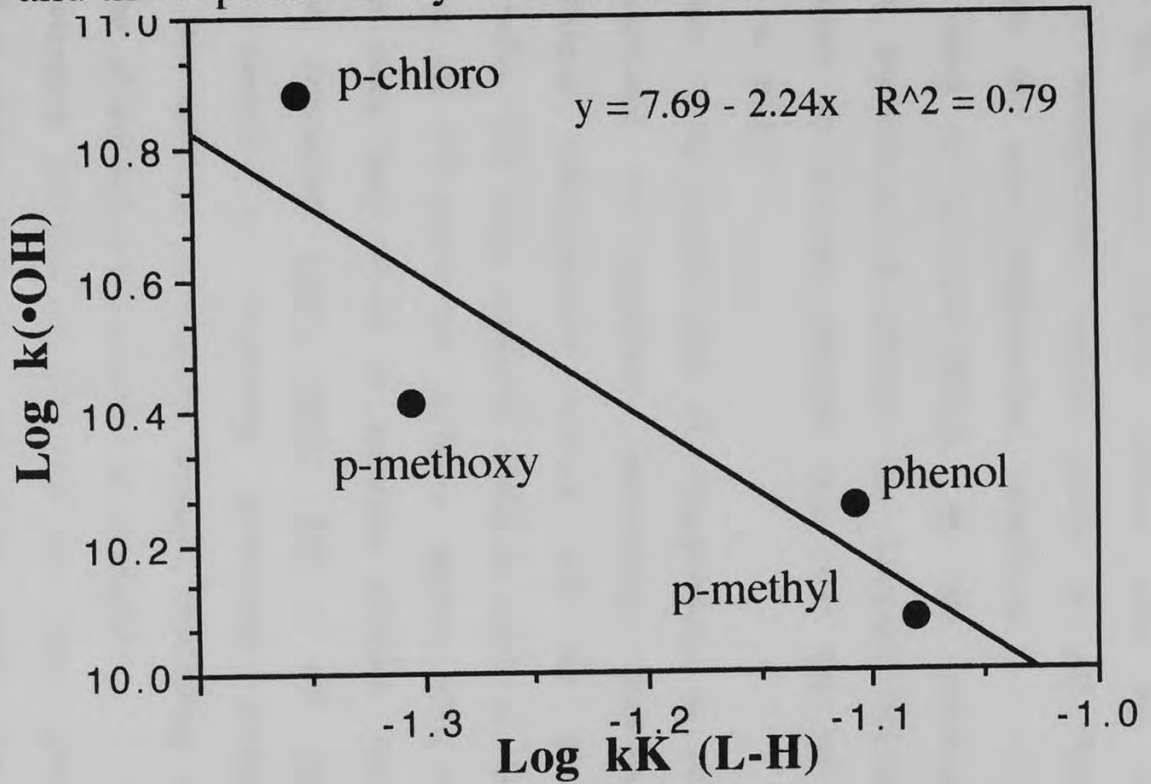

The correlation between the L-H kinetic parameters and the $k_{\bullet OH}$ seems to support the proposal and predictions raised by Ollis and Turchi[8] with regard to the generation and subsequent reaction of •OH. While our observations support the previous findings, more conclusive hypothesis could be drawn if the rate constants of the hydroxyl radical reaction with the studied phenols, in a homogeneous aqueous media at pH 3.0, are measured under the same experimental conditions.

In the study of the pH effects on the semiconductor photocatalyzed degradation of phenol, the Langmuir-Hinshelwood model also seems to fit the obtained data over the pH range examined, 1.0 to 13.7.

A decrease in the initial rates of disappearance at pH 11.0 has been attributed to repulsive interactions between the negatively charged semiconductor surface and the phenoxide species (pK_a 9.89). The same argument could be used to describe the decrease at pH 1.0 where the oxidative species, •OH, is less likely to form since there would be repulsion between the hole (h^+) and the protonated water (H_3O^+). Also at pH 1.0, the semiconductor surface is completely protonated causing a weakening in the substrate adsorption through H-bonding and a decrease in the photocatalyzed oxidation is expected.

The acceleration observed at pH 13.7 has been previously reported [21,27] in studies of phenol at pH values higher than 12.0 and has been attributed to the increased number of hydroxyl ions

at the semiconductor surface, but this effect should have been observed at pH 11.0 instead of the detected decrease. In a previous study of chlorobenzene,[24] an increase in initial rates of disappearance was also reported at pH values above 12.0 after remaining constant in the pH range of 6.0 to 11.0. We suggest the enhancement in the reaction is due to a new oxidizing species formed under very alkaline media, the unprotonated hydroxyl radical, $\bullet O^-$, pK_a = 11.8.[61] This species can react in a different manner to hydroxyl radical affecting the initial rates of disappearance. In a homogeneous aqueous media, this oxide radical ion generally reacts with organic substrates either by Eq. 25, Eq. 26, or both.[62,63]

$$\bullet O^- + R\text{-}H \longrightarrow {}^-OH + R\bullet \qquad (25)$$

and/or

$$\bullet O^- + R \longrightarrow O^{-2} + R\bullet^+ \qquad (26)$$

It has been reported that, in a homogeneous aqueous media, the reaction (Eq. 27) of the oxide radical ion with the phenoxide species has a rate constant, k, equal to 6.5 X 10^8 $M^{-1}sec.$[63,64]

$$\bullet O^- + C_6H_5O^- \xrightarrow{H_2O} {}^-OH + C_6H_5O\bullet \qquad (27)$$

which produces a species with no charge. If this reaction is occurring in the heterogeneous photocatalyzed process, the

electrostatic repulsion observed at pH 11.0 is not expected to occur at pH 13.7 and the phenoxide radical can interact with the semiconductor surface to greater extent or be degradated by reactions with other species in solution such as O_2.

Although the initial rates are accelerated at pH 13.7, the removal efficiency is significantly low compared to reactions carried out at lower pH values after four hours of irradiation. A possible explanation to this observation could be the competitive adsorption for active sites between the phenoxide and its products of degradation which may inhibit the initial reaction leading to its disappearance.[23] A decrease in the pH of the reaction mixture has been observed in the TiO_2 photocatalyzed oxidation of substrates, including phenols, which has been attributed to the formation of acidic by-products, such as carboxylic acids.[54] The reactions at pH 13.7 (2.0 N NaOH) are so alkaline, however, that no pH change is observed after 4 hours of light exposure and the carboxylate species produced may form strongly adsorbed complexes with the excited TiO_2 surface inhibiting adsorption of the phenoxide species thus reducing the extent of degradation.

Future studies should be pursued at different pH values on the effect of salts of dicarboxylic acids, such as oxalates (^-OOC-COO^-) and malonates (^-OOC-CH_2-COO^-), on the initial rates of TiO_2 catalyzed photodegradation of phenol, as well as on the overall removal efficiency. These dicarboxylates are expected by-

products in the oxidation of the aromatic moiety. These additional studies will help in the interpretation of our results and will help clarify the role of adsorption in the photocatalyzed heterogeneous reaction.

6. REFERENCES.

1) Legrini, O.; Oliveros, E.; Braun, A.M., *Chem. Rev.*, **1993**, *93*, 671.

2) Ollis, D.F.; Pelizzetti, E.; Serpone, N., *Env. Sci. Tech.*, **1991**, *25*, 1523.

3) Bockris, J. O'M.; Reddy, A.K.N., *Modern Electrochemistry*, Volume 2, Plenum Press, New York, N.Y., 1970.

4) Fox, M.A., *Topics in Current Chemistry*, Volume 142, Springer-Verlag, Berlin Heidelberg, 1987.

5) Fox, M.A., *Photochem. Photobiol.*, **1990**, *52*, 617.

6) Fox, M.A., *Acc. Chem. Res.*, **1983**, *16*, 314.

7) Fox, M.A., *Chemtech*, **1992**,

8) Turchi, G.S.; Ollis, D.F., *J. Catal.*, **1990**, *122*, 178.

9) Lawless, D.; Serpone, N.; Meisel, D., *J. Phys. Chem.*, **1991**, *95*, 5166.

10) Fox, M.A.; Draper, B.; Dulay, M.; O'Shea, K., *Photochemical Conversion and Storage of Solar Energy*, E. Pelizzetti, M. Schiavello (eds.), Kluger Academic Publishers, Netherlands, 1991.

11) Al-Ekabi, H.; de Mayo, P., *J. Phys. Chem.*, **1986**, *90*, 4075.

12) Al-Ekabi, H.; de Mayo, P., *Tetrahedron*, **1986**, *42*, 6277.

13) Gerischer, H.; Heller, A., *J. Electrochem. Soc.*, **1992**, *139*, 113.

14) Gerischer, H.; Heller, A., *J. Phys. Chem.*, **1991**, *95*, 5261.

15) Gonzalez-Elipe, A.R.; Munuera, G.; Soria, J., *J. Chem. Faraday Trans. I*, **1979**, *75*, 748.

16) Howe, R.F.; Grätzel, M., J. *Phys. Chem.*, **1987**, *91*, 3906.

17) Augugliaro, V.; Palmisano, L.; Sclafani, A.; Minero, C.; Pelizzetti, E., *Toxicol. Envir. Chem.*, **1988**, *16*, 89.

18) Hansch, C.; Leo, A.; Taft, R.W., *Chem. Rev.*, **1991**, *91*, 165.

19) Fox, M.A., *Tetrahedron Lett.*, **1983**, *24*, 547.

20) Lowry, T.H.; Richardson, K.S., *Mechanism and Theory in Organic Chemistry*, 2nd Ed., 130pp, Harper and Row Publications, New York, N.Y., 1981.

21) Ritchie, C.D.; Sager, W.F., *Prog. Phys. Org. Chem.*, **1964**, *2*, 323.

22) March, J., *Advance Organic Chemistry*, 4th Ed., 273pp, Wiley-Interscience Publications, New York, N.Y., 1992.

23) D'Oliviera, J.; Al-Sayyed, G.; Pichat, P., *Envir. Sci. Tech.*, **1990**, *24*, 990.

24) Sabin, F.; Türk, T.; Vogler, A., *J. Photochem. Photobiol. A: Chem.*, **1989**, *48*, 155.

25) Tanak, K.; Hisanga, T.; Harada, K., *J. Photochem. Photobiol. A: Chem.*, **1989**, *48*, 155.

26) Brown, G.T.; Darwent, J., *J. Phys. Chem.*, **1984**, *88*, 4955.

27) Rose, T.L.; Nanjundiah, C., *J. Phys. Chem.*, **1985**, *89*, 3766.

28) Harada, H.; Ueda, T.; Sakata, T., *J. Phys. Chem.*, **1989**, *93*, 1542.

29) Wei, A.P.; Wan, C., *Ind. Eng. Chem. Res.*, **1991**, *30*, 1293.

30) Davis, A.P.; Huang, C.P., *Ind. Eng. Chem. Res.*, **1989**, *21*, 455.

31) Tunesi, S.; Anderson, M., *J. Phys. Chem.*, **1991**, *95*, 3399.

32) Tseng, J.M.; Huang, C.P., *Wat. Sci. Tech.*, **1991**, *23*, 377.

33) Schackelford, W.M.; Keith, L.H., *Frequency of Organic Compounds Identified in Water*, U.S. EPA, EPA600/4-76-062, 617pp, Athens, Ga., 1976.

34) *IARC Monographs*, **1975**, *9*, 117.

35) Dorfman, L.M.; Adams, G.E., *Reactivity of Hydroxyl Radical in Aqueous Solutions*, NSRDS-NBS-46. NTIS:COM-73-50623. Springfield, Va., 1973.

36) Vershueren, K., *Handbook of Environmental Data on Organic Chemicals*, 657pp, Van Nostrand/Reinhold, New York, N.Y., 1977.

37) Leo, A.; Hansch, C.; Elkins, D., *Chem. Rev.*, **1971**, *71*, 525.

38) Dilling, W.L.; Tefertiller, N.B.: Kallos, G.J., *Envir. Sci. Tech.*, **1975**, *833*.

39) Branson, D.R., *Aquatic Toxicology and Hazard Evaluation.* ASTM Special Technical Publication, 634pp, F.L. Mayer, J.L. Hamelick (eds.), American Society for Testing and Materials, Philadelphia, Pa., 1977.

40) Branson, D.R., *Estimating the Hazard of Chemical Substances to Aquatic Life.* ASTM Special Technical Publication, 657pp, J.Cairns, K.L. Dickson, A.W. Maki (eds.), American Society for Testing and Materials, Philadelphia, Pa., 1978.

41) Dreisbach, R.R., *Pressure-Volume-Temperature Relationship of Organic Compounds*, 3rd Ed., 349pp, Handbook Publishers, Inc., Cleveland, Oh., 1952.

42) Dulin, D.; Drossman, H.; Mill, T., *Envir. Sci. Tech.*, **1986**, *20*, 72.

43) Calvert, J.; Pitts, J.N., *Photochemistry*, Wiley, New York, N.Y., 1966. Hatchard, G.C.; Parker, C.A., *Proc. Roy. Soc. A.*, **1953**, *220*, 104.

44) Rabek, J.F., *Experimental Methods in Photochemistry and Photophysics*, part 2, 943pp, Wiley-Interscience Publications, New York, N.Y., 1982.

45) D'Oliviera, J-C.; Minero, C.; Pelizzetti, E.; Pichat, P., *J. Photochem. Photobiol. A: Chem.*, **1993**, *72*, 261.

46) Milano, J.C.; Bernat-Escallon, C.; Vernet, J.L., *Envir. Tech. Lett.*, **1989**, *10*, 291.

47) Nickelson, M.G.; Cooper, W.J.; Kuricz, C.N.; Waite, T.D., *Envir. Sci. Tech.*, **1992**, *26*, 115.

48) Hoshika, Y.; Muto, G., *J. Chrom.*, **1979**, *179*, 105.

49) Serpone, N.; Pelizzetti, E., *Photocatalysis: Fundamentals and Applications*, Wiley, New York, N.Y., 1989.

50) Neta, P.; Madhavan, V.; Zemel, H.; Fessenden, R.W., *J.A.C.S.*, **1977**, *99*, 163.

51) Neta, P.; Dorfman, L.M., *Adv. Chem. Ser.*, **1968**, *81*, 222.

52) Savel'eva, O.S.; Shevchuk, L.G.; Vysotskaya, N.A., *J. Org. Chem. of the USSR.*, **1972**, *8*, 283.

53) Boule, P.; Guyon, C.; Tissot, A.; Lamaire, J., *Photochemistry of Environmental Aquatic Systems*, ACS Symposium Series, R.G. Zika, W.J. Cooper (eds.), 1987.

54) El-Ekabi, H.; Serpone, N.; Pelizzetti, E.; Minero, C.; Fox, M.A.; Draper, R.B., *Langmuir*, **1985**, *5*, 250.

55) Serpone, N.; Terzian, R.; Minero, C.; Pelizzetti, E., *Heterogeneous Photocatalyzed Oxidation, Photosensitive Metal-Organic Systems*, ACS, 1992.

56) Moriguchi, I., *Chem. Pharm. Bull.*, **1975**, *23*, 247.

57) Ebert, M.; Keene, J.P.; Swallow, A.J., *Pulse Radiolysis*, **1965**.

58) O'Neill, P.; Stinken, S., *Ber. Bundenges Phys. Chem.*, **1977**, *81*, 550.

59) Feitelson, J.; Hayon, E., *J. Phys. Chem.*, **1973**, *77*, 10.

60) Shetiya, R.S.; Raw, K.N., *Indian J. Chem.*, **1976**, *14a*, 575.

61) Rabani, J.; Matheson, M.S., *J. Phys. Chem.*, **1966**, *70*(8), 761. Weeks, J.L.; Rabani, J., *J. Phys. Chem.*, **1966**, *70*(7), 2100.

62) Neta, P.; Schuler, R.H., *J. Phys. Chem.*, **1975**, *79*, 1.

63) Neta, P.; Schuler, R.H., *Radiation Research*, **1975**, *64*, 233.

64) Neta, P.; Schuler, R.H., *J.A.C.S.*, **1975**, *97*, 912.

APPENDIX I.

ACTINOMETRIC PROCEDURE, CALIBRATION CURVE AND RESULTS.

Potassium ferrioxalate was employed as the actinometer because it is very sensitive over the wavelength range of 253.7 to 577 nm and it is easy to use. When a solution of potassium ferrioxalate is irradiated, the Fe^{+3} ions are reduced to Fe^{+2} as shown below [42]

$$[Fe^{+3}(C_2O_4)_3]^{-3} \longrightarrow [Fe^{+2}(C_2O_4)_2]^{-2} + C_2O_4^{-}$$

$$[Fe^{+3}(C_2O_4)_3]^{-3} + C_2O_4^{-} \longrightarrow [Fe^{+3}(C_2O_4)_3]^{-2} + (C_2O_4)^{-2}$$

$$[Fe^{+3}(C_2O_4)_3]^{-2} \longrightarrow [Fe^{+2}(C_2O_4)_2]^{-2} + 2CO_2$$

The product, Fe^{+2}, is measured spectrophotometrically as the red-colored complex with 1,10-phenanthroline.

PREPARATION OF A CALIBRATION CURVE. [41,42]

The following three standard solutions are required for the preparation of ten data points in the calibration curve and for the experimental measurements of the intensity of the lamp:

(Solution A.) A 0.1 M (± 0.2 mM) $FeSO_4$ solution, made with 0.1 M H_2SO_4, is diluted to 4 X 10^{-4} M with 0.1 N H_2SO_4.

(Solution B.) A 0.1 % by wt. 1,10-phenanthroline in deionized water. This solution need to be stored in the dark and kept for no longer than three months.

(Solution C.) A buffer prepared with 600 mL of a 1 N CH_3COONa, 360 mL of 1 N H_2SO_4 and diluted to one liter with deionized water.

Determined volumes of Solution A (0.0, 0.5, 1.0, 1.5, 2.0, 2.5, 3.0, 3.5, 4.0, 4.5, 5.0) were placed in eleven 25.0 mL volumetric flasks and enough 0.1 N H_2SO_4 was added to bring the total volume to 10.0 mL. Then, 2.0 mL of Solution B were added to each volumetric flask and Solution C was added up to the mark. The eleven flask were shaken and let to stand for an hour to allow the red-complex to form. The absorbance of each solution was measured at 510 nm in a 1 cm cell using as reference the blank (iron-free) solution. The calibration curve obtained is shown below.

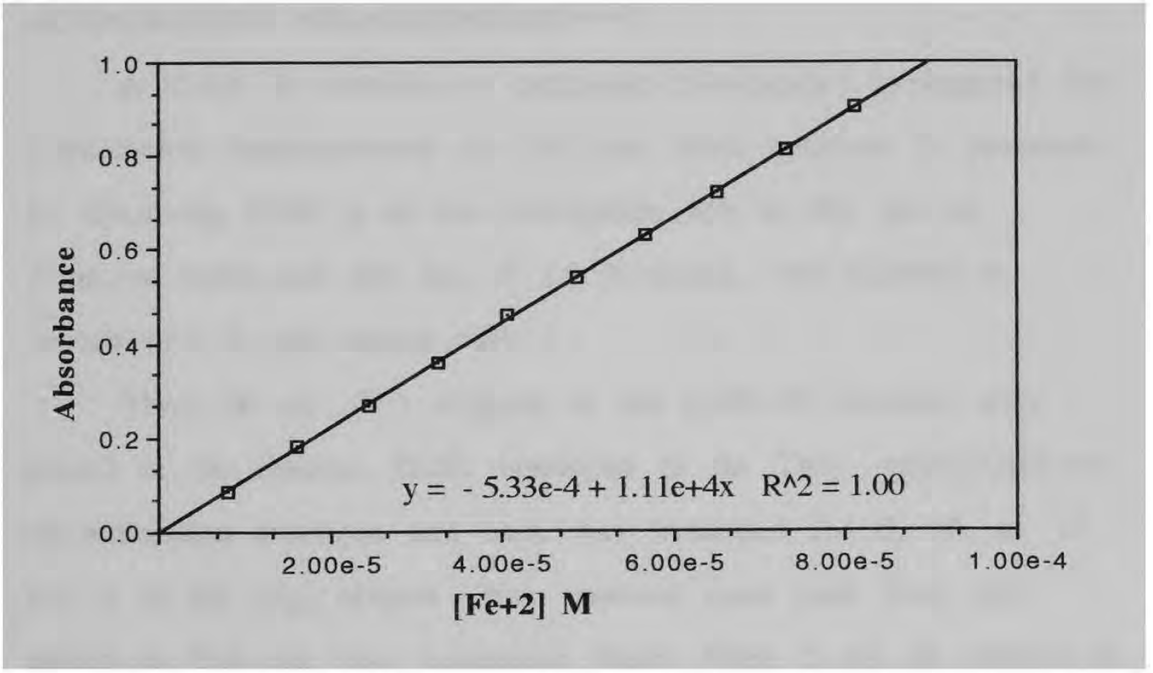

The molar extinction coefficient of the complex solution (slope of the calibration curve) should not differ greatly from ε=1.11 X 10^4 L/mole cm. [41] The procedure was carried out in the dark.

PREPARATION OF THE ACTINOMETER.[41,42]

The potassium ferrioxalate, $K_3Fe(C_2O_4)\cdot 3H_2O$, salt was prepared in a dark room by mixing equal volumes of 1.5 M $K_2C_2O_4$ and 1.5 $FeCl_3$ while stirring vigorously. The precipitate, $K_3Fe(C_2O_4)_3\cdot 3H_2O$, was recrystallized from warm water twice and allowed to dry in a desiccator. This salt can be stored in dark bottles for long periods of time.

ACTINOMETRIC MEASUREMENTS.[41,42]

A 0.006 M solution of potassium ferrioxalate is required for actinometric measurements at 350 nm. This solution is prepared by dissolving 2.947 g of the ferrioxalate salt in 800 mL of deionized water and 100 mL of 1.0 N H_2SO_4. The solution is diluted to 1 L and mixed well.

Three 50 mL (V_1) aliquots of the 0.006 M Solution were placed in the reactive flasks employed in the TiO_2 photocatalyzed decomposition reactions and each was irradiated for 5, 10, or 15 sec. A 10 mL (V_2) aliquot was removed from each flask and placed in 25.0 mL (V_3) volumetric flasks. Then, 2 mL of solution B and 5 mL of buffer B (calibrated pipettes) were added to each.

The solutions were diluted with deionized water to the mark of the volumetric flask (V_3). The solutions were well shaken and allowed to stand for an hour.

The number of moles of Fe^{+2} ($n_{Fe^{+2}}$) formed are calculated from Eq. I and the light intensity (I_0) incident just inside the photolysis flask is obtained from Eq. II.

$$n_{Fe^{+2}} = (6.023 \times 10^{20} V_1 V_3 A)/(V_2 l \varepsilon) \qquad (I)$$

$$I_0 = (n_{Fe^{+2}}) / (\Phi_\lambda t) \qquad (II)$$

Φ_λ is the quantum yield of the reaction at the corresponding wavelength employed in the irradiation. In this case, Φ_λ is 1.21 at a wavelength of 350 nm.[41] The absorbance of the solution (A) was measured at 510.00 nm and l, the path length of the spectrophotometer, was 1 cm. Under our experimental conditions, $I_0 = 7.88 \times 10^{17}$ photon/sec or $1.6 \pm 0.3 \times 10^{16}$ photon/sec cm^3 while the manufacture of the rayonet, The Southern New England Ultraviolet Company, reports approx. 1.5 to 5×10^{16} photon/sec mL.

APPENDIX II.

STANDARDIZATION CURVES OF THE STUDIED HALOETHERS.

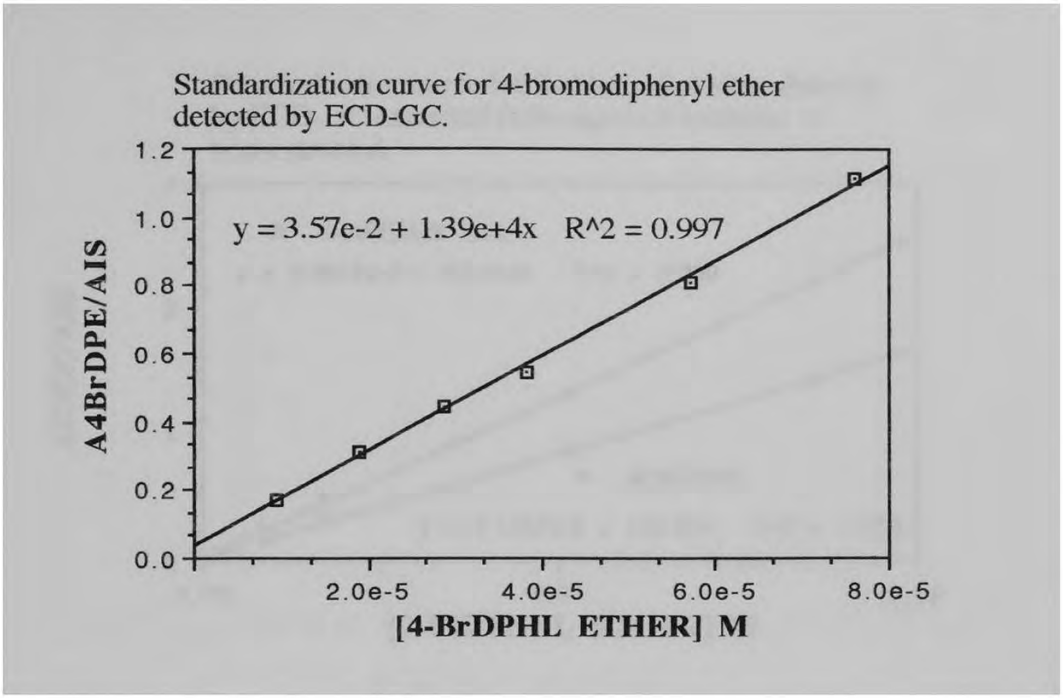
Standardization curve for 4-bromodiphenyl ether detected by ECD-GC.
y = 3.57e-2 + 1.39e+4x R^2 = 0.997
A4BrDPE/AIS
[4-BrDPHL ETHER] M
0.0
0.2
0.4
0.6
0.8
1.0
1.2
2.0e-5
4.0e-5
6.0e-5
8.0e-5

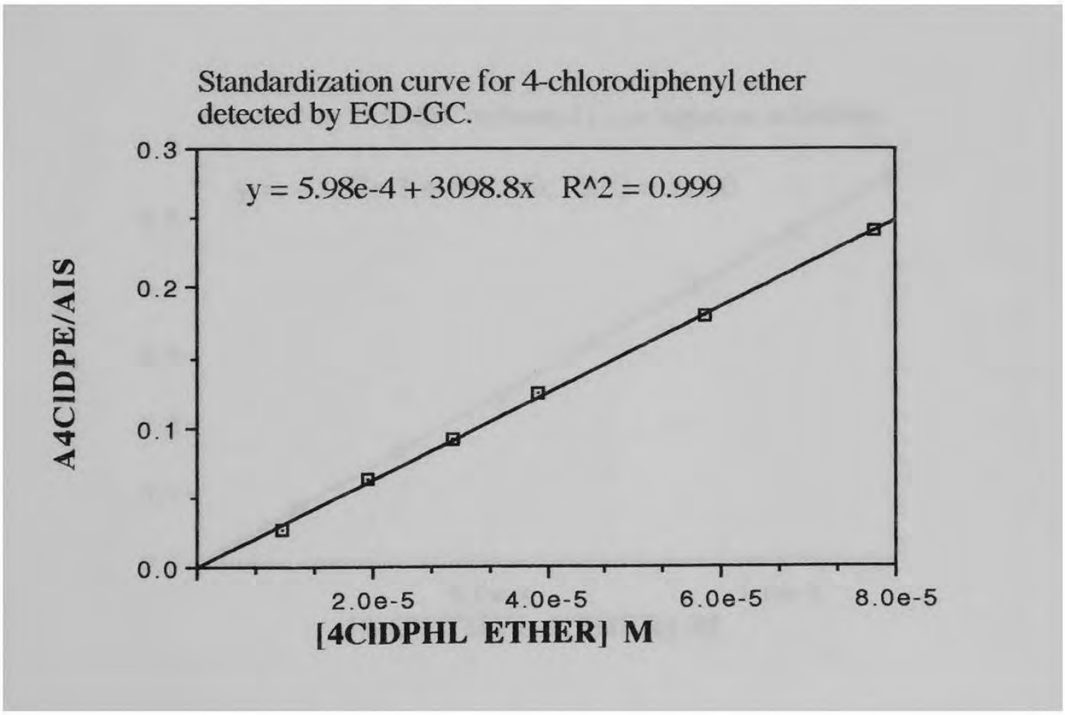
Standardization curve for 4-chlorodiphenyl ether detected by ECD-GC.
y = 5.98e-4 + 3098.8x R^2 = 0.999
A4ClDPE/AIS
[4ClDPHL ETHER] M
0.0
0.1
0.2
0.3
2.0e-5
4.0e-5
6.0e-5
8.0e-5

Standardization curve for 2-chloroethyl ether detected by ECD-GC extracted from aqueous solutions vs non-extracted.

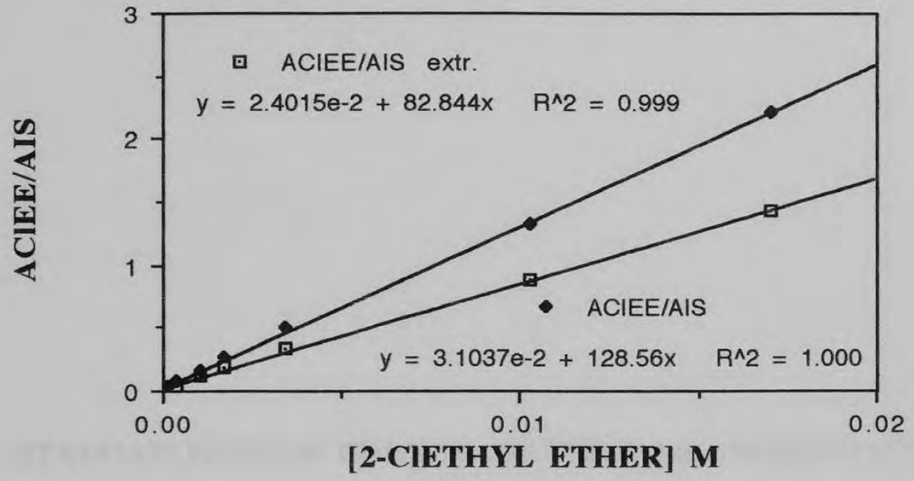

Standardization curve for 2-chloroethyl ether detected by FID-GC extracted from aqueous solutions.

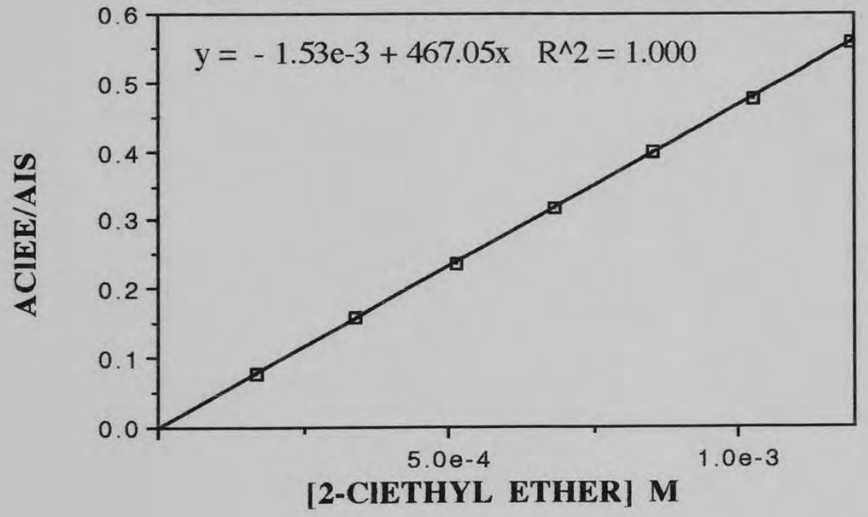

APPENDIX III.

STANDARDIZATION CURVES OF THE *PARA*-SUBSTITUTED PHENOLS STUDIED.

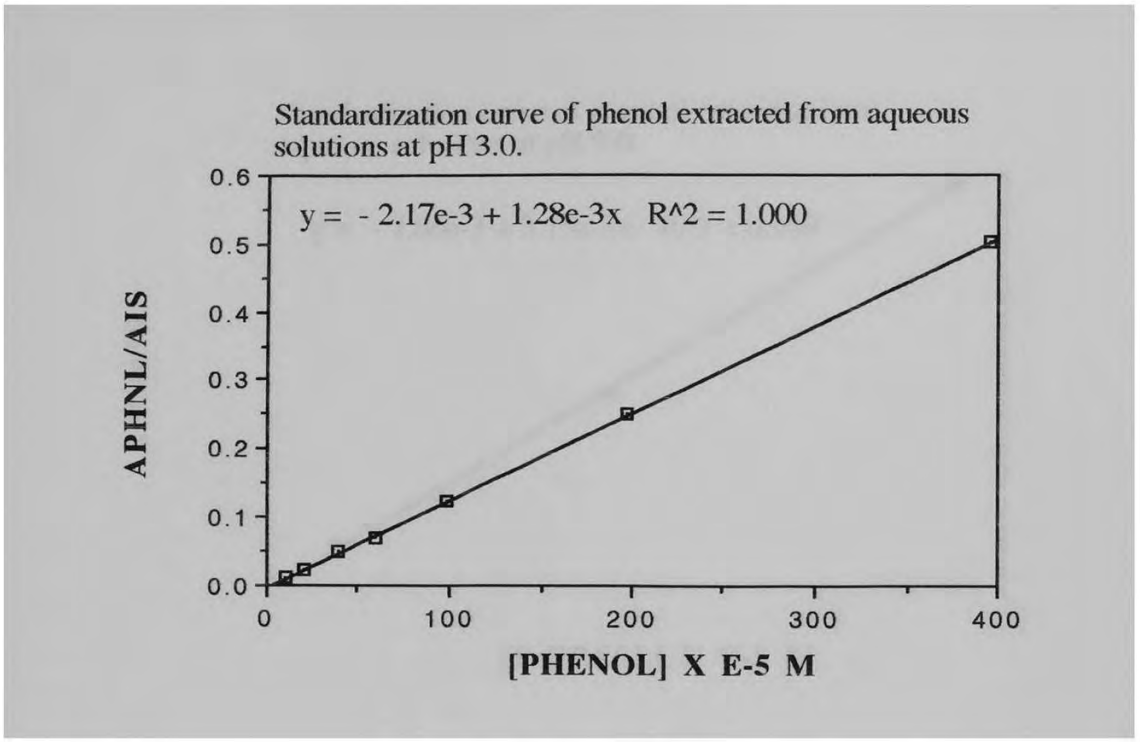
Standardization curve of phenol extracted from aqueous solutions at pH 3.0.
y = - 2.17e-3 + 1.28e-3x R^2 = 1.000
APHNL/AIS
0.6
0.5
0.4
0.3
0.2
0.1
0.0
0
100
200
300
400
[PHENOL] X E-5 M

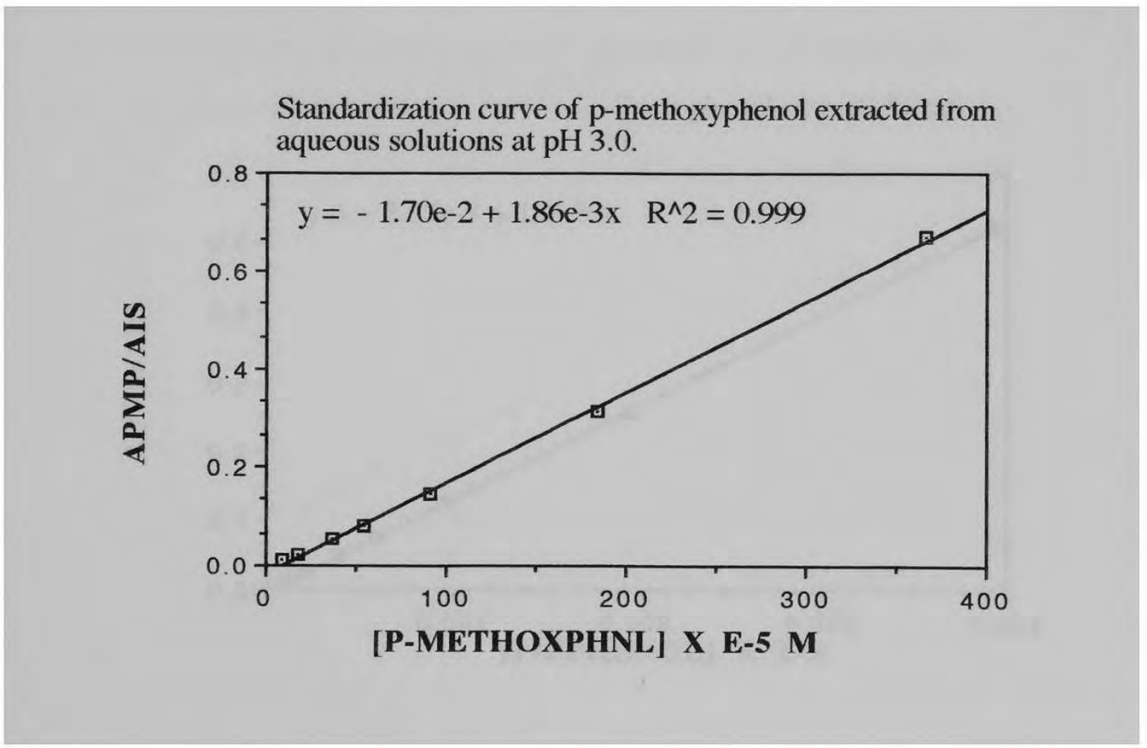
Standardization curve of p-methoxyphenol extracted from aqueous solutions at pH 3.0.
y = - 1.70e-2 + 1.86e-3x R^2 = 0.999
APMP/AIS
0.8
0.6
0.4
0.2
0.0
0
100
200
300
400
[P-METHOXPHNL] X E-5 M

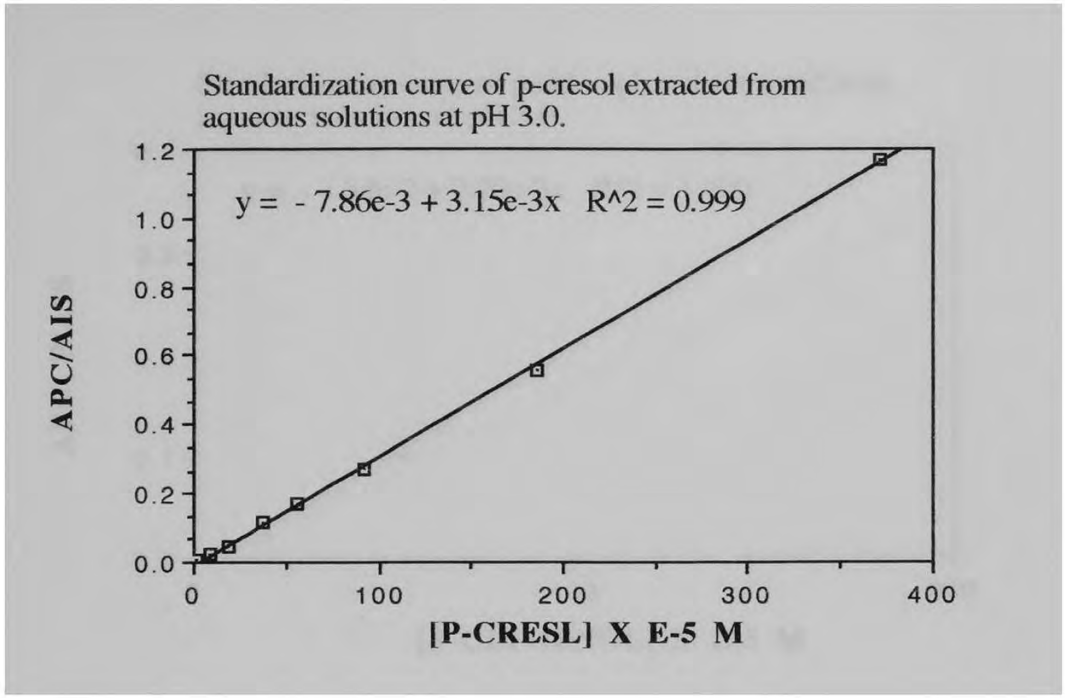
Standardization curve of p-cresol extracted from aqueous solutions at pH 3.0.
y = - 7.86e-3 + 3.15e-3x R^2 = 0.999
APC/AIS
1.2
1.0
0.8
0.6
0.4
0.2
0.0
0
100
200
300
400
[P-CRESL] X E-5 M

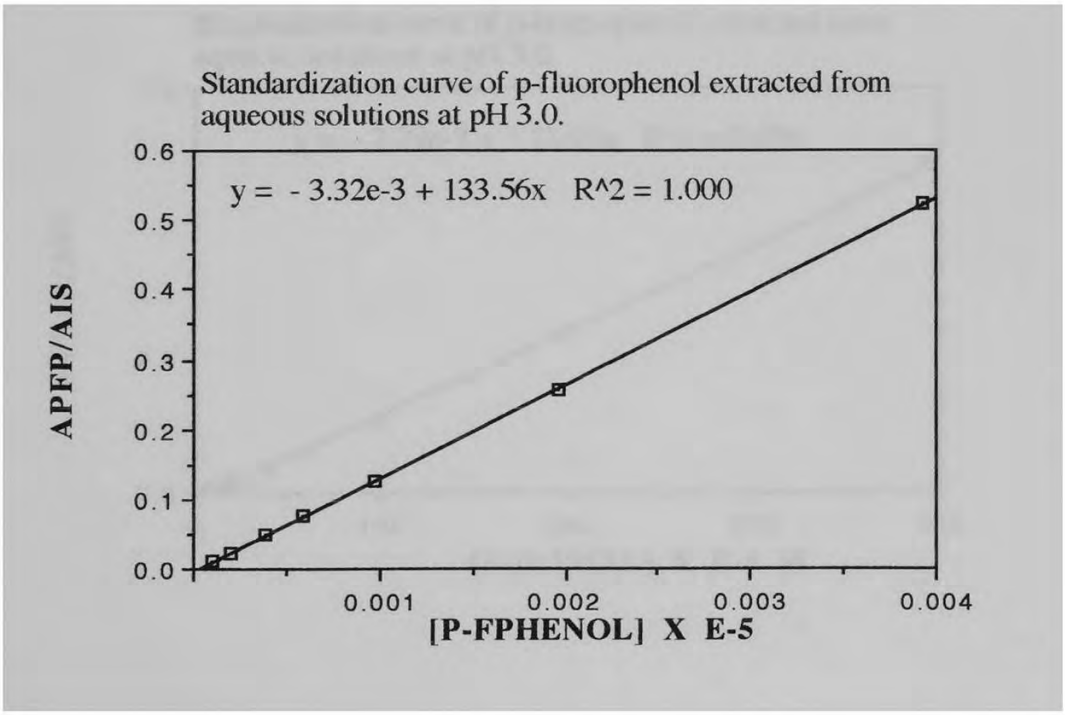
Standardization curve of p-fluorophenol extracted from aqueous solutions at pH 3.0.
y = - 3.32e-3 + 133.56x R^2 = 1.000
APFP/AIS
0.6
0.5
0.4
0.3
0.2
0.1
0.0
0.001
0.002
0.003
0.004
[P-FPHENOL] X E-5

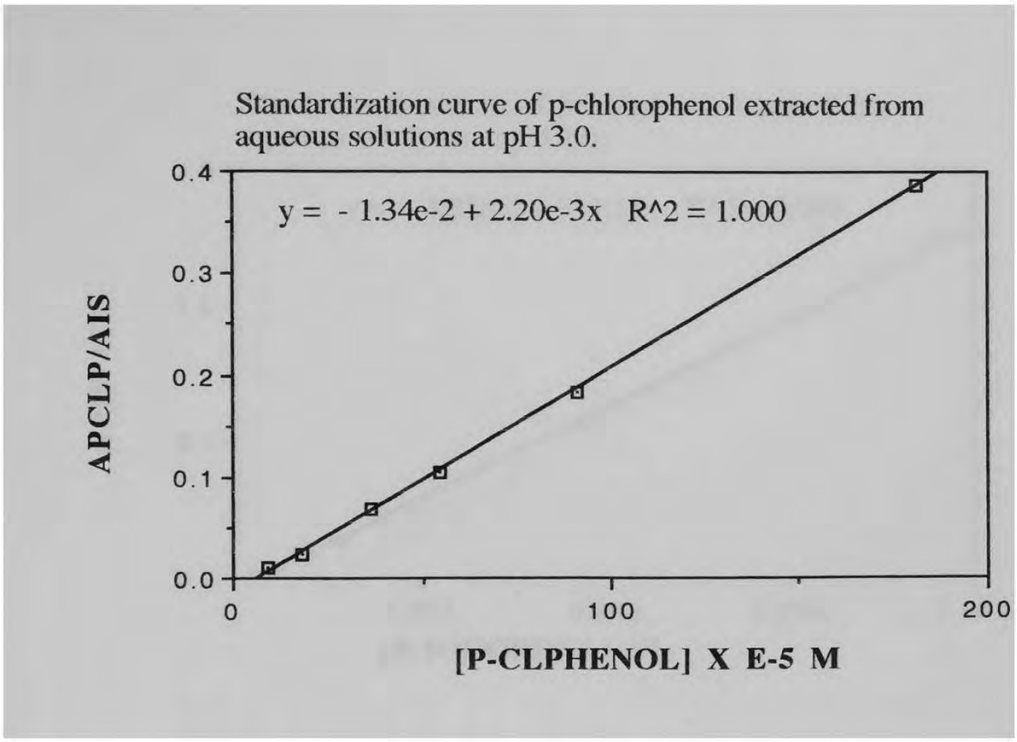
Standardization curve of p-chlorophenol extracted from aqueous solutions at pH 3.0.
y = - 1.34e-2 + 2.20e-3x R^2 = 1.000
APCLP/AIS
0.4
0.3
0.2
0.1
0.0
0
100
200
[P-CLPHENOL] X E-5 M

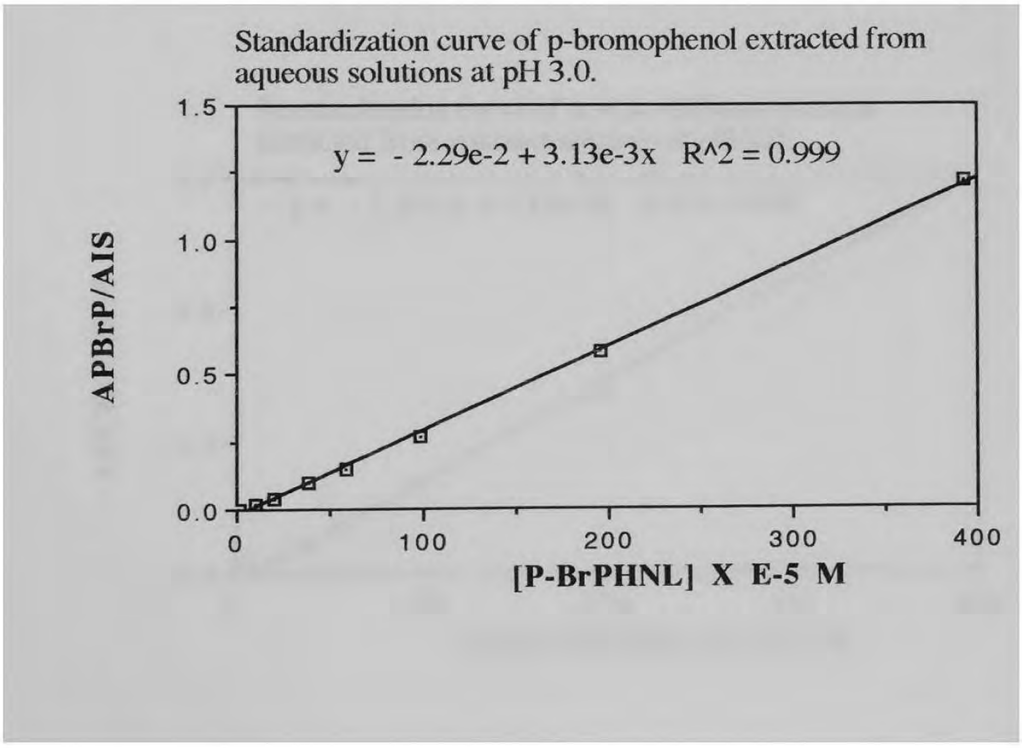
Standardization curve of p-bromophenol extracted from aqueous solutions at pH 3.0.
y = - 2.29e-2 + 3.13e-3x R^2 = 0.999
APBrP/AIS
1.5
1.0
0.5
0.0
0
100
200
300
400
[P-BrPHNL] X E-5 M

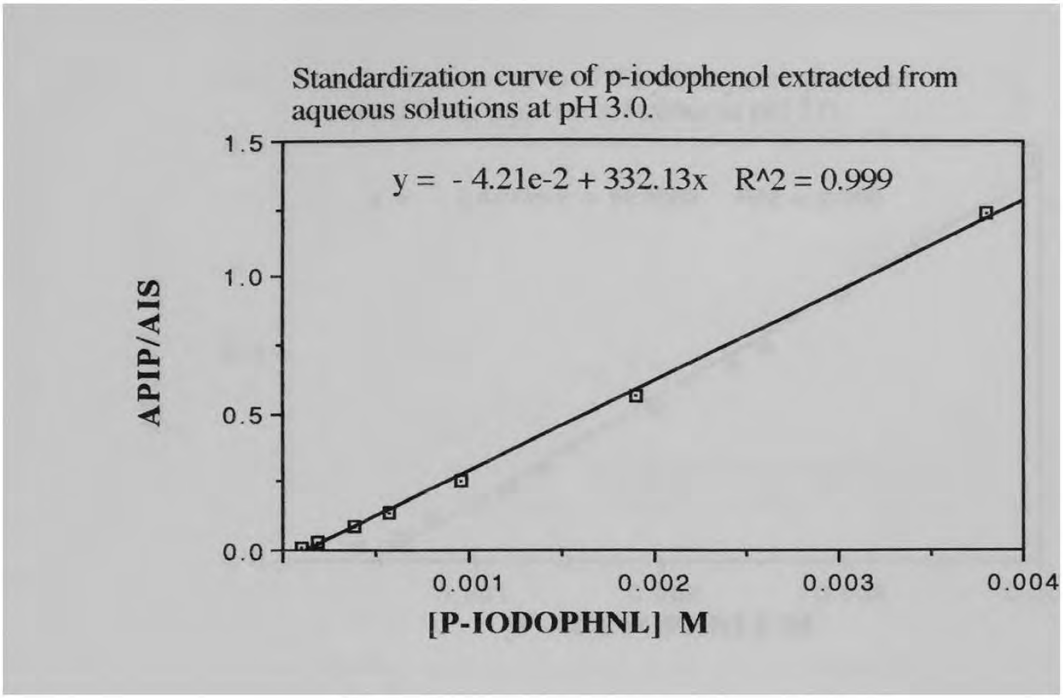
Standardization curve of p-iodophenol extracted from aqueous solutions at pH 3.0.
y = - 4.21e-2 + 332.13x R^2 = 0.999
APIP/AIS
1.5
1.0
0.5
0.0
0.001
0.002
0.003
0.004
[P-IODOPHNL] M

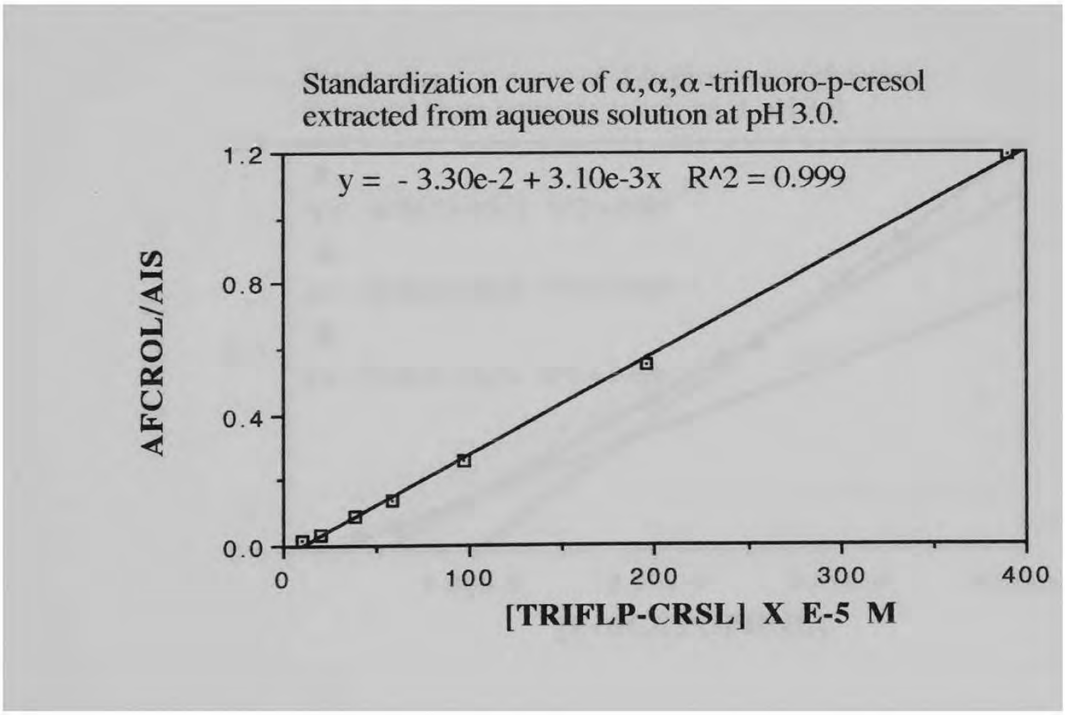
Standardization curve of α,α,α-trifluoro-p-cresol extracted from aqueous solution at pH 3.0.
y = - 3.30e-2 + 3.10e-3x R^2 = 0.999
AFCROL/AIS
1.2
0.8
0.4
0.0
0
100
200
300
400
[TRIFLP-CRSL] X E-5 M

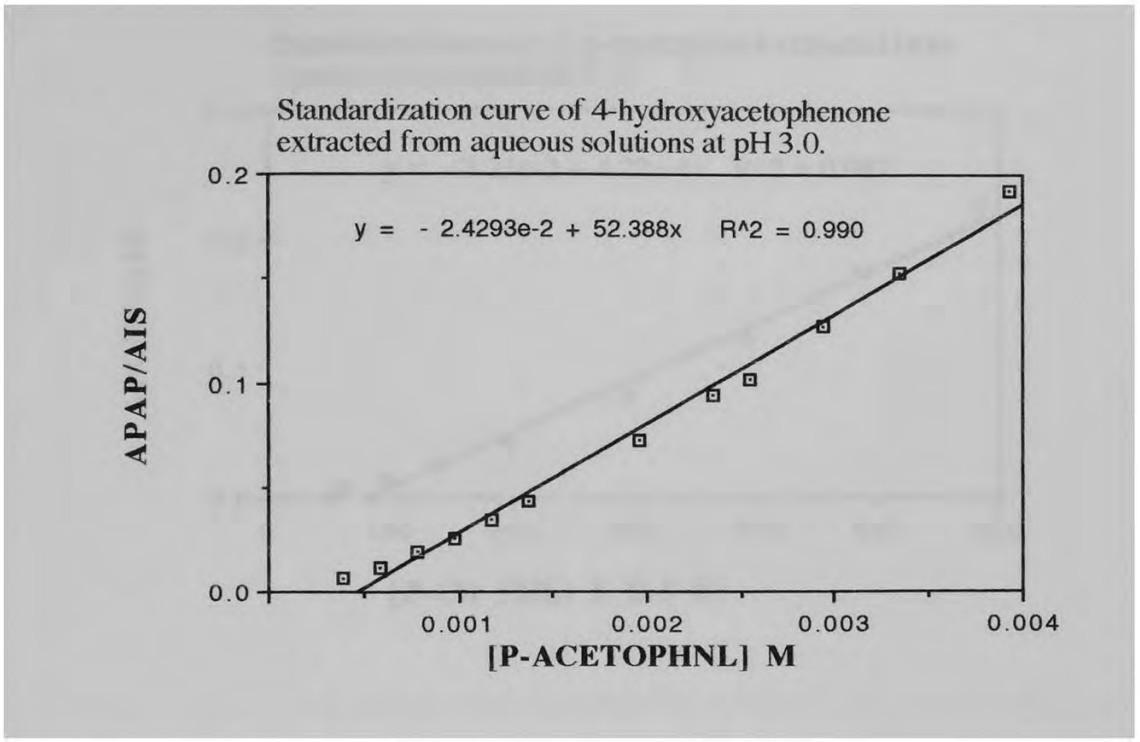
Standardization curve of 4-hydroxyacetophenone
extracted from aqueous solutions at pH 3.0.
y = - 2.4293e-2 + 52.388x R^2 = 0.990
APAP/AIS
0.2
0.1
0.0
0.001
0.002
0.003
0.004
[P-ACETOPHNL] M

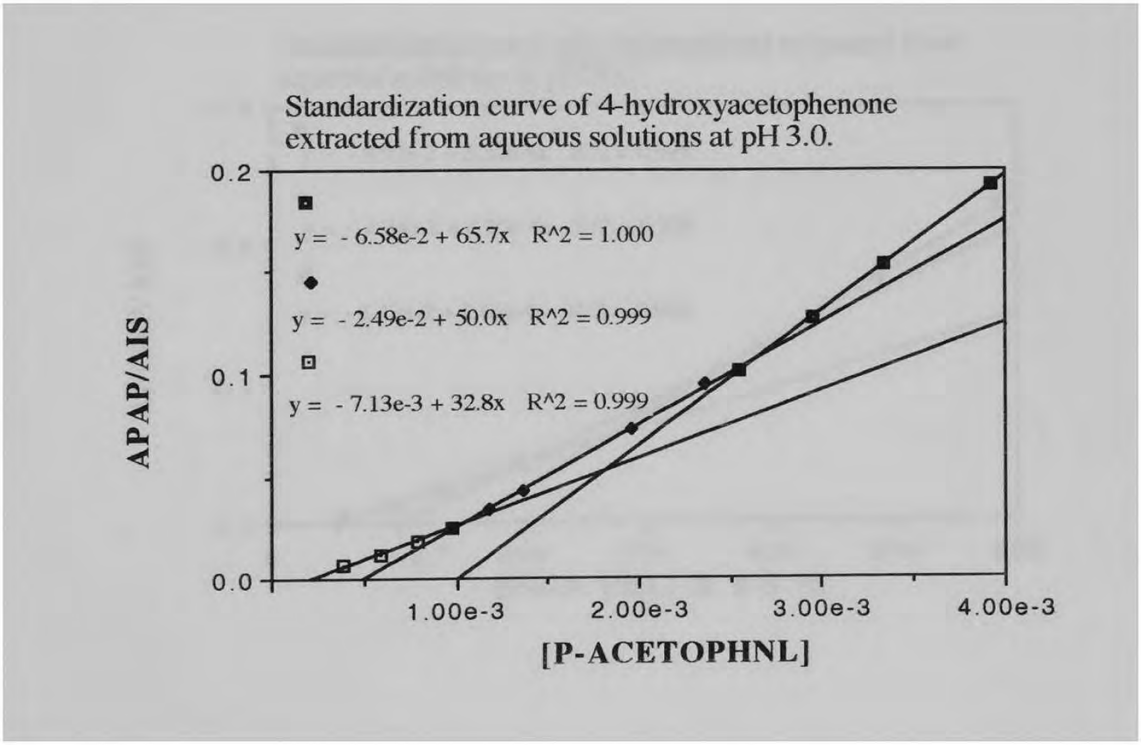
Standardization curve of 4-hydroxyacetophenone
extracted from aqueous solutions at pH 3.0.
y = - 6.58e-2 + 65.7x R^2 = 1.000
y = - 2.49e-2 + 50.0x R^2 = 0.999
y = - 7.13e-3 + 32.8x R^2 = 0.999
APAP/AIS
0.2
0.1
0.0
1.00e-3
2.00e-3
3.00e-3
4.00e-3
[P-ACETOPHNL]

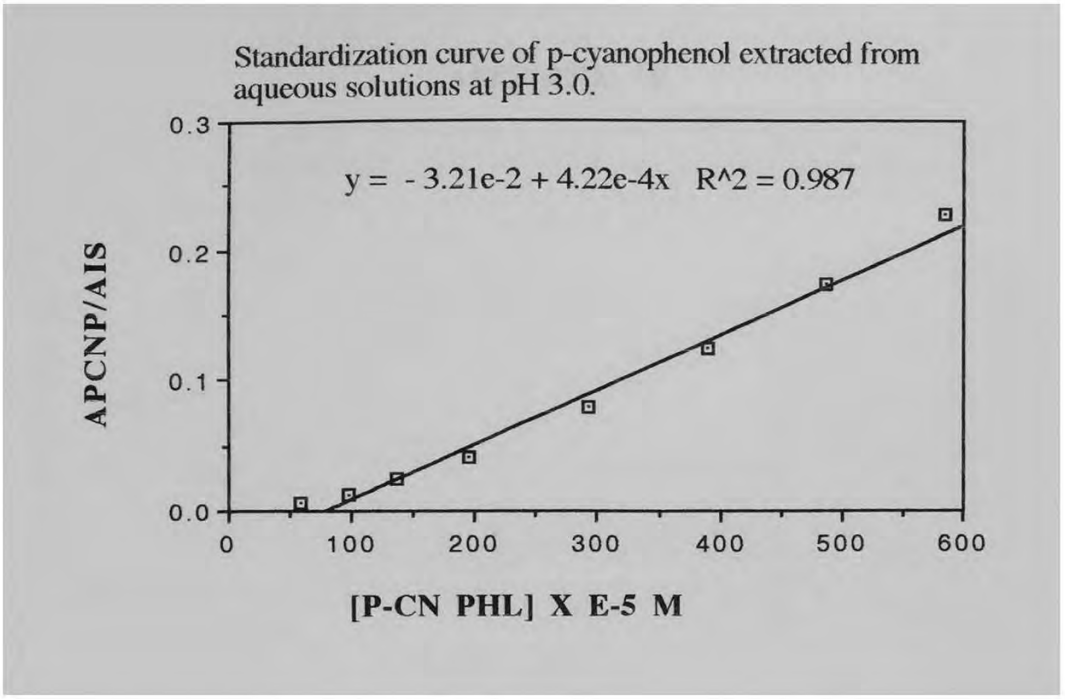
Standardization curve of p-cyanophenol extracted from aqueous solutions at pH 3.0.
y = - 3.21e-2 + 4.22e-4x R^2 = 0.987
APCNP/AIS
0.3
0.2
0.1
0.0
0
100
200
300
400
500
600
[P-CN PHL] X E-5 M

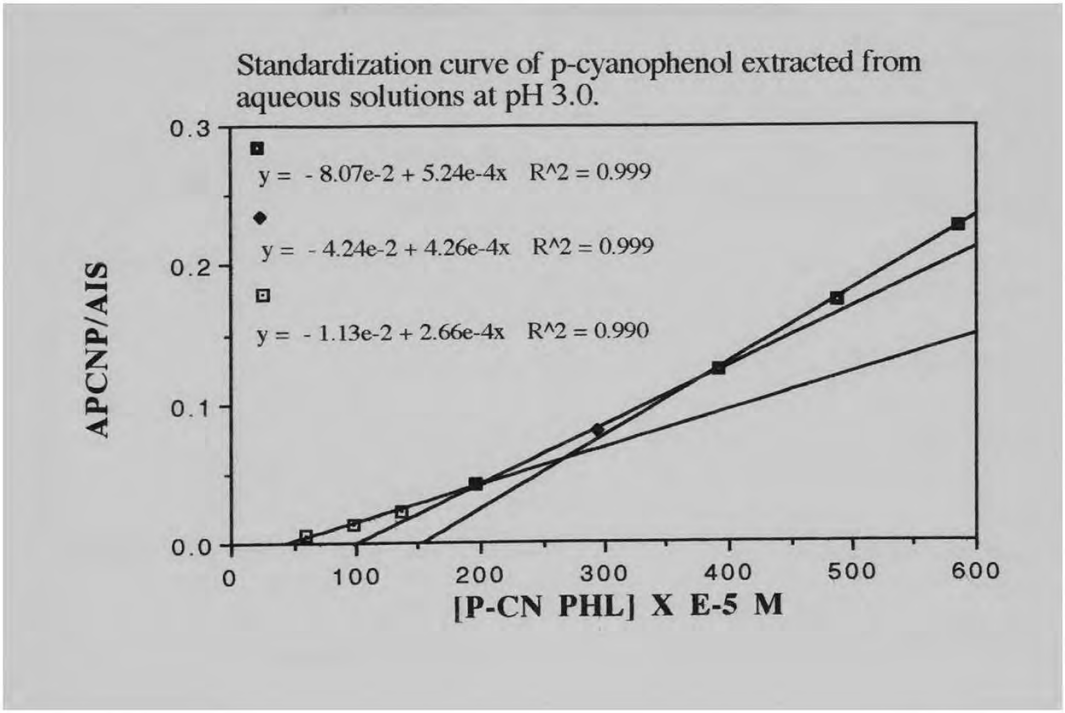
Standardization curve of p-cyanophenol extracted from aqueous solutions at pH 3.0.
y = - 8.07e-2 + 5.24e-4x R^2 = 0.999
y = - 4.24e-2 + 4.26e-4x R^2 = 0.999
y = - 1.13e-2 + 2.66e-4x R^2 = 0.990
APCNP/AIS
0.3
0.2
0.1
0.0
0
100
200
300
400
500
600
[P-CN PHL] X E-5 M

APPENDIX IV.

INITIAL RATES OF DISAPPEARANCE OF THE PHENOLS STUDIED AT DIFFERENT CONCENTRATIONS.

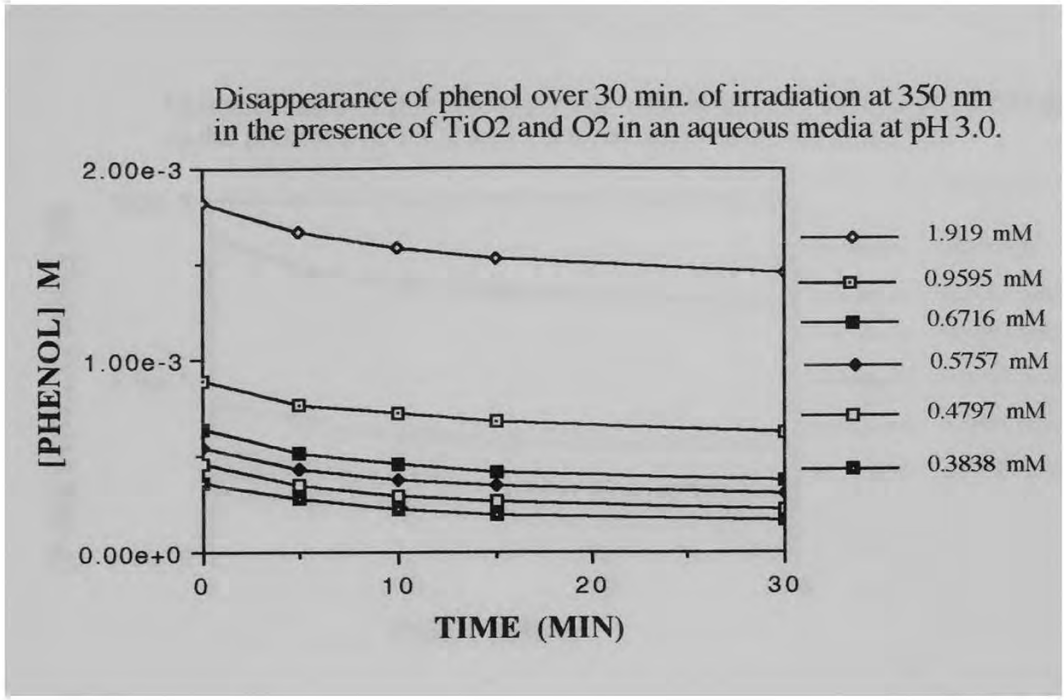
Disappearance of phenol over 30 min. of irradiation at 350 nm
in the presence of TiO2 and O2 in an aqueous media at pH 3.0.
2.00e-3
1.00e-3
0.00e+0
[PHENOL] M
0
10
20
30
TIME (MIN)
1.919 mM
0.9595 mM
0.6716 mM
0.5757 mM
0.4797 mM
0.3838 mM

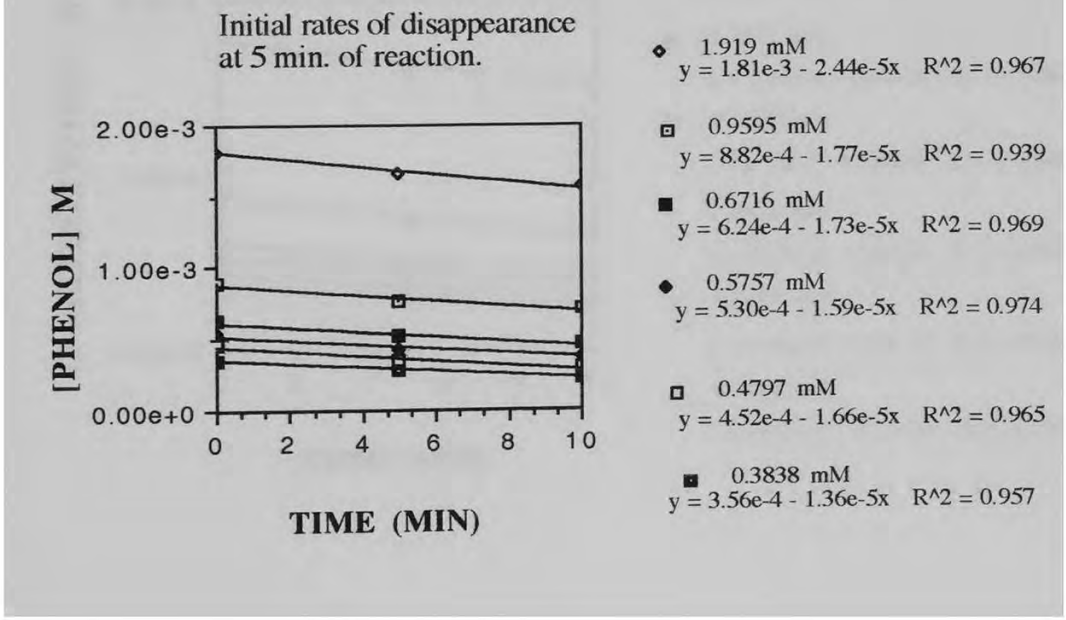
Initial rates of disappearance
at 5 min. of reaction.
2.00e-3
1.00e-3
0.00e+0
[PHENOL] M
0
2
4
6
8
10
TIME (MIN)
1.919 mM
y = 1.81e-3 - 2.44e-5x R^2 = 0.967
0.9595 mM
y = 8.82e-4 - 1.77e-5x R^2 = 0.939
0.6716 mM
y = 6.24e-4 - 1.73e-5x R^2 = 0.969
0.5757 mM
y = 5.30e-4 - 1.59e-5x R^2 = 0.974
0.4797 mM
y = 4.52e-4 - 1.66e-5x R^2 = 0.965
0.3838 mM
y = 3.56e-4 - 1.36e-5x R^2 = 0.957

Disappearance of p-methoxyphenol over 30 min. of irradiation at 350 nm in the presence of TiO2 and O2 in an aqueous media at pH 3.0.

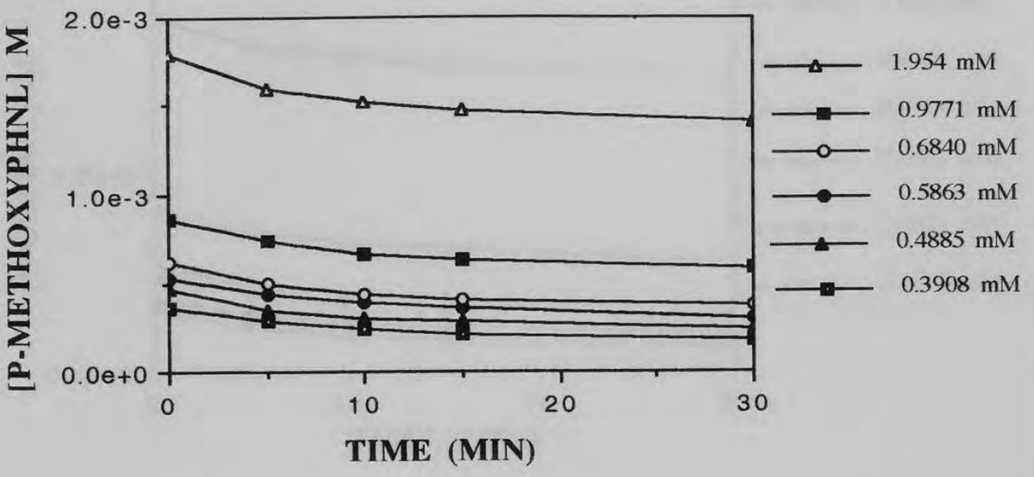

Initial rates of disappearance at 5 min. of reaction.

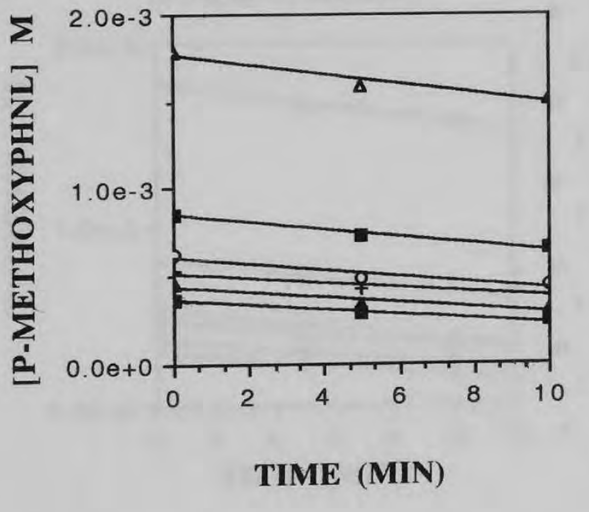

△ 1.954 mM
y = 1.76e-3 - 2.70e-5x R^2 = 0.927

■ 0.9771 mM
y = 8.53e-4 - 2.06e-5x R^2 = 0.984

○ 0.6840 mM
y = 6.08e-4 - 1.78e-5x R^2 = 0.943

+ 0.5863 mM
y = 5.18e-4 - 1.38e-5x R^2 = 0.950

▲ 0.4885 mM
y = 4.46e-4 - 1.55e-5x R^2 = 0.917

▣ 0.3908 mM
y = 3.59e-4 - 1.23e-5x R^2 = 0.957

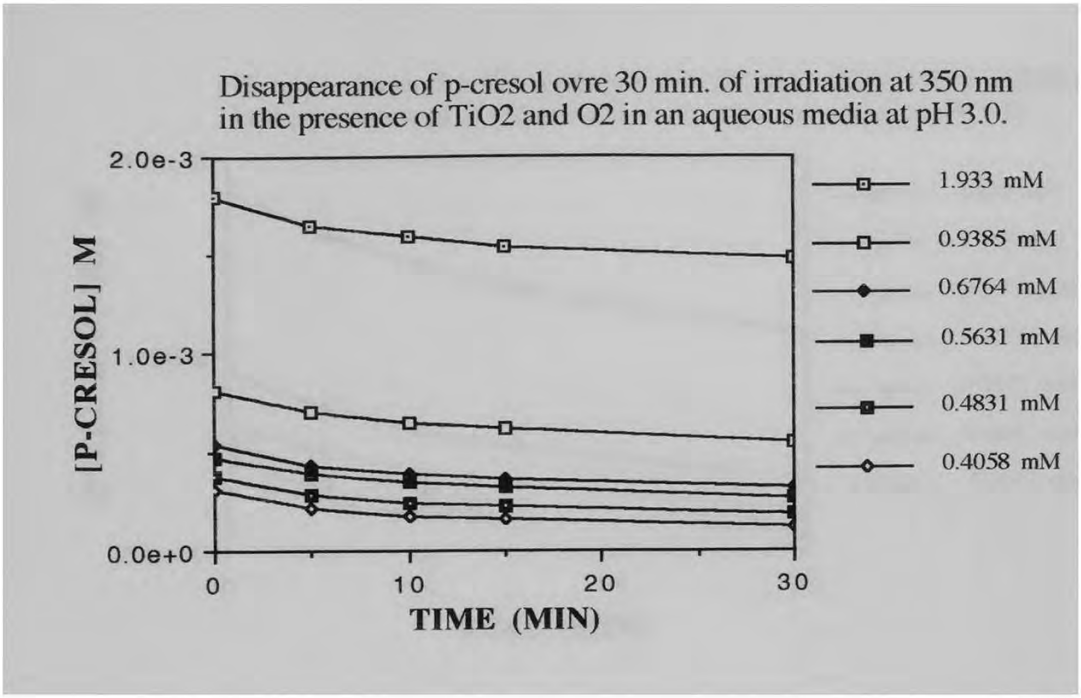
Disappearance of p-cresol ovre 30 min. of irradiation at 350 nm
in the presence of TiO2 and O2 in an aqueous media at pH 3.0.
[P-CRESOL] M
2.0e-3
1.0e-3
0.0e+0
0
10
20
30
TIME (MIN)
1.933 mM
0.9385 mM
0.6764 mM
0.5631 mM
0.4831 mM
0.4058 mM

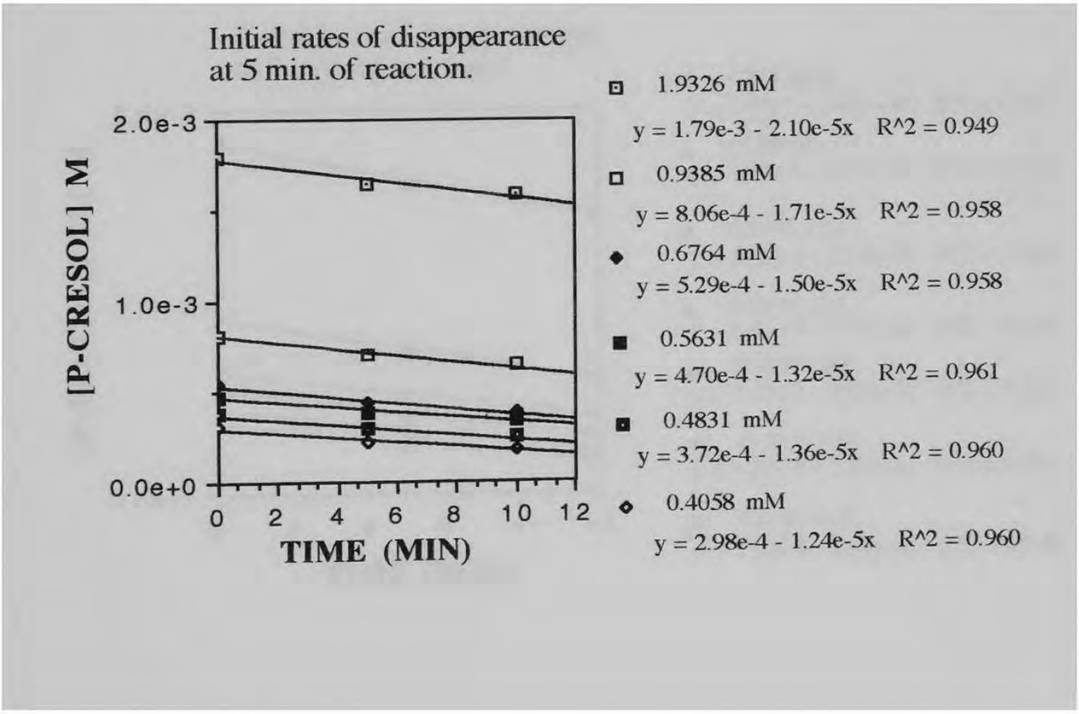
Initial rates of disappearance
at 5 min. of reaction.
[P-CRESOL] M
2.0e-3
1.0e-3
0.0e+0
0
2
4
6
8
10
12
TIME (MIN)
1.9326 mM
y = 1.79e-3 - 2.10e-5x R^2 = 0.949
0.9385 mM
y = 8.06e-4 - 1.71e-5x R^2 = 0.958
0.6764 mM
y = 5.29e-4 - 1.50e-5x R^2 = 0.958
0.5631 mM
y = 4.70e-4 - 1.32e-5x R^2 = 0.961
0.4831 mM
y = 3.72e-4 - 1.36e-5x R^2 = 0.960
0.4058 mM
y = 2.98e-4 - 1.24e-5x R^2 = 0.960

Disappearance of p-fluorophenol over 30 min. of irradiation at 350 nm in the presence of TiO2 and O2 in an aqueous media at pH 3.0.

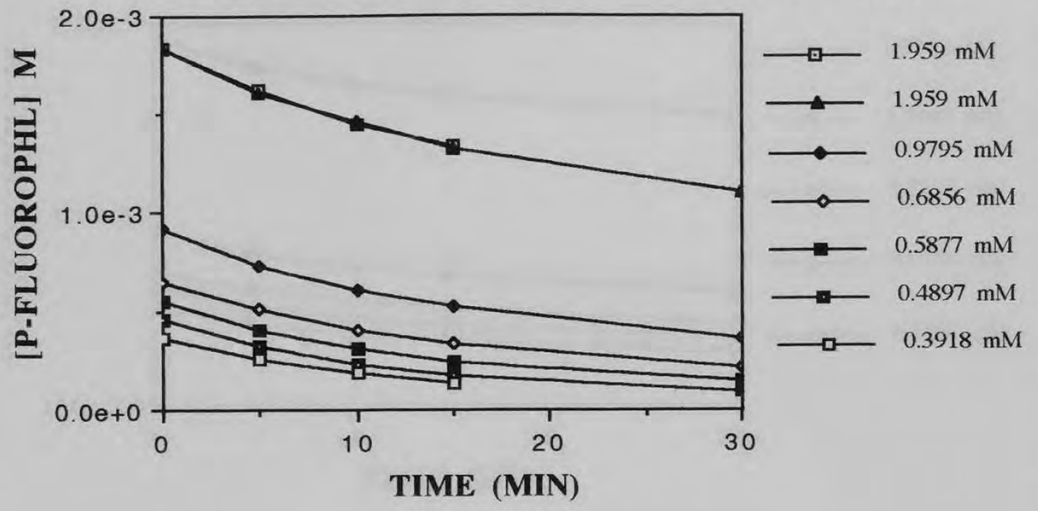

Initial rates of disappearance at 5 min. of reaction.

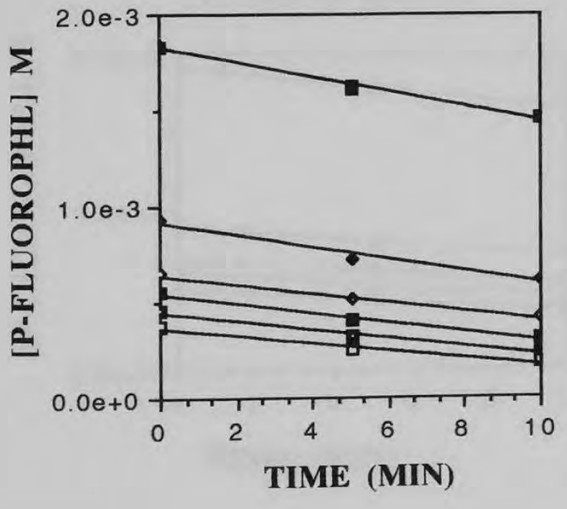

1.959 mM
y = 1.83e-3 - 3.81e-5x R^2 = 0.997

1.959 mM
y = 1.83e-3 - 3.83e-5x R^2 = 0.981

0.9795 mM
y = 9.11e-4 - 3.14e-5x R^2 = 0.980

0.6856 mM
y = 6.41e-4 - 2.37e-5x R^2 = 0.989

0.5877 mM
y = 5.48e-4 - 2.49e-5x R^2 = 0.991

0.4897 mM
y = 4.50e-4 - 2.28e-5x R^2 = 0.981

0.3918 mM
y = 3.63e-4 - 1.86e-5x R^2 = 0.978

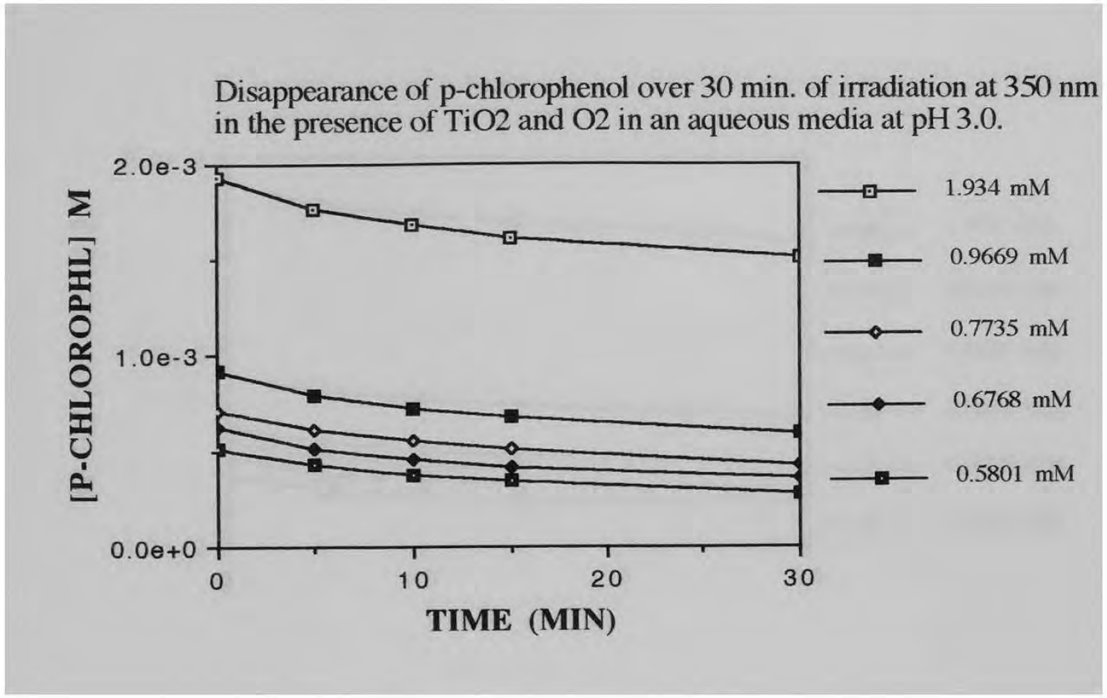
Disappearance of p-chlorophenol over 30 min. of irradiation at 350 nm in the presence of TiO2 and O2 in an aqueous media at pH 3.0.
[P-CHLOROPHL] M
2.0e-3
1.0e-3
0.0e+0
0
10
20
30
TIME (MIN)
1.934 mM
0.9669 mM
0.7735 mM
0.6768 mM
0.5801 mM

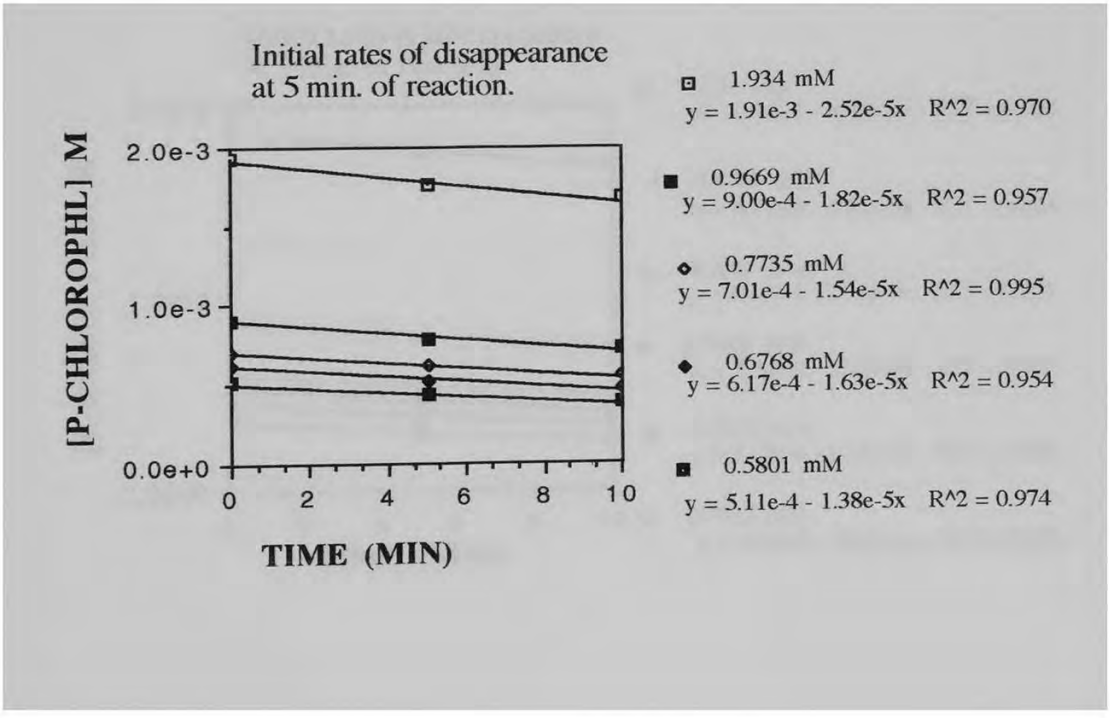
Initial rates of disappearance at 5 min. of reaction.
[P-CHLOROPHL] M
2.0e-3
1.0e-3
0.0e+0
0
2
4
6
8
10
TIME (MIN)
1.934 mM
y = 1.91e-3 - 2.52e-5x R^2 = 0.970
0.9669 mM
y = 9.00e-4 - 1.82e-5x R^2 = 0.957
0.7735 mM
y = 7.01e-4 - 1.54e-5x R^2 = 0.995
0.6768 mM
y = 6.17e-4 - 1.63e-5x R^2 = 0.954
0.5801 mM
y = 5.11e-4 - 1.38e-5x R^2 = 0.974

Disappearance of p-bromophenol over 30 min. of irradiation at 350 nm in the presence of TiO2 and O2 in an aqueous media at pH 3.0.

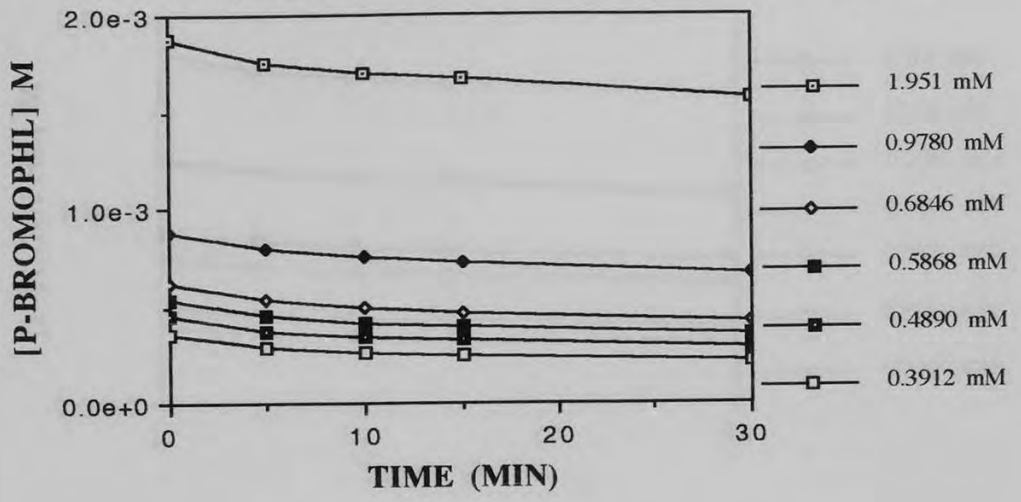

Initial rates of disappearance at 5 min. of reaction.

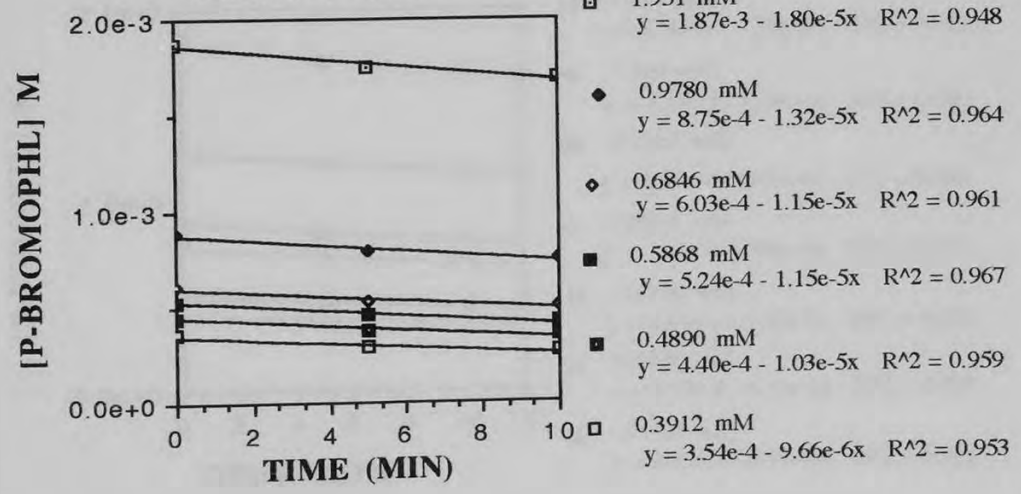

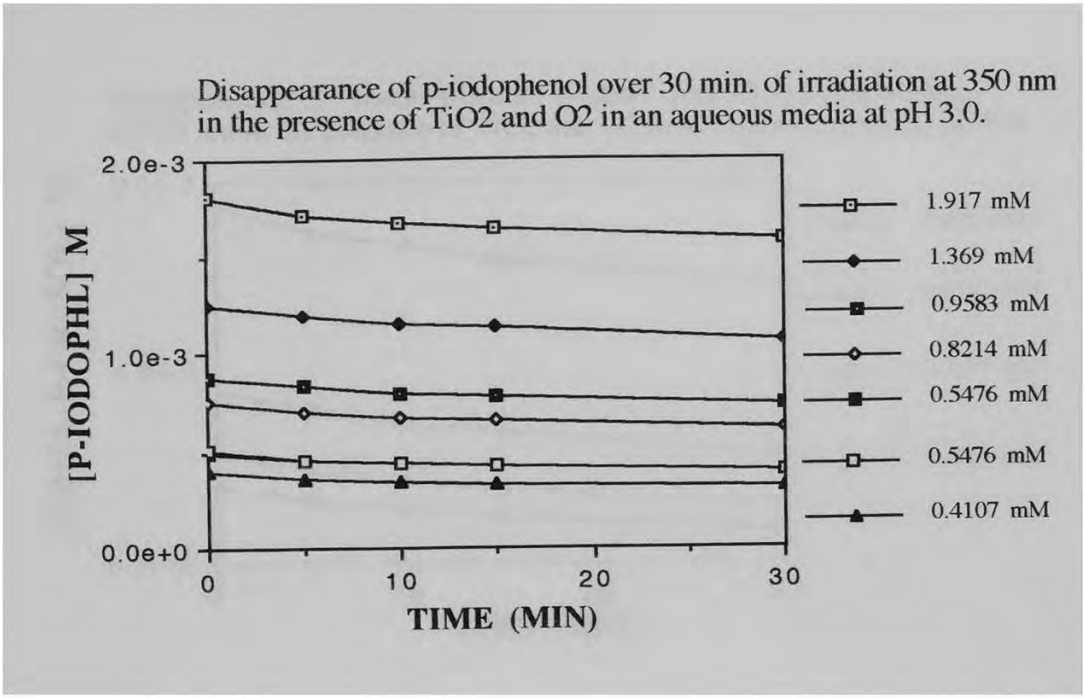
Disappearance of p-iodophenol over 30 min. of irradiation at 350 nm in the presence of TiO2 and O2 in an aqueous media at pH 3.0.
[P-IODOPHL] M
2.0e-3
1.0e-3
0.0e+0
0
10
20
30
TIME (MIN)
1.917 mM
1.369 mM
0.9583 mM
0.8214 mM
0.5476 mM
0.5476 mM
0.4107 mM

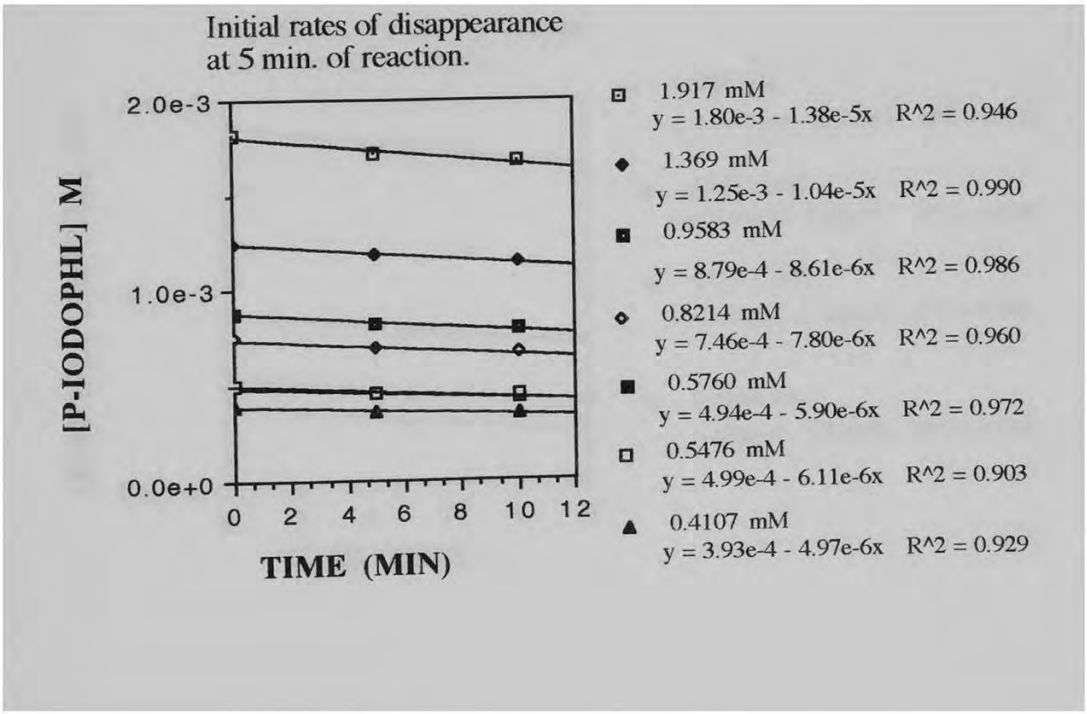
Initial rates of disappearance at 5 min. of reaction.
[P-IODOPHL] M
2.0e-3
1.0e-3
0.0e+0
0
2
4
6
8
10
12
TIME (MIN)
1.917 mM
y = 1.80e-3 - 1.38e-5x R^2 = 0.946
1.369 mM
y = 1.25e-3 - 1.04e-5x R^2 = 0.990
0.9583 mM
y = 8.79e-4 - 8.61e-6x R^2 = 0.986
0.8214 mM
y = 7.46e-4 - 7.80e-6x R^2 = 0.960
0.5760 mM
y = 4.94e-4 - 5.90e-6x R^2 = 0.972
0.5476 mM
y = 4.99e-4 - 6.11e-6x R^2 = 0.903
0.4107 mM
y = 3.93e-4 - 4.97e-6x R^2 = 0.929

Disappearance of α,α,α -trifluoro-p-cresol over 30 min of irradiation at 350 nm in the presence of TiO2 and O2 in an aqueous media at pH 3.0.

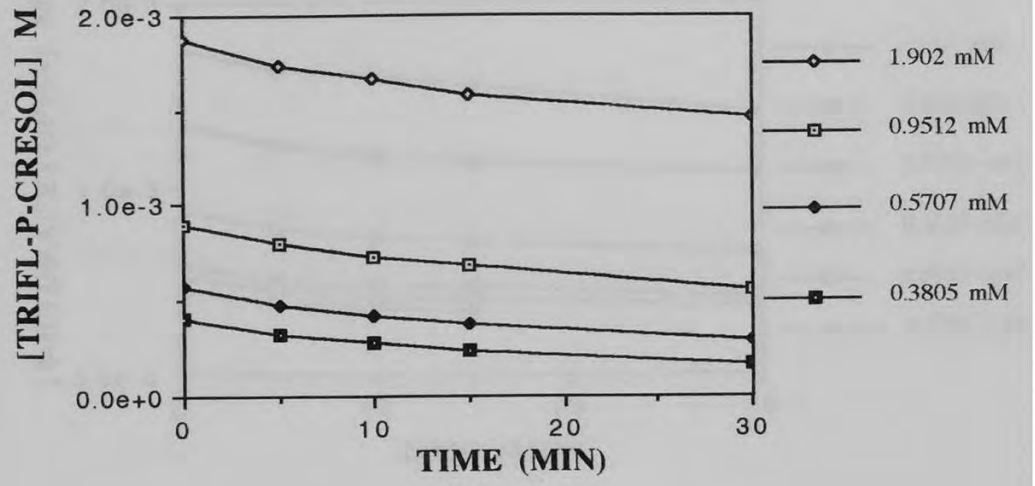

Initial rates of disappearance at 5 min. of reaction.

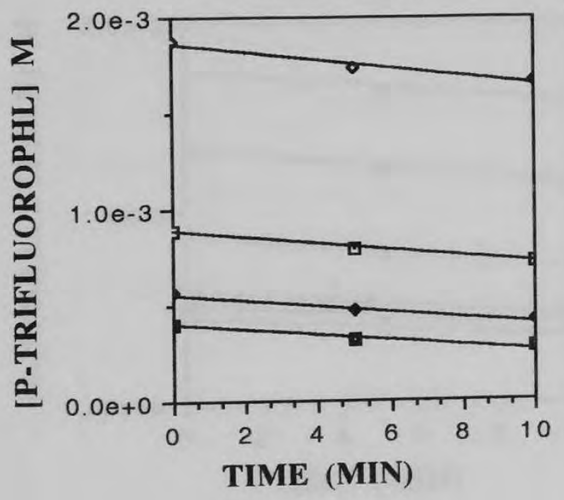

1.902 mM
y = 1.87e-3 - 2.12e-5x R^2 = 0.971

0.9512 mM
y = 8.88e-4 - 1.65e-5x R^2 = 0.990

0.5707 mM
y = 5.61e-4 - 1.47e-5x R^2 = 0.965

0.3804 mM
y = 4.02e-4 - 1.34e-5x R^2 = 0.979

Disappearance of 4-hydroxyacatophenone over 30 min. irradiation at 350 nm in the presence of TiO2 and O2 in an aqueous media at pH 3.0.

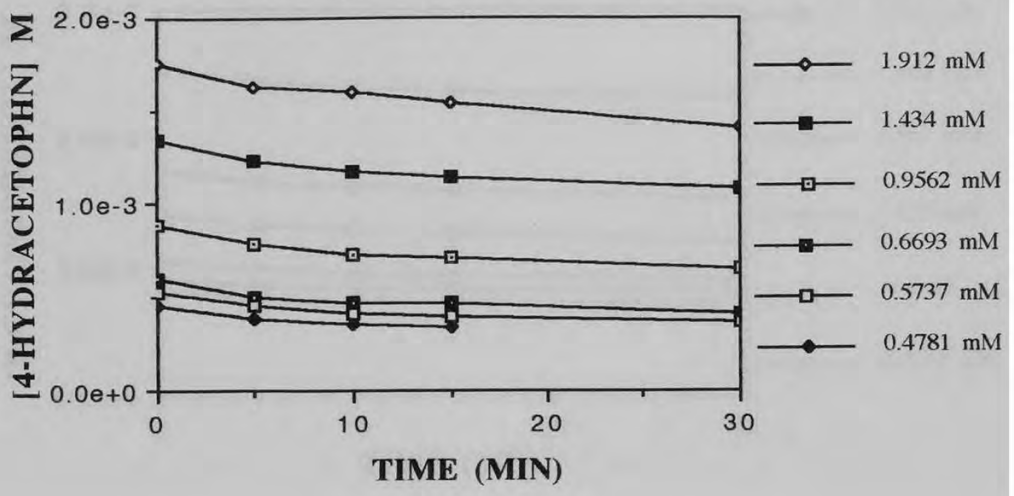

Initial rates of disappearance at 5 min. of reaction.

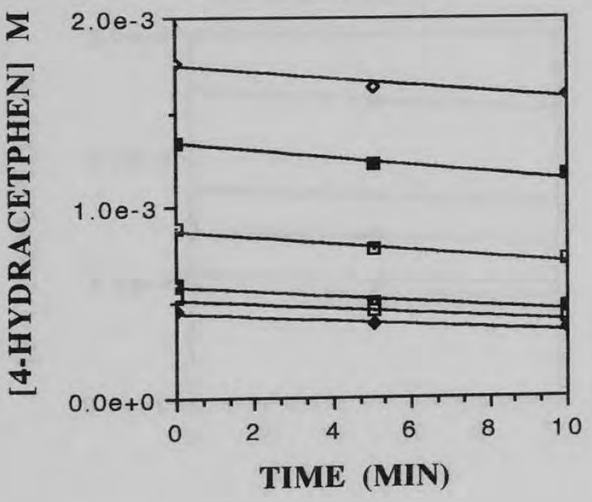

◇ 1.912 mM
y = 1.74e-3 - 1.66e-5x R^2 = 0.903

■ 1.434 mM
y = 1.34e-3 - 1.78e-5x R^2 = 0.951

▣ 0.9562 mM
y = 8.84e-4 - 1.65e-5x R^2 = 0.972

▣ 0.6693 mM
y = 5.93e-4 - 1.28e-5x R^2 = 0.902

□ 0.5737 mM
y = 5.20e-4 - 1.07e-5x R^2 = 0.968

◆ 0.4781 mM
y = 4.52e-4 - 9.46e-6x R^2 = 0.945

Disappearance of p-cyanophenol over 30 min. of irradiation at 350 nm in the presence of TiO2 and O2 in an aqueous media at pH 3.0.

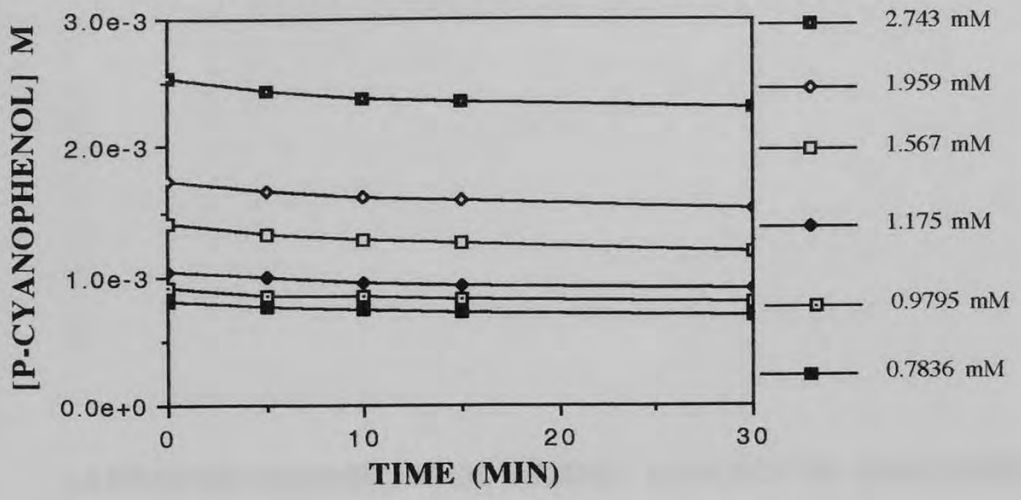

Initial rates of disappearance at 5 min. of reaction.

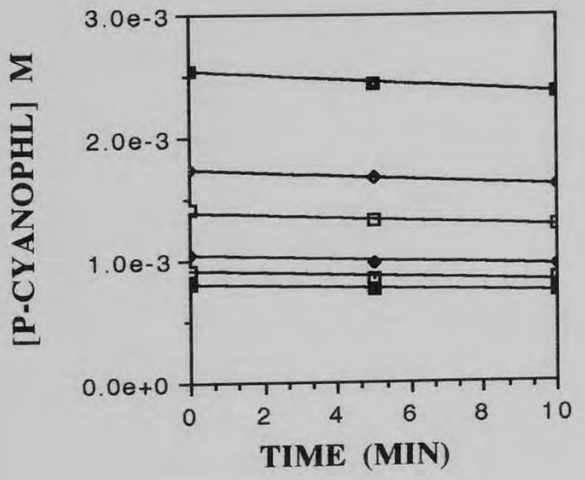

2.743 mM
y = 2.53e-3 - 1.64e-5x R^2 = 0.968

1.959 mM
y = 1.74e-3 - 1.30e-5x R^2 = 0.992

1.567 mM
y = 1.40e-3 - 1.16e-5x R^2 = 0.931

1.175 mM
y = 1.04e-3 - 8.53e-6x R^2 = 0.959

0.9795 mM
y = 9.05e-4 - 7.170e-6x R^2 = 0.855

0.7836 mM
y = 8.05e-4 - 7.17e-6x R^2 = 0.916

APPENDIX V.

LANGMUIR-HINSHELWOOD MODEL APPLIED TO EXAMINED PHENOLS.

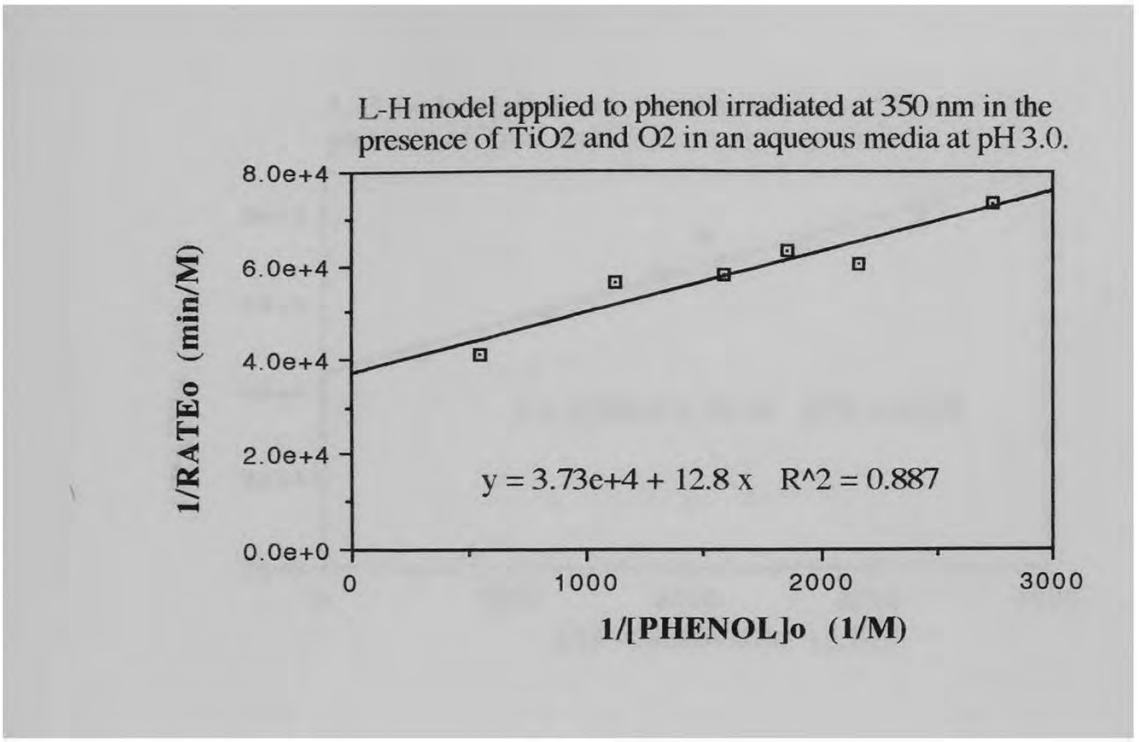
L-H model applied to phenol irradiated at 350 nm in the presence of TiO2 and O2 in an aqueous media at pH 3.0.
8.0e+4
6.0e+4
4.0e+4
2.0e+4
0.0e+0
1/RATEo (min/M)
y = 3.73e+4 + 12.8 x R^2 = 0.887
0
1000
2000
3000
1/[PHENOL]o (1/M)

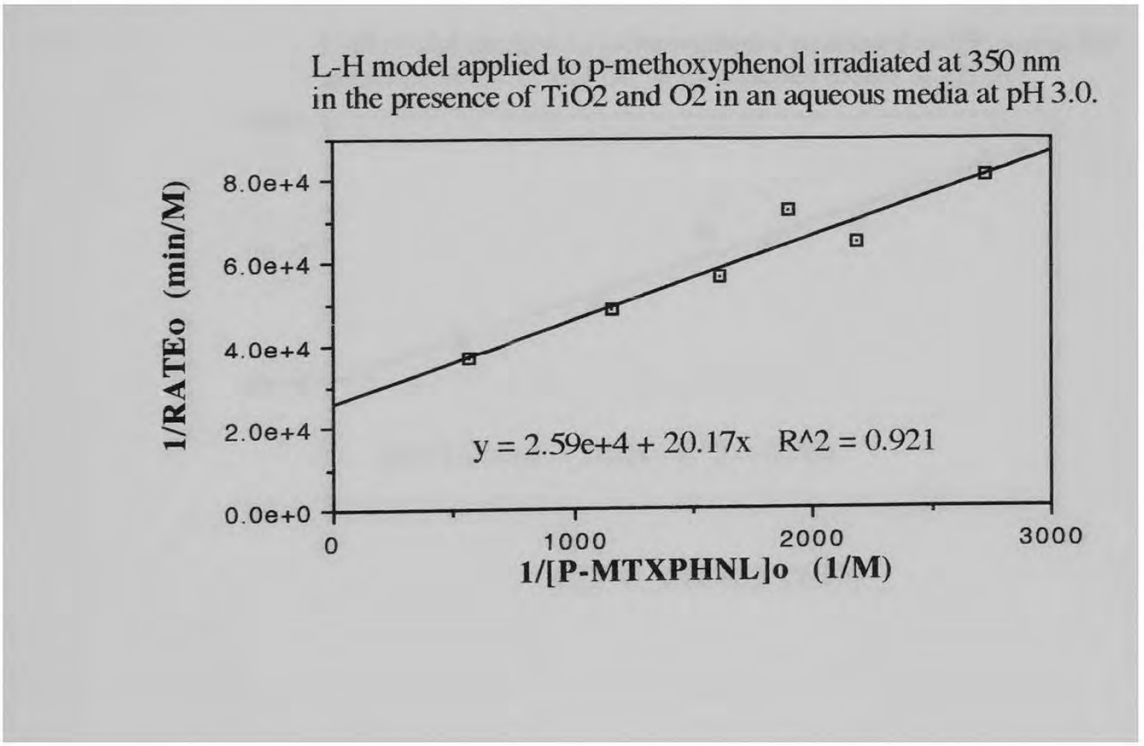
L-H model applied to p-methoxyphenol irradiated at 350 nm in the presence of TiO2 and O2 in an aqueous media at pH 3.0.
8.0e+4
6.0e+4
4.0e+4
2.0e+4
0.0e+0
1/RATEo (min/M)
y = 2.59e+4 + 20.17x R^2 = 0.921
0
1000
2000
3000
1/[P-MTXPHNL]o (1/M)

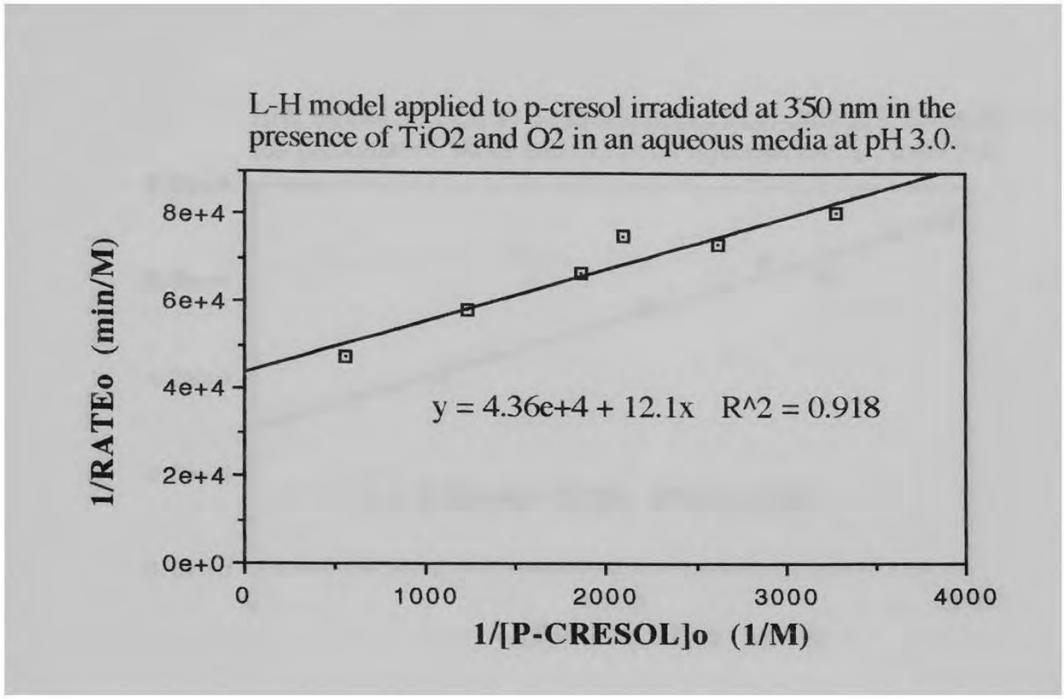
L-H model applied to p-cresol irradiated at 350 nm in the presence of TiO2 and O2 in an aqueous media at pH 3.0.
1/RATEo (min/M)
8e+4
6e+4
4e+4
2e+4
0e+0
0
1000
2000
3000
4000
y = 4.36e+4 + 12.1x R^2 = 0.918
1/[P-CRESOL]o (1/M)

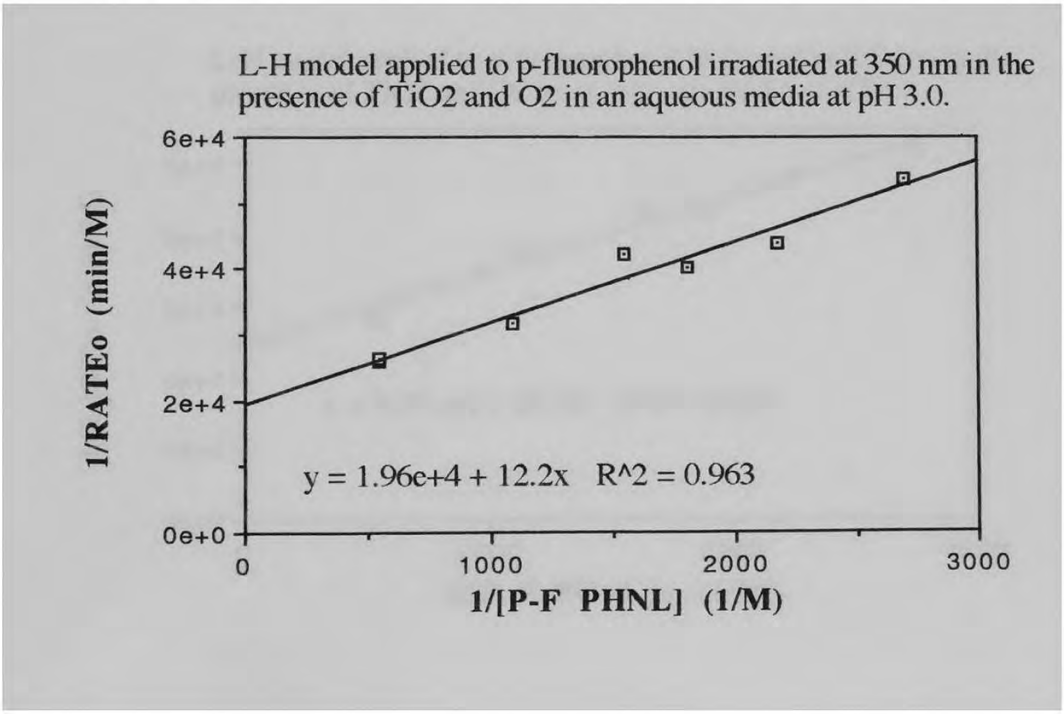
L-H model applied to p-fluorophenol irradiated at 350 nm in the presence of TiO2 and O2 in an aqueous media at pH 3.0.
1/RATEo (min/M)
6e+4
4e+4
2e+4
0e+0
0
1000
2000
3000
y = 1.96e+4 + 12.2x R^2 = 0.963
1/[P-F PHNL] (1/M)

L-H model applied to p-chlorophenol irradiated at 350 nm in the presence of TiO2 and O2 in an aqueous media at pH 3.0.

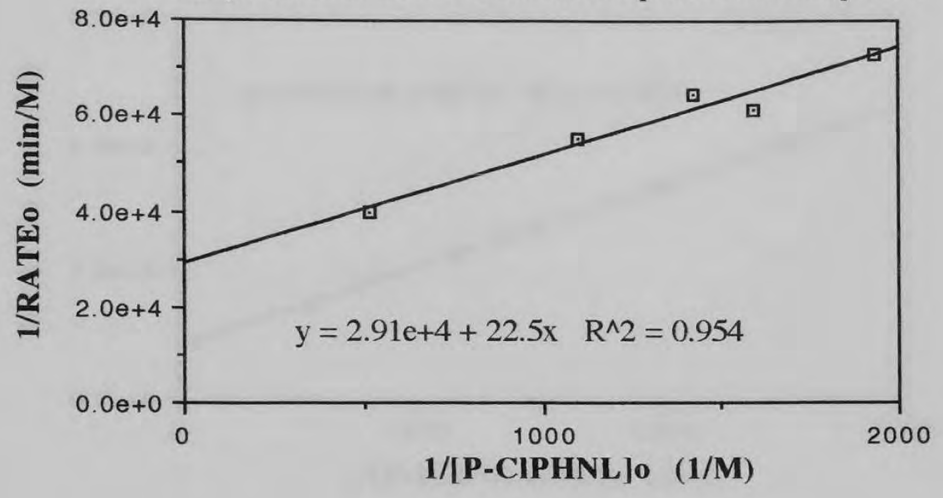

L-H model applied to p-bromophenol irradiated at 350 nm in the presence of TiO2 and O2 in an aqueous media at pH 3.0.

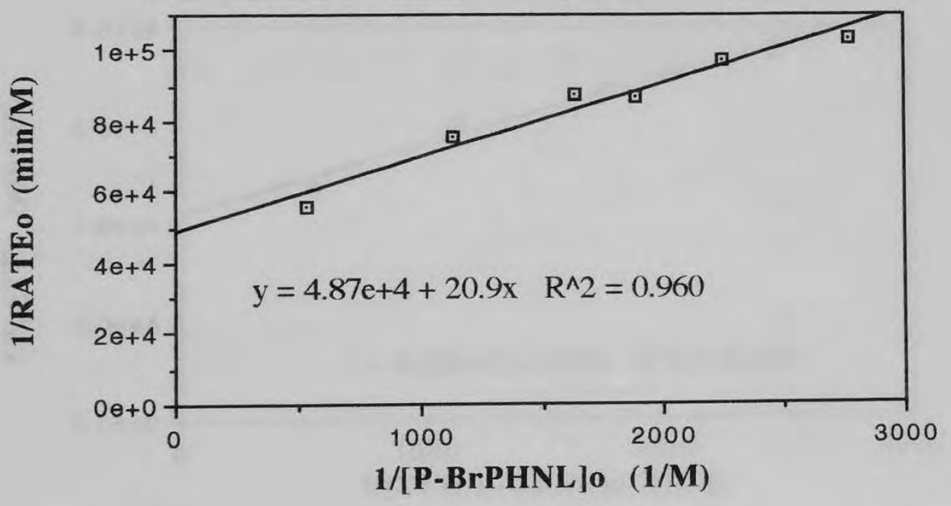

L-H model applied to p-iodophenol irradiated at 350 nm in the presence of TiO2 and O2 in an aqueous media at pH 3.0.

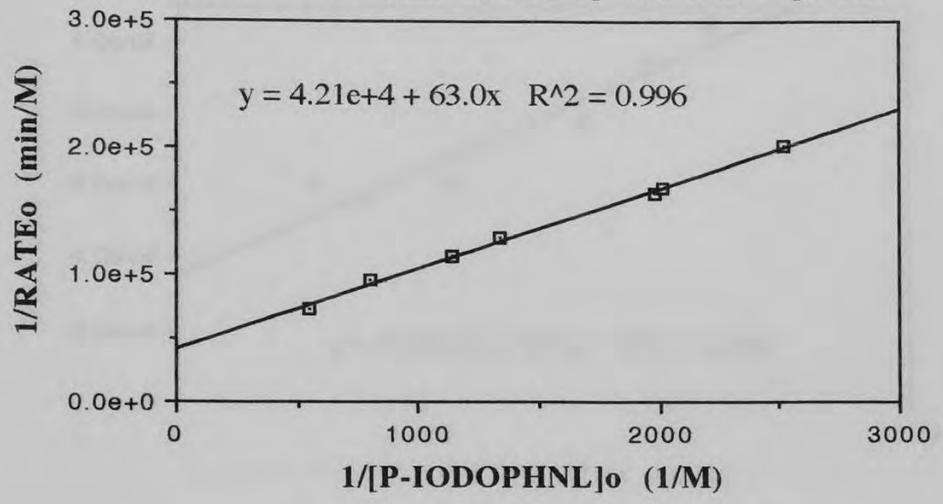

L-H model applied to α,α,α -trifluoro-p-cresol irradiated at 350 nm in the presence of TiO2 and O2 in an aqueous media at pH 3.0.

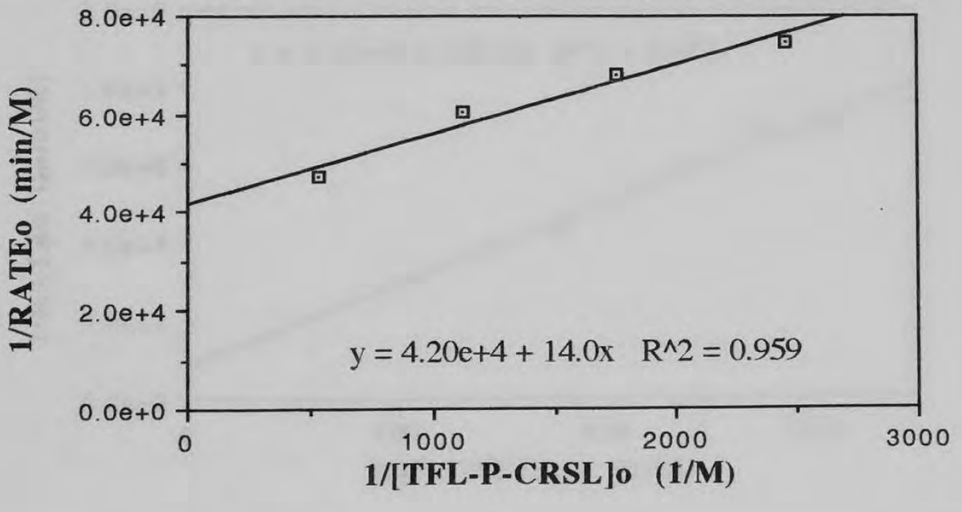

L-H model applied to 4-hydroxyactophenone irradiated at 350 nm in the presence of TiO2 and O2 in an aqueous media at pH 3.0.

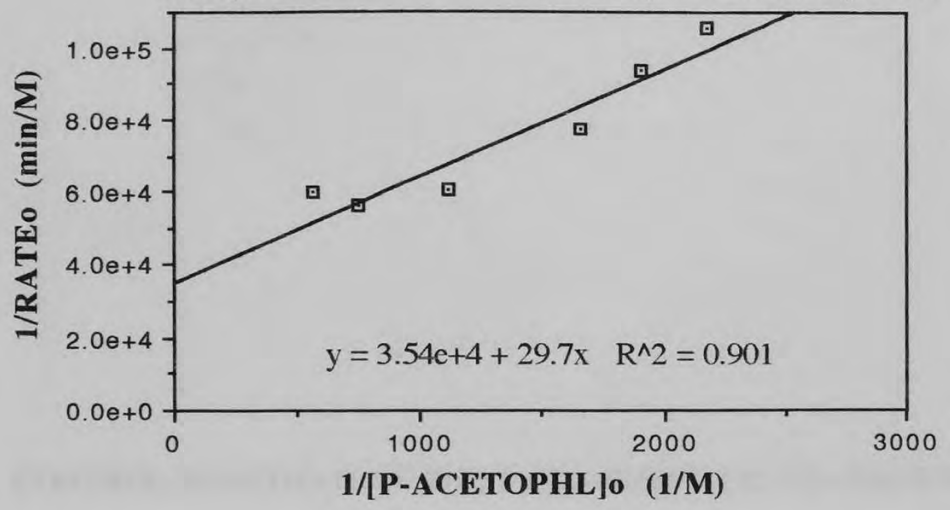

L-H model applied to p-cyanophenol irradiated at 350 nm in the presence of TiO2 and O2 in an aqueous media at pH 3.0.

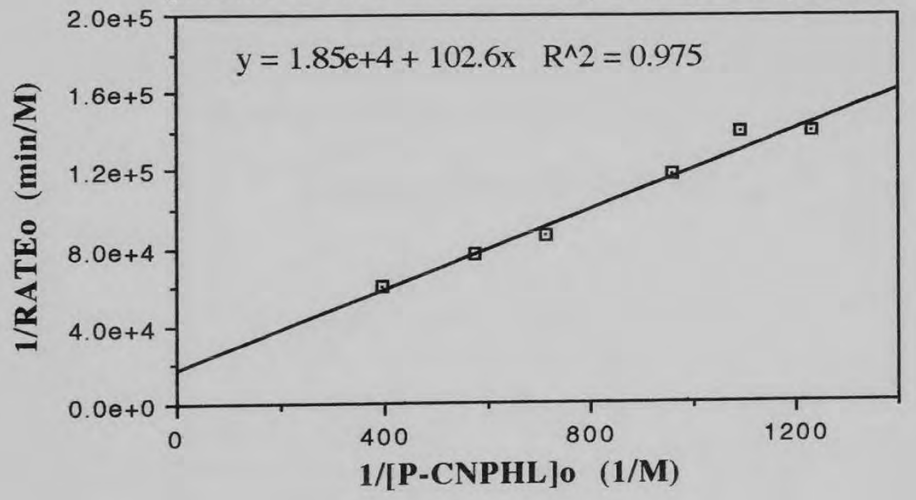

APPENDIX VI.

CONTROL REACTIONS OF THE *PARA*-SUBSTITUTED PHENOLS STUDIED OVER A 4 HOUR PERIOD AT pH 3.0.

Disappearance of phenol under oxic and anoxic conditions when irradiated at 350 nm in the presence of TiO2 in an aqueous media at pH 3.0.

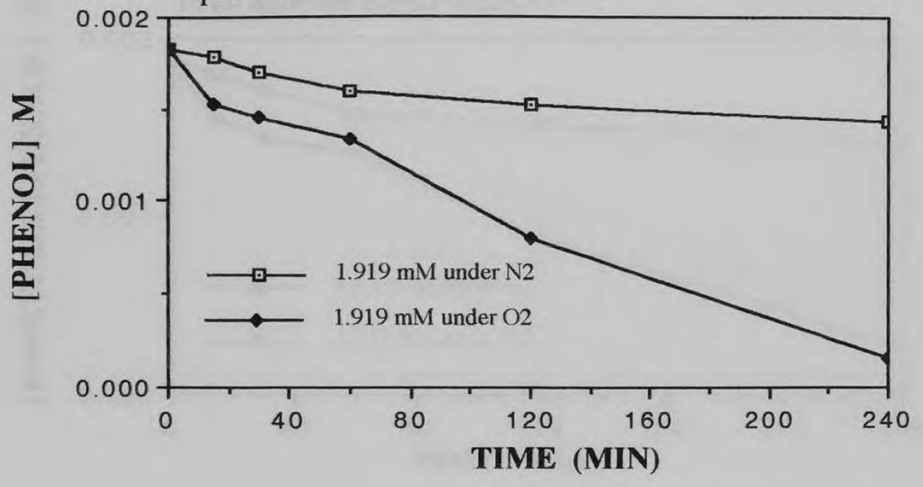

Control reactions of phenol irradiated at 350 nm in the absence of TiO2 and kept in the dark with TiO2 for a period of 4 hours.

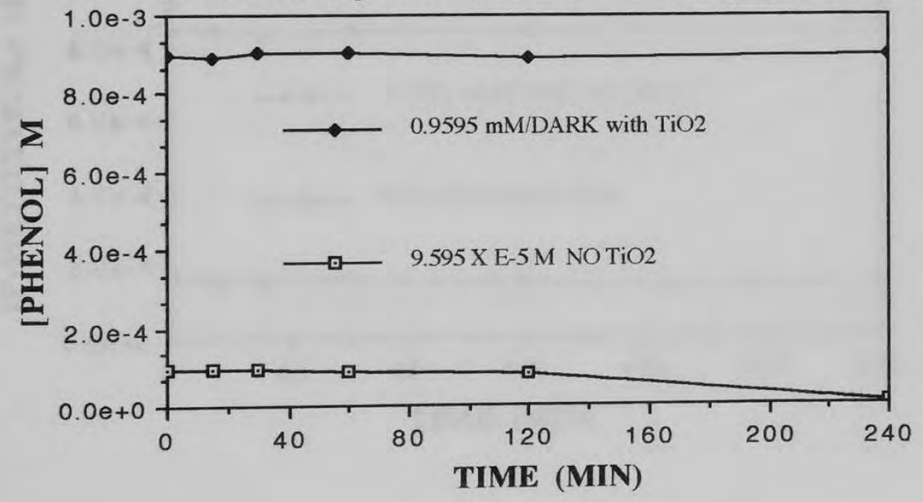

Disappearance of p-methoxyphenol under oxic and anoxic conditions when irradiated at 350 nm in the presence of TiO2 in an aqueous media at pH 3.0.

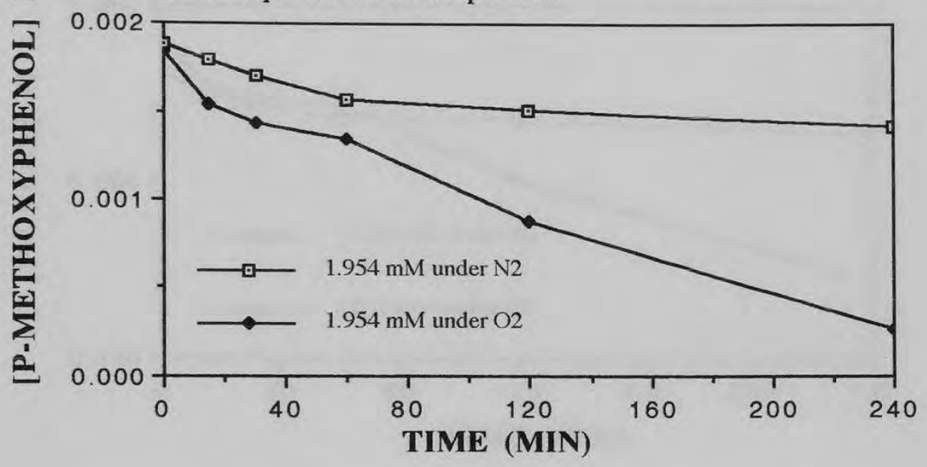

Control reactions of p-methoxyphenol irradiated at 350 nm in the absence of TiO2 and kept in the dark with TiO2 for a period of 4 hours

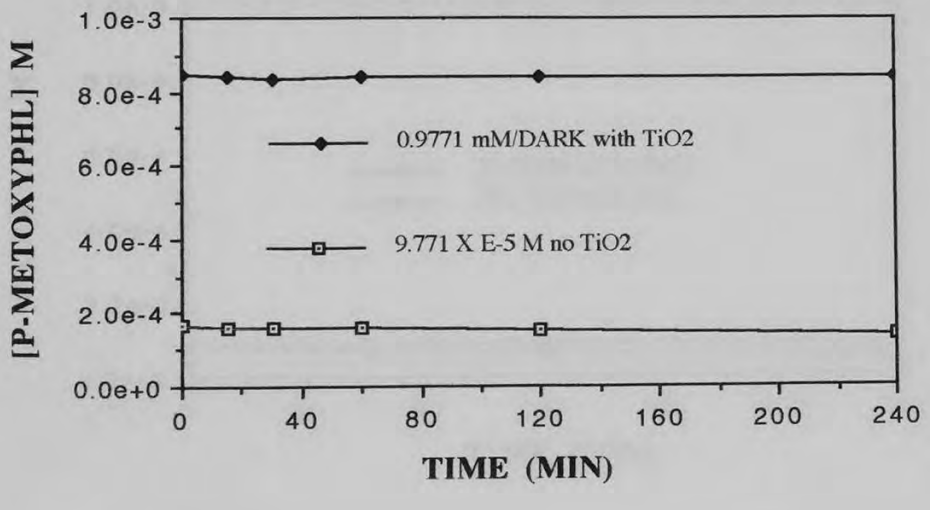

Disappearance of p-cresol under oxic and anoxic conditions when irradiated at 350 nm in the presence of TiO2 in an aqueous media at pH 3.0.

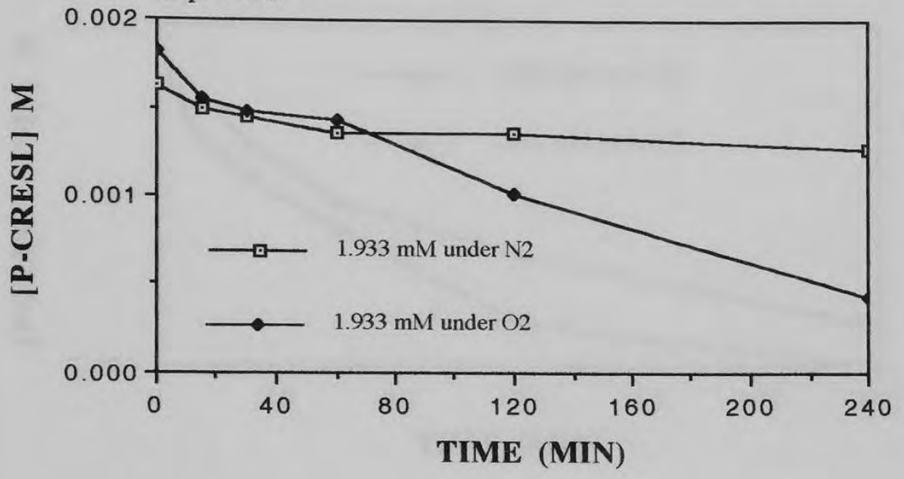

Control reactions of p-cresolirradiated at 350 nm in the absence of TiO2 and kept in the dark with TiO2 for a period of 4 hours.

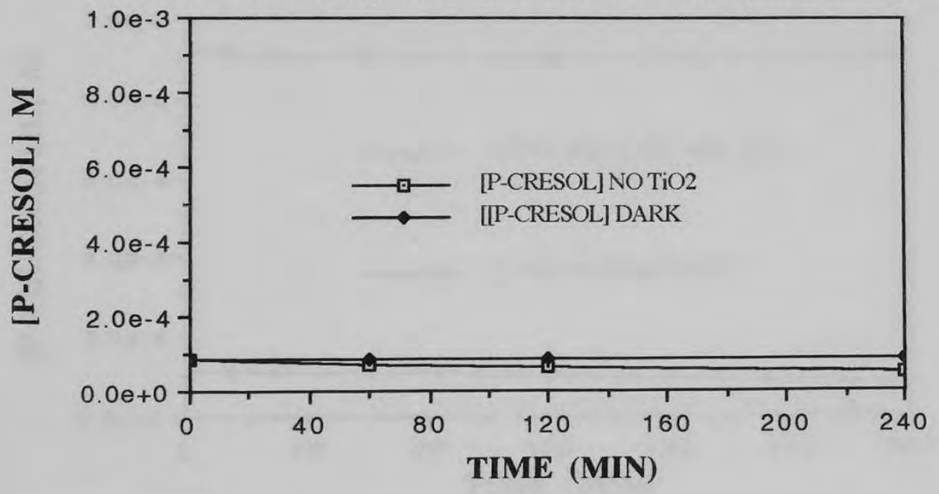

Disappearance of p-fluorophenol under oxic and anoxic conditions when irradiated at 350 nm in the presence of TiO2 in an aqueous media at pH 3.0.

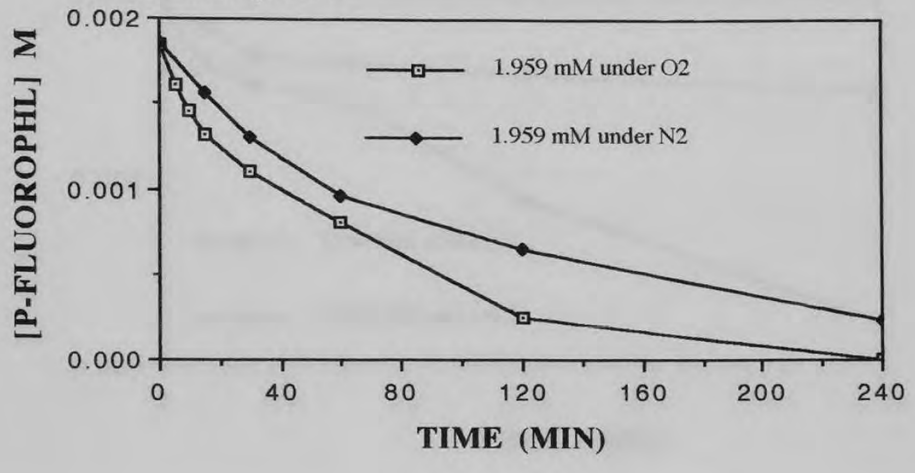

Control reations of p-fluorophenol irradiated at 350 nm in the absence of TiO2 and kept in the dark with TiO2 for a period of 4 hours.

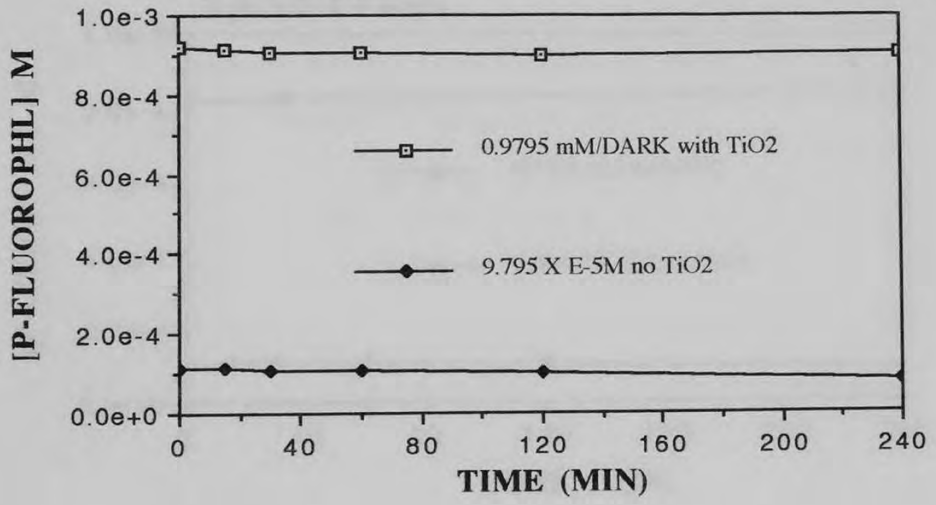

Disappearance of p-chlorophenol under oxic and anoxic conditions when irradiated at 350 nm in the presence of

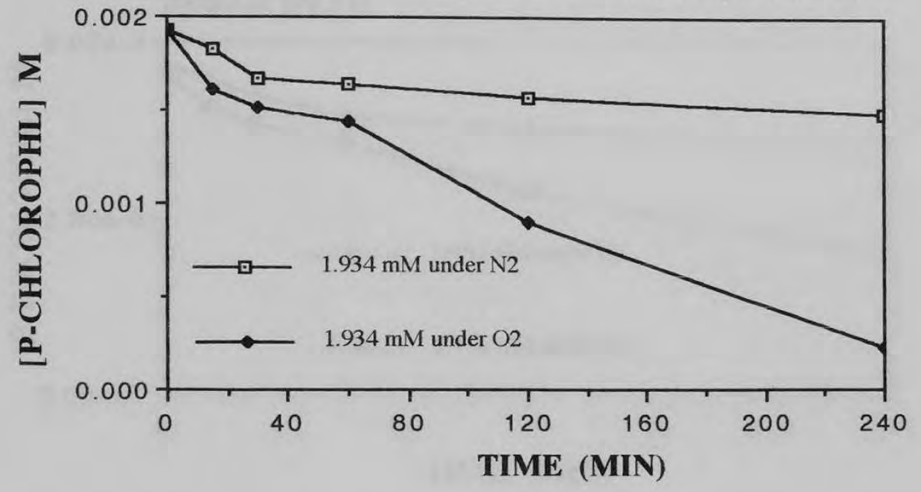

Control reactions of p-chlorophenol irradiated at 350 nm in the absence of TiO2 and kept in the dark with TiO2 for a period of 4 hours.

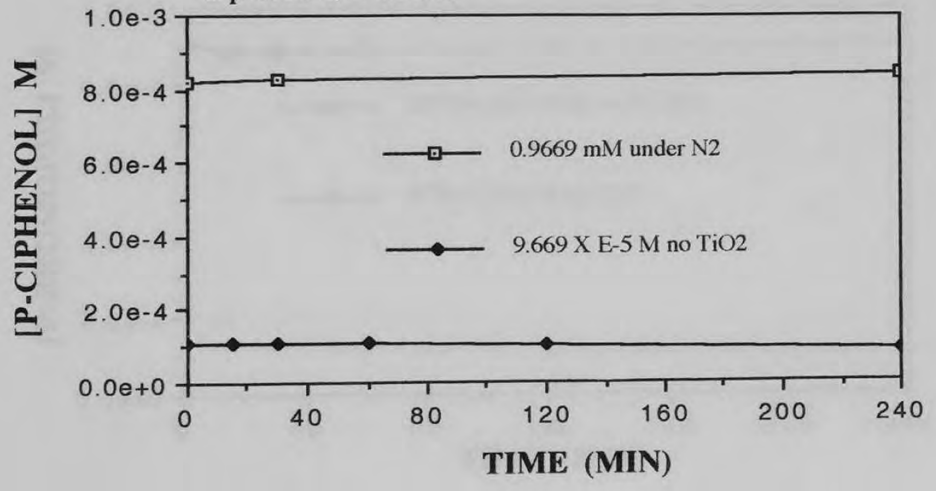

Disappearance of p-bromophenol under oxic and anoxic conditions when irradiated at 350 nm in the presence of TiO2 in an aqueous media at pH 3.0.

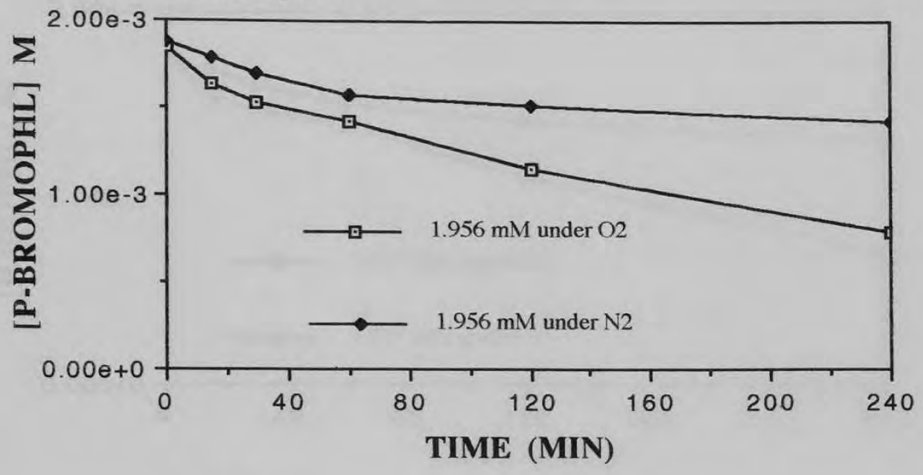

Control recations of p-bromophenol irradiated at 350 nm in the absence of TiO2 and kept in the dark with TiO2 for a period of 4 hours.

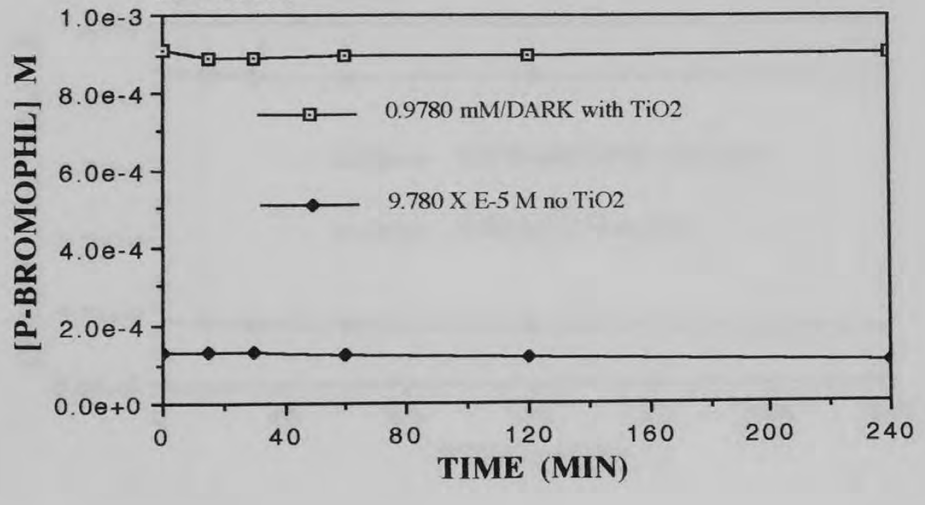

Disappearance of p-iodophenol under oxic and anoxic conditions when irradiated at 350 nm in the presence of TiO2 in an aqueous media at pH 3.0.

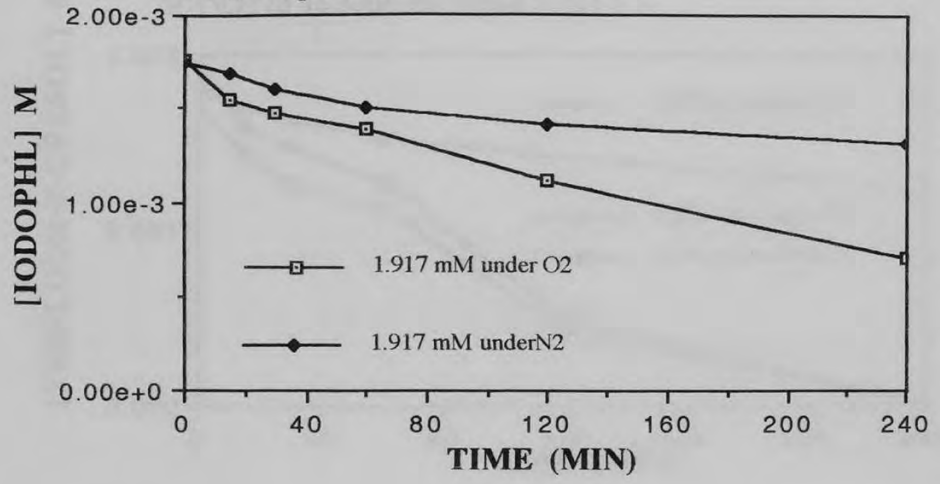

Control reactions of p-iodophenol irradiated at 350 nm in the absence of TiO2 and kept in the dark with TiO2 for a period of 4 hours.

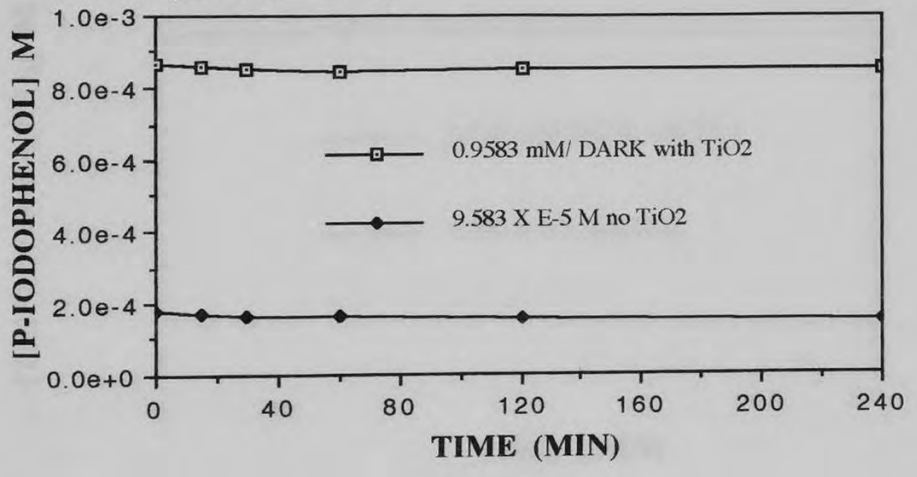

Disappearance of α,α,α -trifluoro-p-cresol under oxic and anoxic conditions when irradiated at 350 nm in the presence of TiO2 in an aqueous media at pH 3.0.

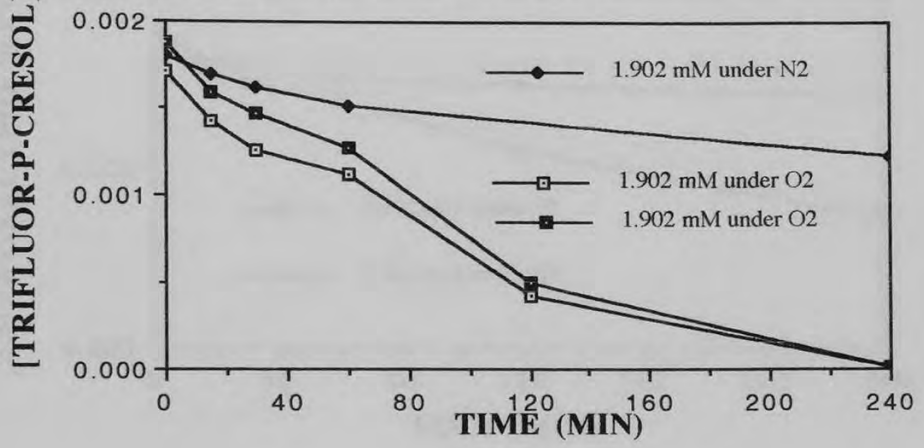

Control reactions of trifluoro-p-cresol irradiated at 350 nm in the absence of TiO2 and kept in the dark with TiO2 for a period of 4 hours.

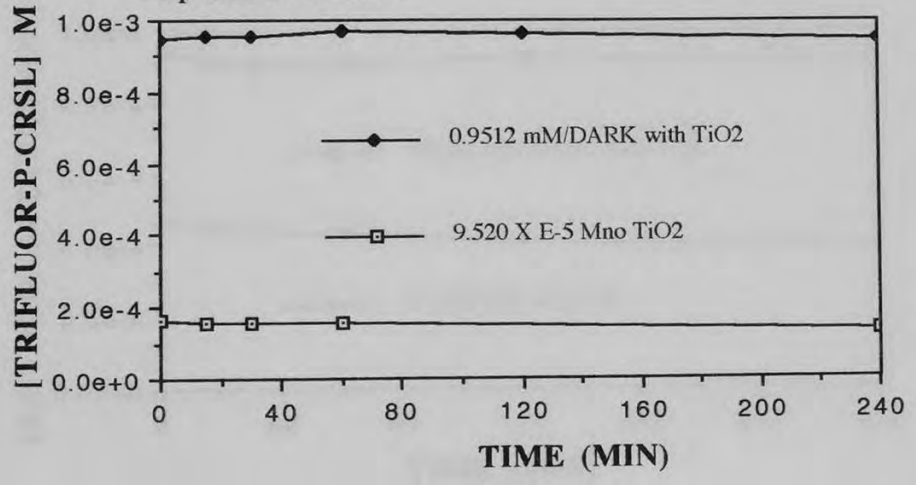

Disappearance of 4-hydroxyacetophenone under oxic and anoxic conditions when irradiated at 350 nm in the presence of TiO2 in an aqueous media at pH 3.0.

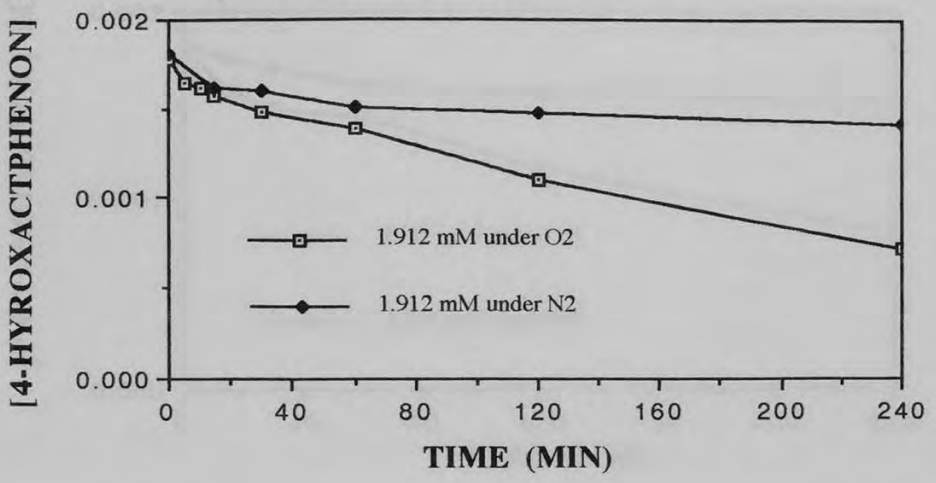

Control reactions of 4-hydroxyacetophenone irradiated at 350 nm in the absence of TiO2 and kept in the dark with TiO2 for a period of 4 hours.

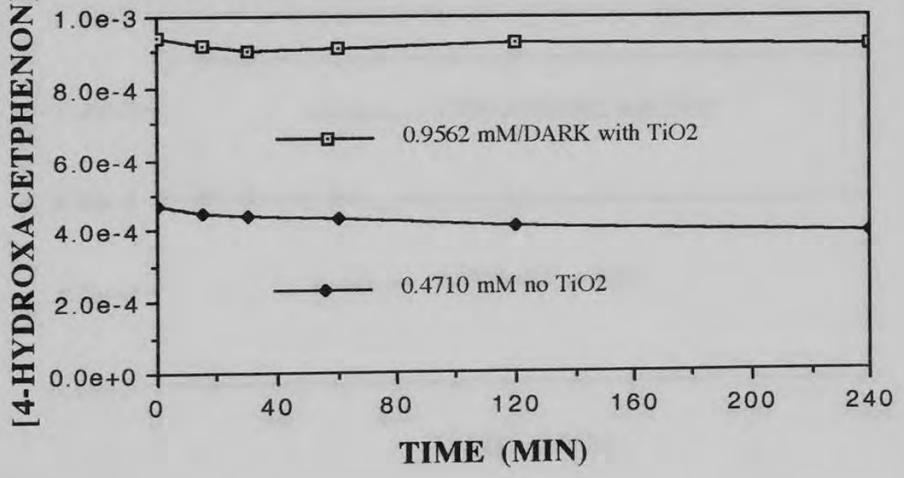

Disappearance of p-cyanophenol under oxic and anoxic conditions when irradiated at 350 nm in thepresence of TiO2 in an aqueous media at pH 3.0.

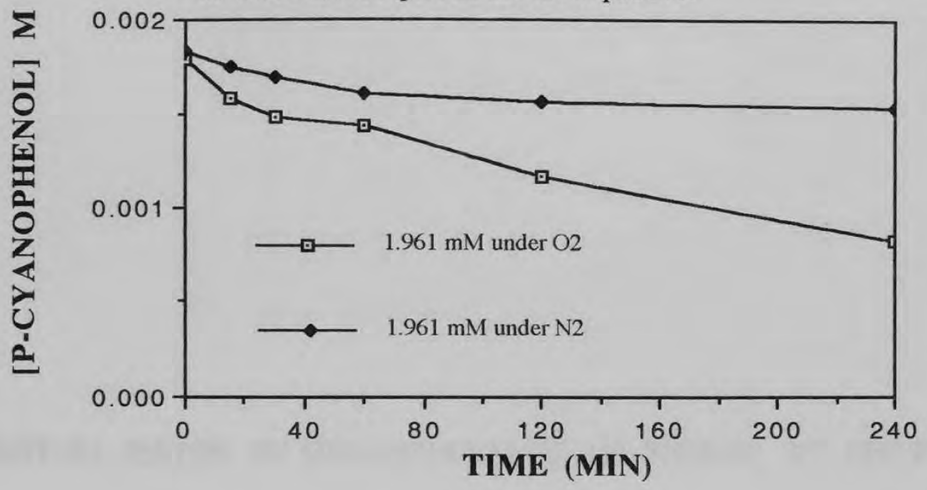

Control recations of p-cyanophenol irradiated at 350 nm in the absence of TiO2 and kept in the dark with TiO2 for a period of 4 hours.

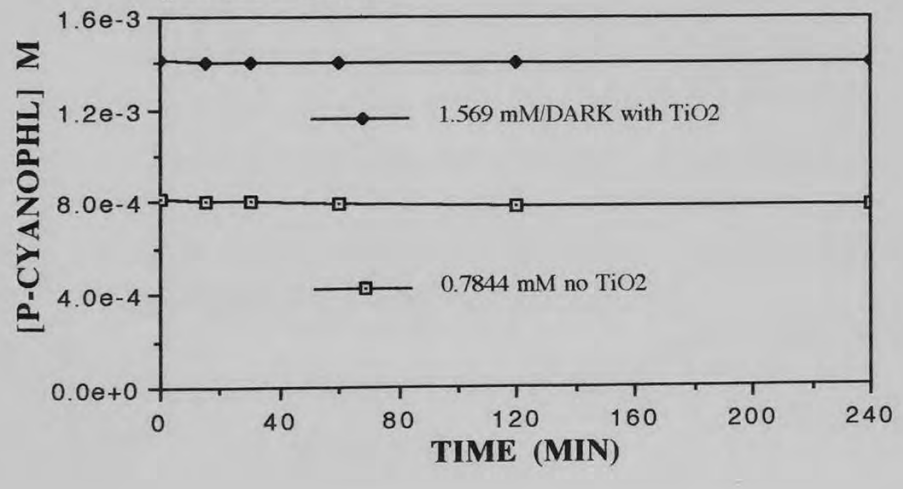

APPENDIX VII.

INITIAL RATES OF DISAPPEARANCE OF PHENOL AT DIFFERENT CONCENTRATIONS OVER THE 1.0 TO 13.7 pH RANGE.

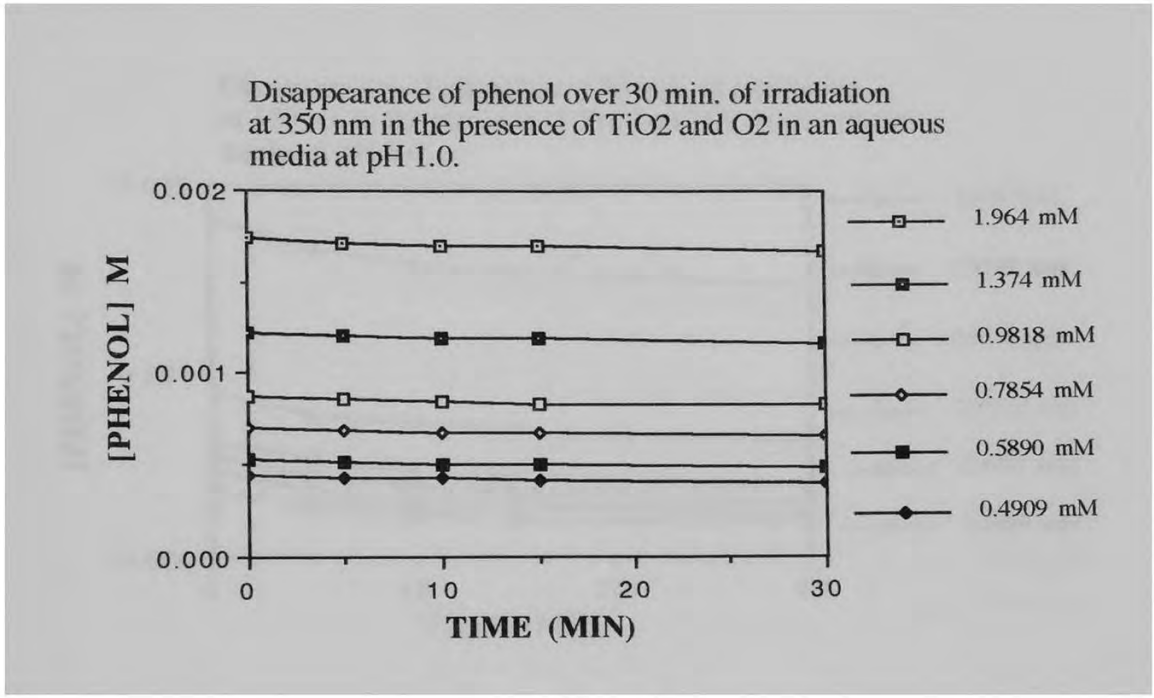
Disappearance of phenol over 30 min. of irradiation at 350 nm in the presence of TiO2 and O2 in an aqueous media at pH 1.0.
[PHENOL] M
0.002
0.001
0.000
0
10
20
30
TIME (MIN)
1.964 mM
1.374 mM
0.9818 mM
0.7854 mM
0.5890 mM
0.4909 mM

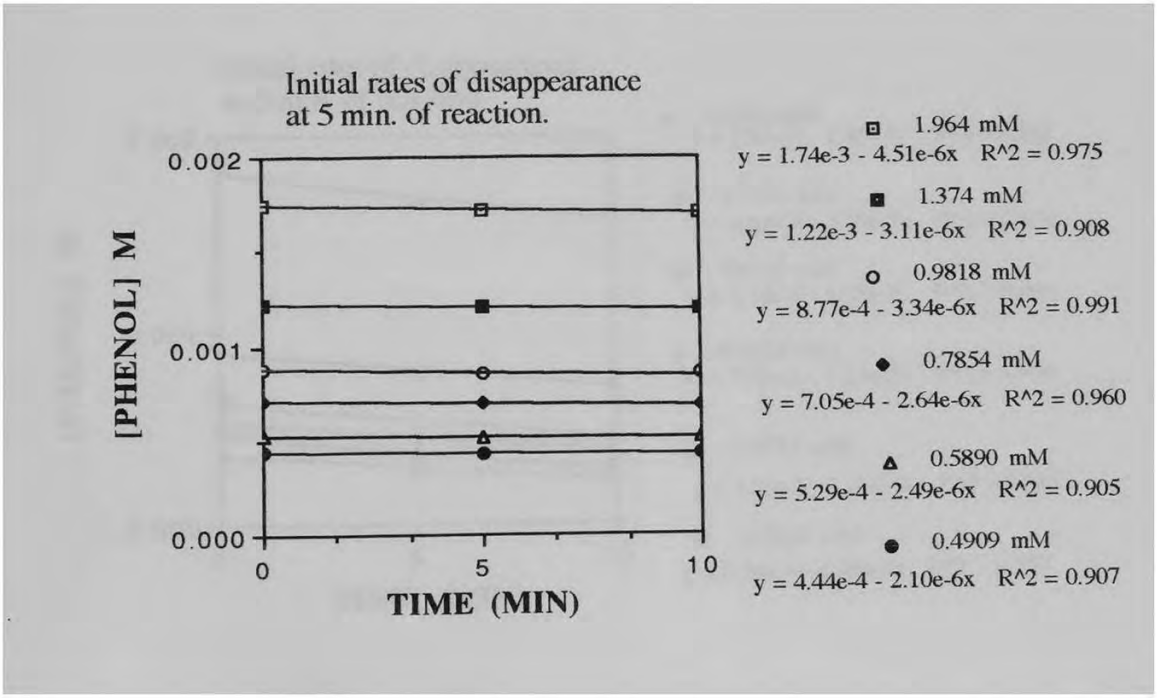
Initial rates of disappearance at 5 min. of reaction.
[PHENOL] M
0.002
0.001
0.000
0
5
10
TIME (MIN)
1.964 mM
y = 1.74e-3 - 4.51e-6x R^2 = 0.975
1.374 mM
y = 1.22e-3 - 3.11e-6x R^2 = 0.908
0.9818 mM
y = 8.77e-4 - 3.34e-6x R^2 = 0.991
0.7854 mM
y = 7.05e-4 - 2.64e-6x R^2 = 0.960
0.5890 mM
y = 5.29e-4 - 2.49e-6x R^2 = 0.905
0.4909 mM
y = 4.44e-4 - 2.10e-6x R^2 = 0.907

Disappearance of phenol over 30 min. of irradiation at 350 nm in the presence of TiO2 and O2 in an aqueous media at pH 3.0.

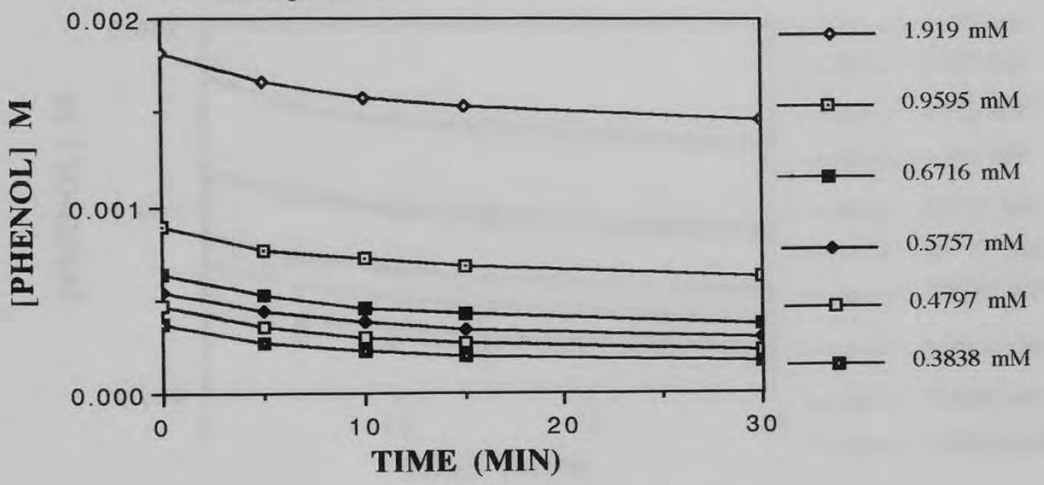

Initial rates of disappearance at 5 min. of reaction.

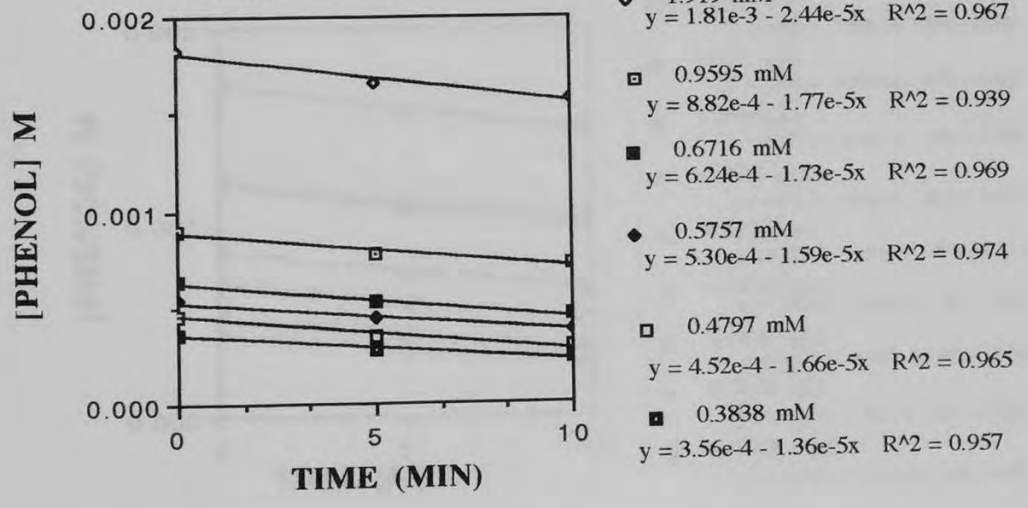

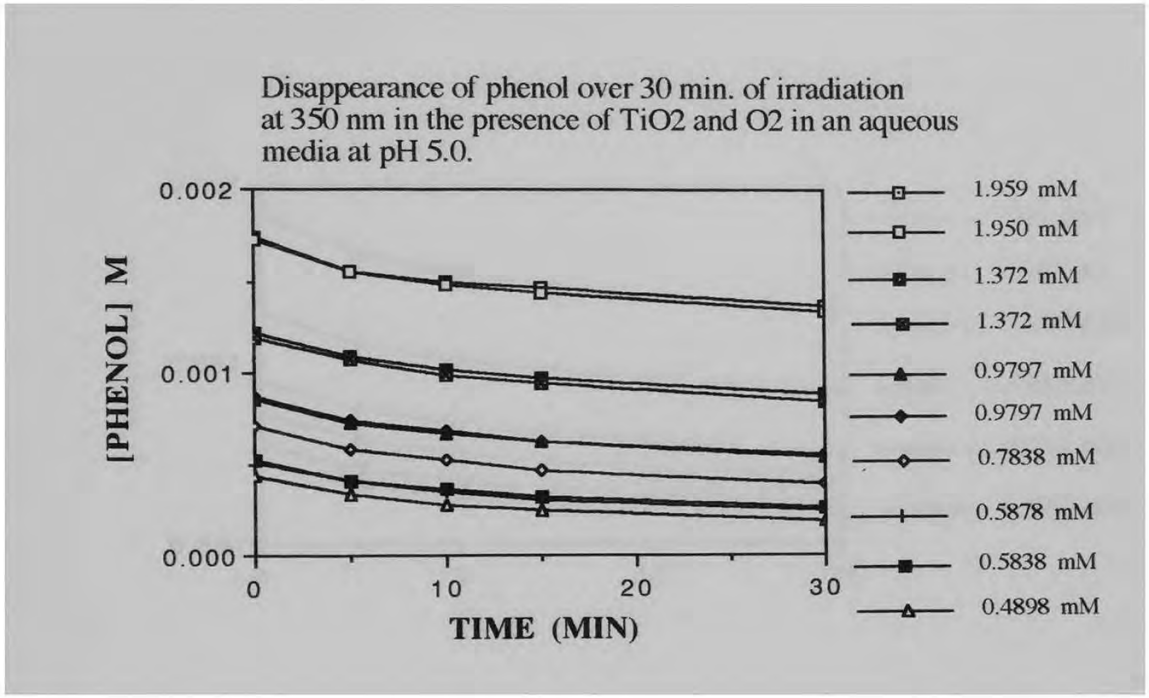
Disappearance of phenol over 30 min. of irradiation at 350 nm in the presence of TiO2 and O2 in an aqueous media at pH 5.0.
[PHENOL] M
0.002
0.001
0.000
0
10
20
30
TIME (MIN)
1.959 mM
1.950 mM
1.372 mM
1.372 mM
0.9797 mM
0.9797 mM
0.7838 mM
0.5878 mM
0.5838 mM
0.4898 mM

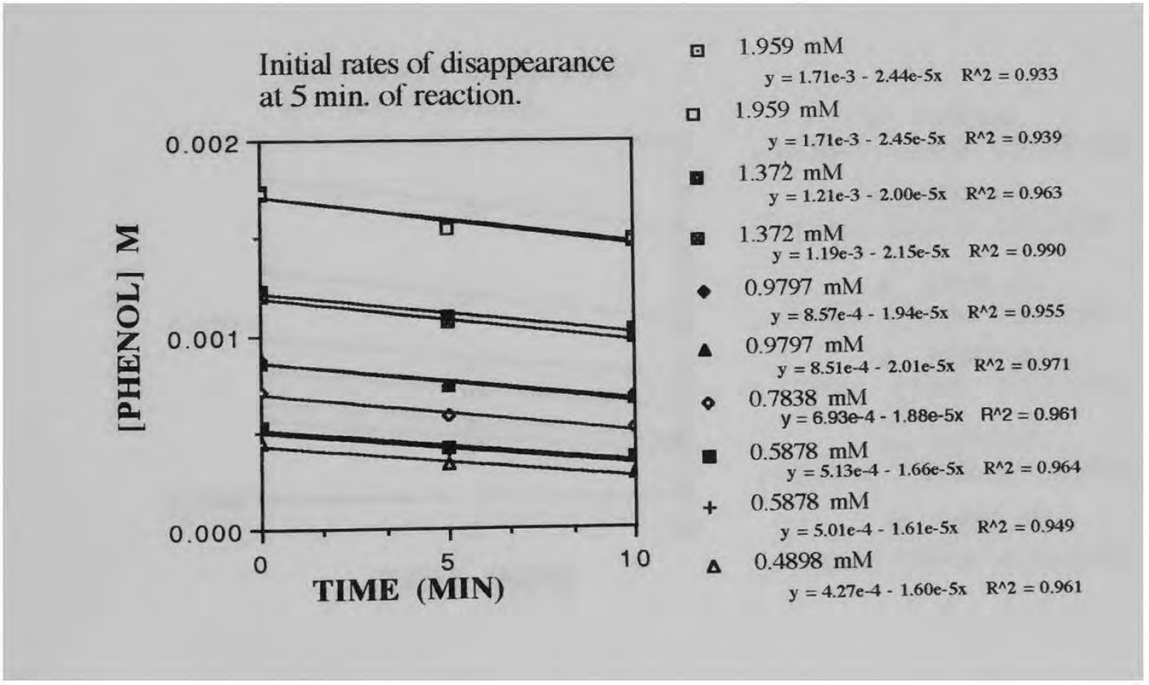
Initial rates of disappearance at 5 min. of reaction.
[PHENOL] M
0.002
0.001
0.000
0
5
10
TIME (MIN)
1.959 mM
y = 1.71e-3 - 2.44e-5x R^2 = 0.933
1.959 mM
y = 1.71e-3 - 2.45e-5x R^2 = 0.939
1.372 mM
y = 1.21e-3 - 2.00e-5x R^2 = 0.963
1.372 mM
y = 1.19e-3 - 2.15e-5x R^2 = 0.990
0.9797 mM
y = 8.57e-4 - 1.94e-5x R^2 = 0.955
0.9797 mM
y = 8.51e-4 - 2.01e-5x R^2 = 0.971
0.7838 mM
y = 6.93e-4 - 1.88e-5x R^2 = 0.961
0.5878 mM
y = 5.13e-4 - 1.66e-5x R^2 = 0.964
0.5878 mM
y = 5.01e-4 - 1.61e-5x R^2 = 0.949
0.4898 mM
y = 4.27e-4 - 1.60e-5x R^2 = 0.961

Disappearance of phenol over 30 min. of irradiation at 350 nm in the presence of TiO2 and O2 in an aqueous media at pH 7.0.

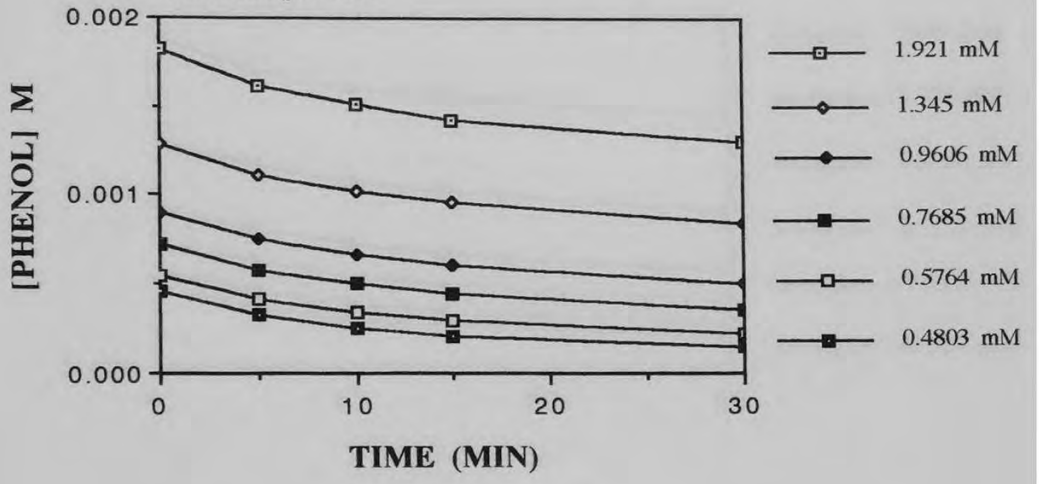

Initial rates of disappearance at 5 min. of reaction.

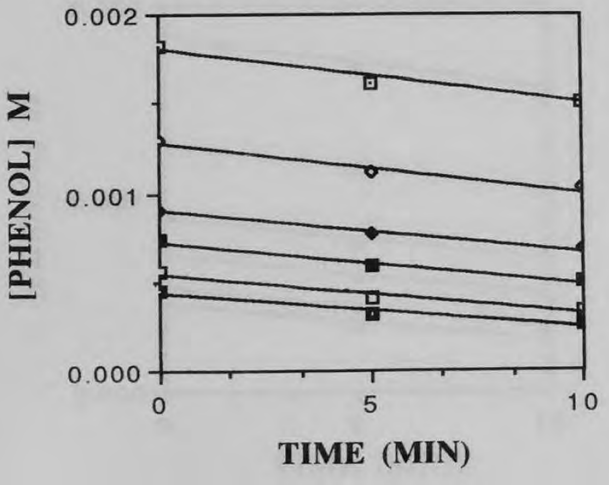

1.921 mM
y = 1.80e-3 - 3.11e-5x R^2 = 0.960

1.345 mM
y = 1.28e-3 - 2.72e-5x R^2 = 0.951

0.9606 mM
y = 8.98e-4 - 2.37e-5x R^2 = 0.981

0.7685 mM
y = 7.22e-4 - 2.35e-5x R^2 = 0.974

0.5764 mM
y = 5.41e-4 - 2.15e-5x R^2 = 0.970

0.4803 mM
y = 4.42e-4 - 2.01e-5x R^2 = 0.968

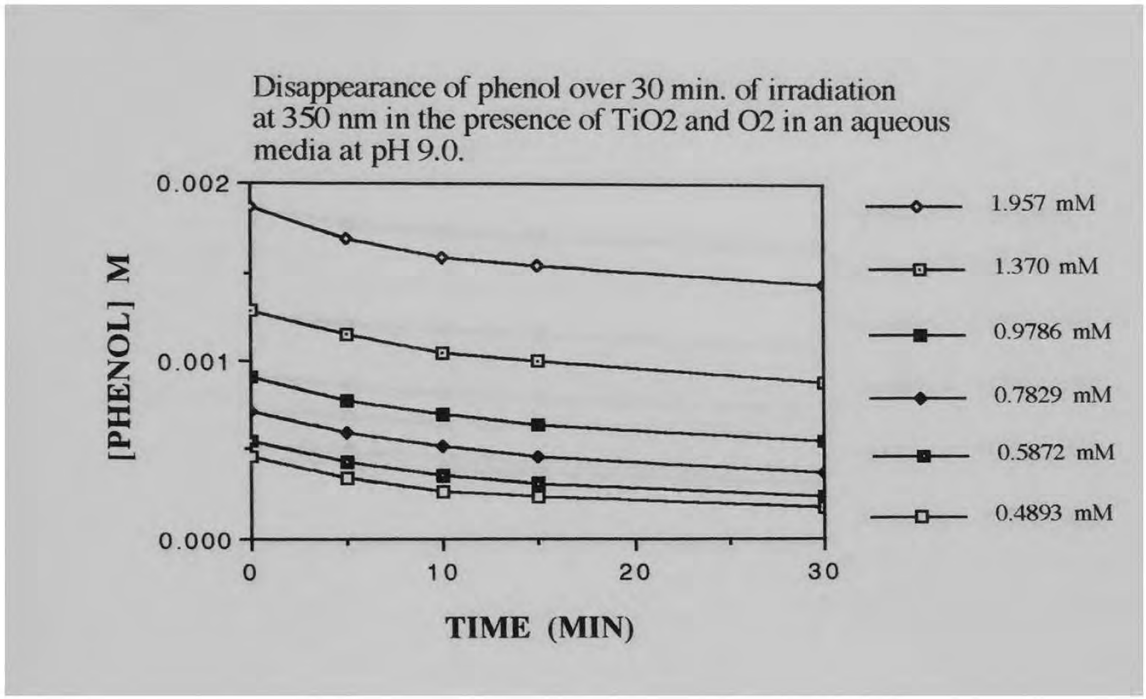
Disappearance of phenol over 30 min. of irradiation at 350 nm in the presence of TiO2 and O2 in an aqueous media at pH 9.0.
[PHENOL] M
0.002
0.001
0.000
0
10
20
30
TIME (MIN)
1.957 mM
1.370 mM
0.9786 mM
0.7829 mM
0.5872 mM
0.4893 mM

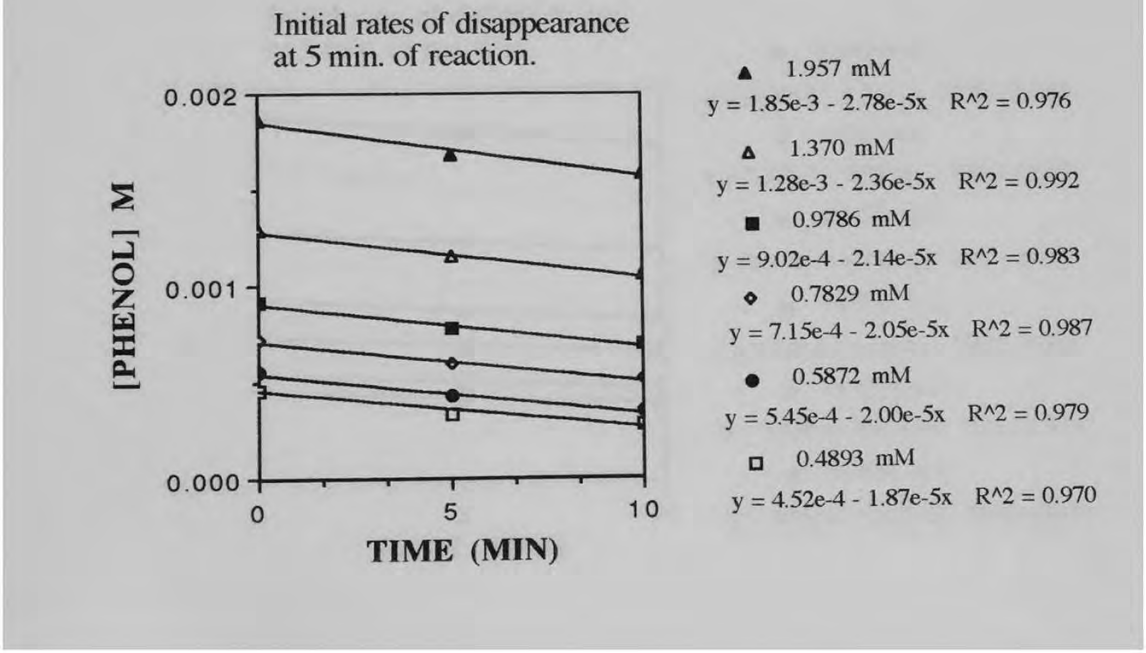
Initial rates of disappearance at 5 min. of reaction.
[PHENOL] M
0.002
0.001
0.000
0
5
10
TIME (MIN)
1.957 mM
y = 1.85e-3 - 2.78e-5x R^2 = 0.976
1.370 mM
y = 1.28e-3 - 2.36e-5x R^2 = 0.992
0.9786 mM
y = 9.02e-4 - 2.14e-5x R^2 = 0.983
0.7829 mM
y = 7.15e-4 - 2.05e-5x R^2 = 0.987
0.5872 mM
y = 5.45e-4 - 2.00e-5x R^2 = 0.979
0.4893 mM
y = 4.52e-4 - 1.87e-5x R^2 = 0.970

Disappearance of phenol over 30 min. of irradiation at 350 nm in the presence of TiO2 and O2 in an aqueous media at pH 11.0.

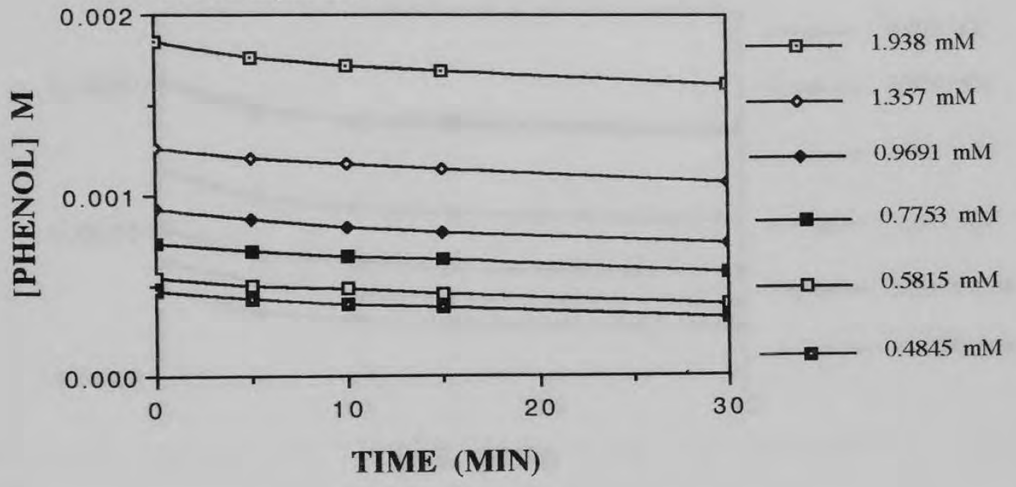

Initial rates of disappearance at 5 min. of reaction.

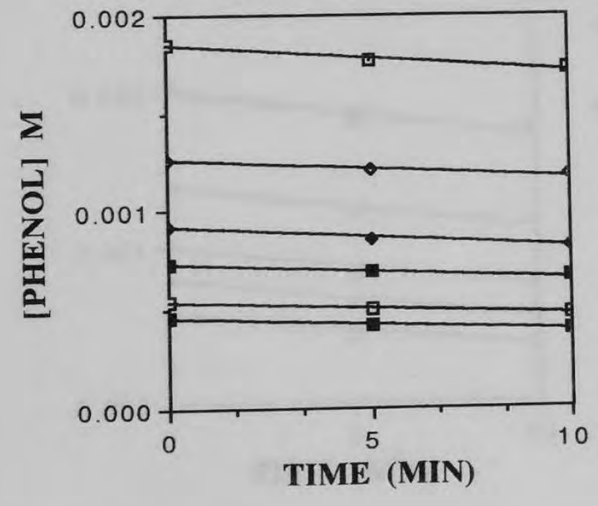

1.938 mM
y = 1.84e-3 - 1.25e-5x R^2 = 0.936
1.357 mM
y = 1.26e-3 - 9.09e-6x R^2 = 0.977
0.9691 mM
y = 9.23e-4 - 1.06e-5x R^2 = 0.979
0.7753 mM
y = 7.34e-4 - 7.54e-6x R^2 = 0.990
0.5815 mM
y = 5.45e-4 - 6.61e-6x R^2 = 0.958
0.4845 mM
y = 4.63e-4 - 7.07e-6x R^2 = 0.975

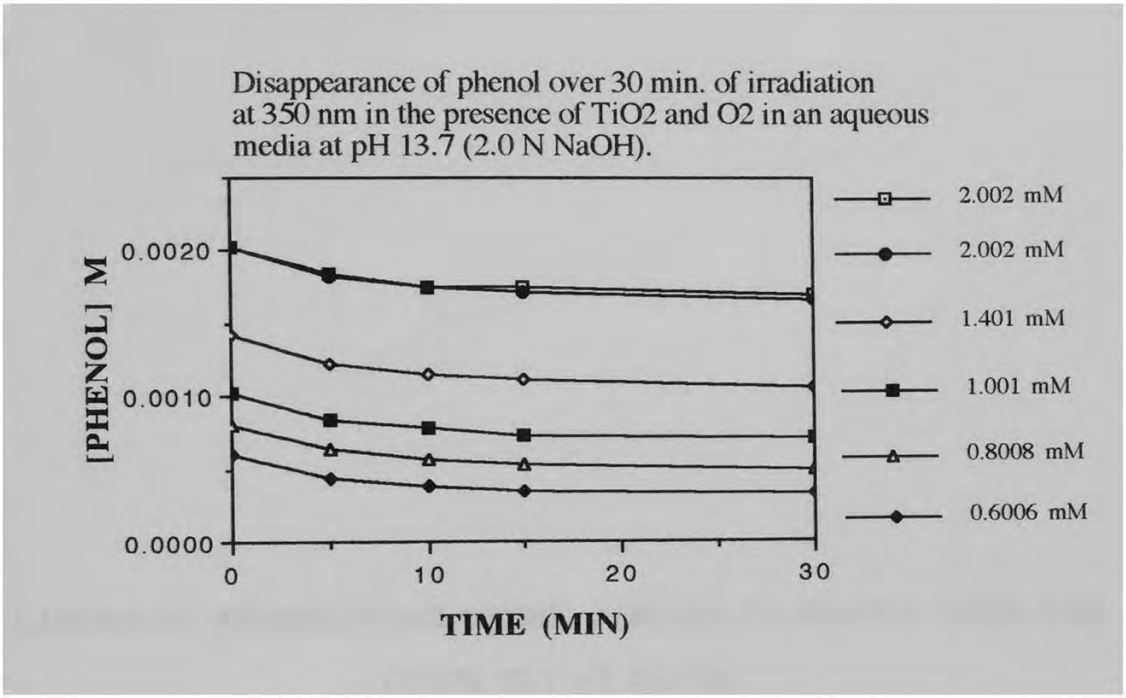
Disappearance of phenol over 30 min. of irradiation at 350 nm in the presence of TiO2 and O2 in an aqueous media at pH 13.7 (2.0 N NaOH).
[PHENOL] M
0.0020
0.0010
0.0000
0
10
20
30
TIME (MIN)
2.002 mM
2.002 mM
1.401 mM
1.001 mM
0.8008 mM
0.6006 mM

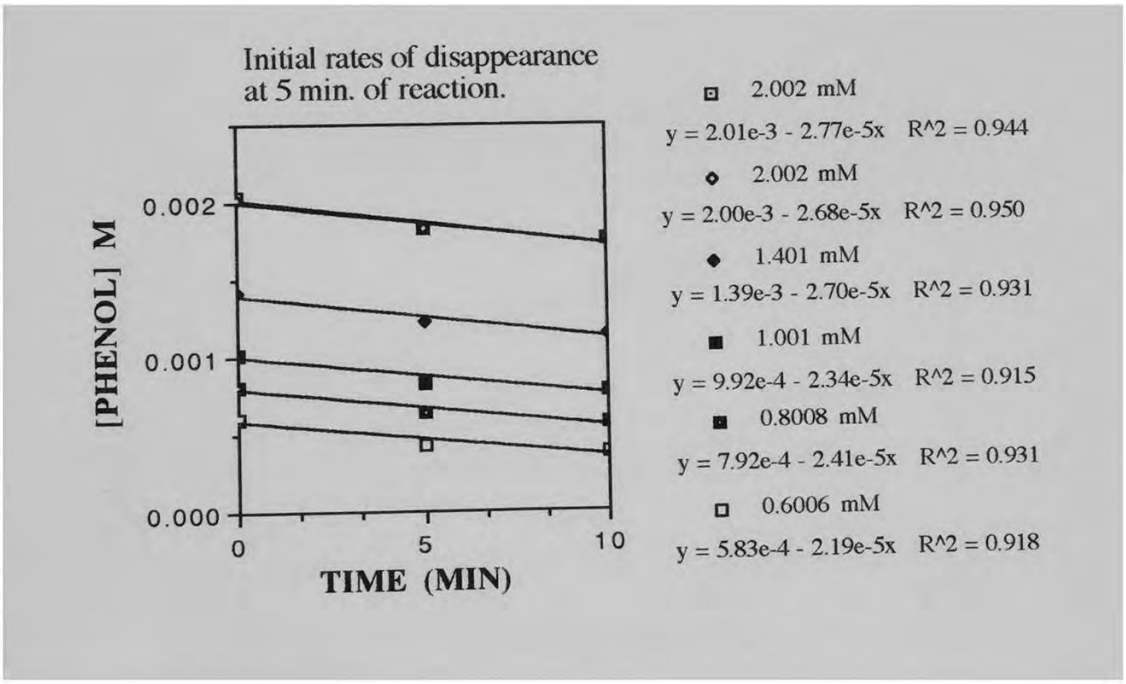
Initial rates of disappearance at 5 min. of reaction.
[PHENOL] M
0.002
0.001
0.000
0
5
10
TIME (MIN)
2.002 mM
y = 2.01e-3 - 2.77e-5x R^2 = 0.944
2.002 mM
y = 2.00e-3 - 2.68e-5x R^2 = 0.950
1.401 mM
y = 1.39e-3 - 2.70e-5x R^2 = 0.931
1.001 mM
y = 9.92e-4 - 2.34e-5x R^2 = 0.915
0.8008 mM
y = 7.92e-4 - 2.41e-5x R^2 = 0.931
0.6006 mM
y = 5.83e-4 - 2.19e-5x R^2 = 0.918

APPENDIX VIII.

LANGMUIR-HINSHELWOOD MODEL APPLIED TO PHENOL OVER THE 1.0 TO 13.7 pH RANGE.

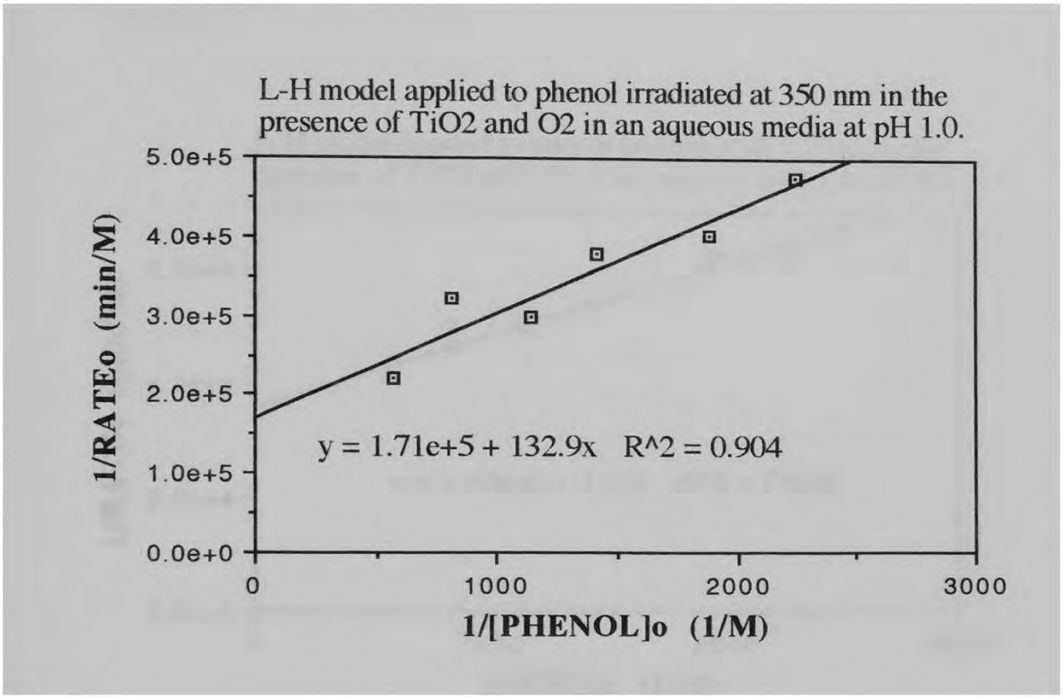
L-H model applied to phenol irradiated at 350 nm in the presence of TiO2 and O2 in an aqueous media at pH 1.0.
5.0e+5
4.0e+5
3.0e+5
2.0e+5
1.0e+5
0.0e+0
1/RATEo (min/M)
y = 1.71e+5 + 132.9x R^2 = 0.904
0
1000
2000
3000
1/[PHENOL]o (1/M)

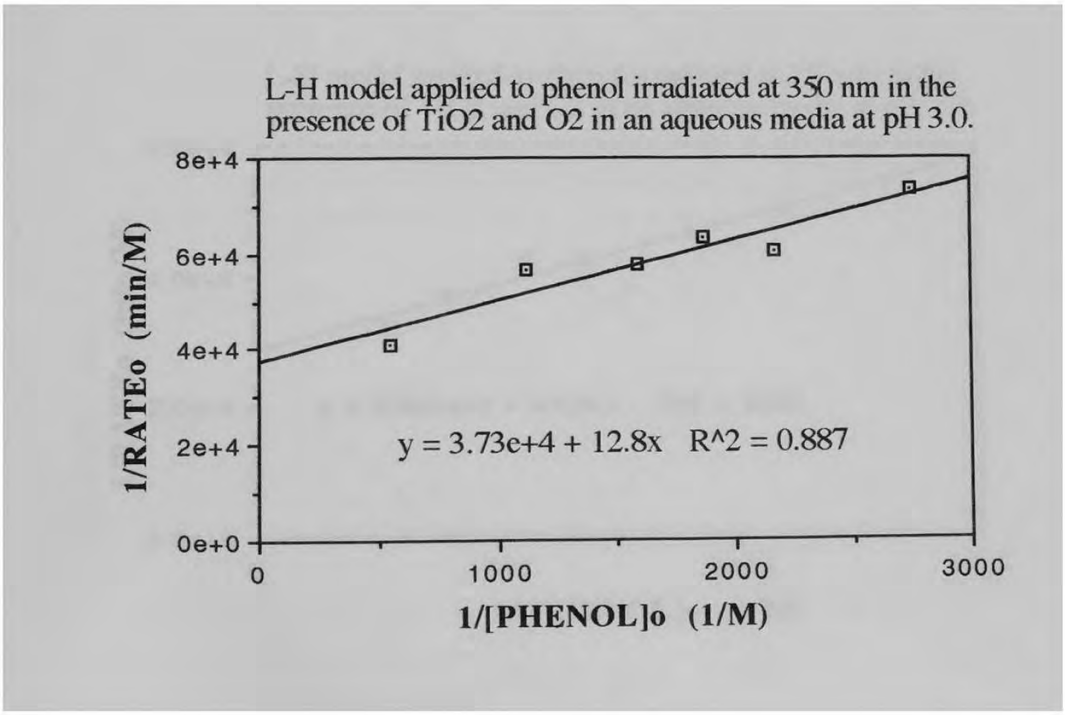
L-H model applied to phenol irradiated at 350 nm in the presence of TiO2 and O2 in an aqueous media at pH 3.0.
8e+4
6e+4
4e+4
2e+4
0e+0
1/RATEo (min/M)
y = 3.73e+4 + 12.8x R^2 = 0.887
0
1000
2000
3000
1/[PHENOL]o (1/M)

L-H model applied to phenol irradiated at 350 nm in the presence of TiO2 and O2 in an aqueous media at pH 5.0.

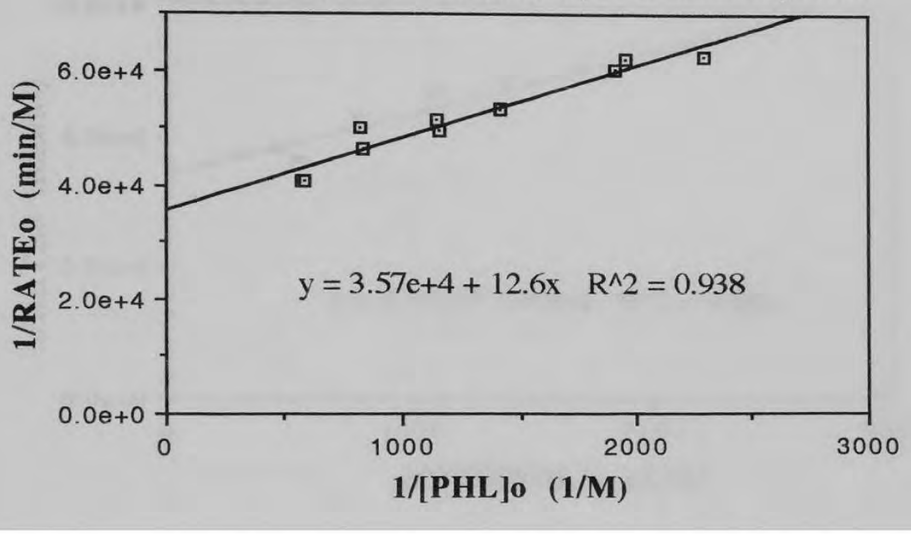

L-H model applied to phenol irradiated at 350 nm in the presence of TiO2 and O2 in an aqueous media at pH 7.0.

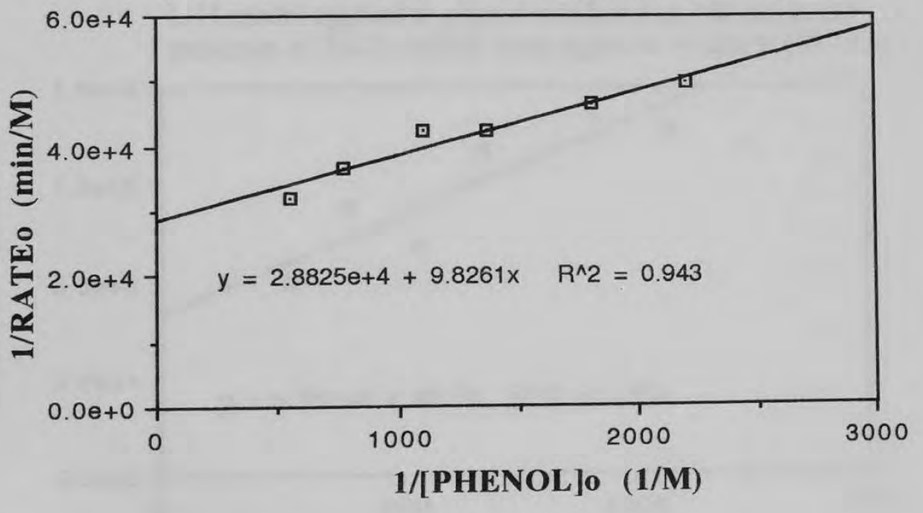

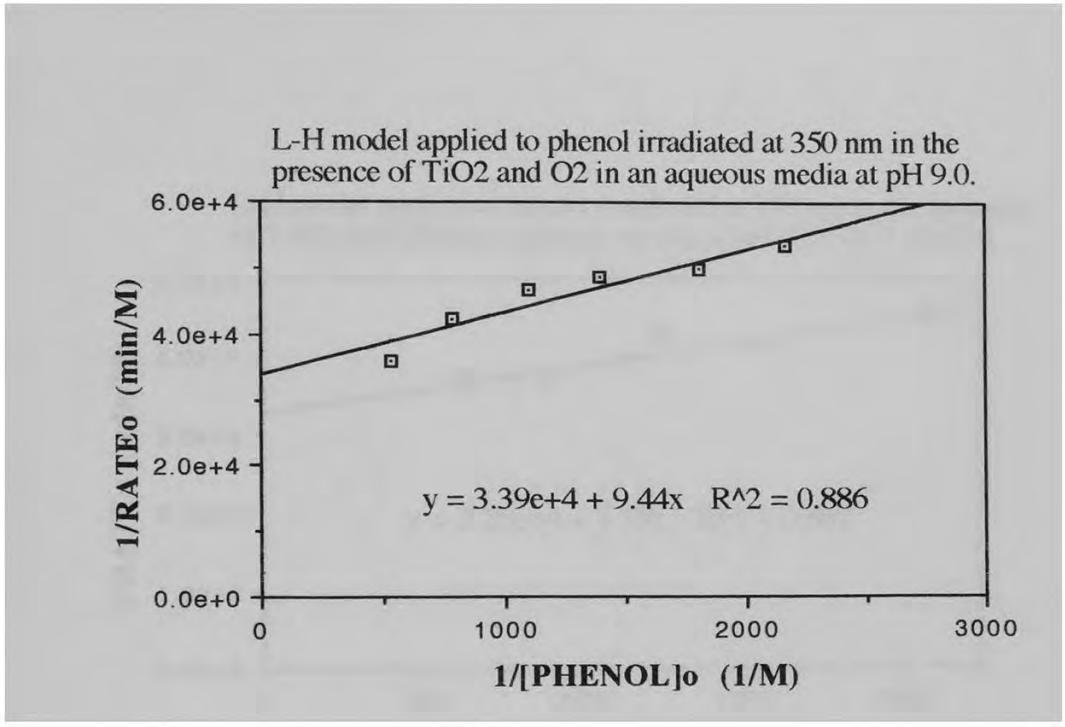
L-H model applied to phenol irradiated at 350 nm in the presence of TiO2 and O2 in an aqueous media at pH 9.0.
6.0e+4
4.0e+4
2.0e+4
0.0e+0
1/RATEo (min/M)
y = 3.39e+4 + 9.44x R^2 = 0.886
0
1000
2000
3000
1/[PHENOL]o (1/M)

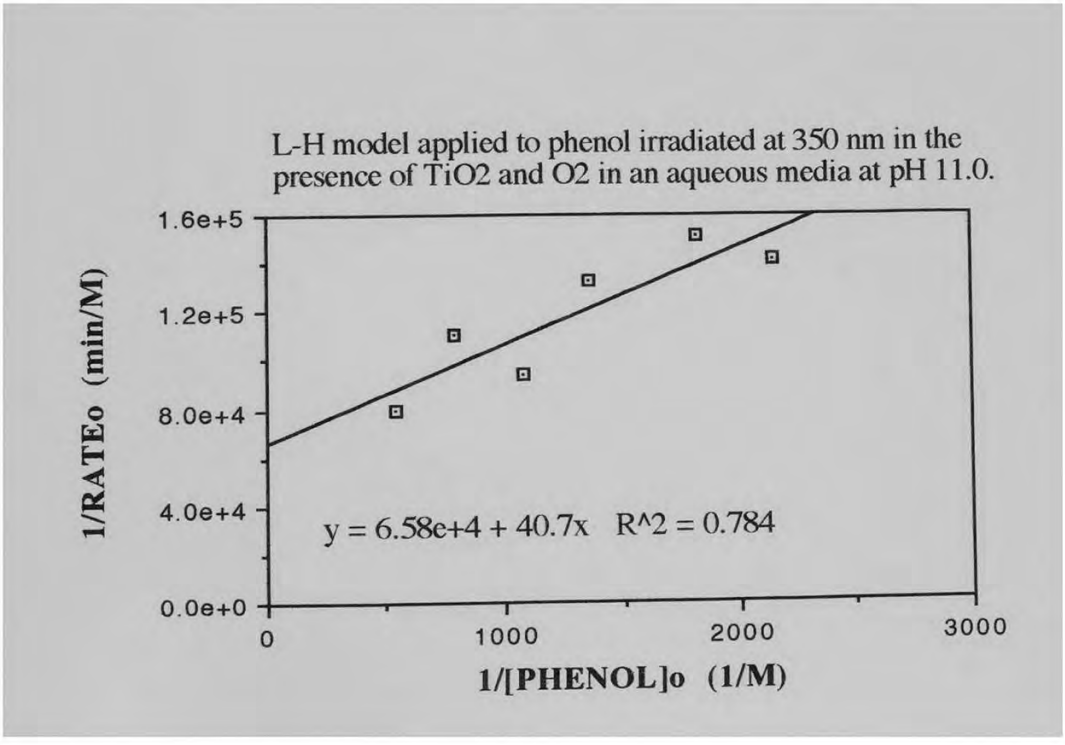
L-H model applied to phenol irradiated at 350 nm in the presence of TiO2 and O2 in an aqueous media at pH 11.0.
1.6e+5
1.2e+5
8.0e+4
4.0e+4
0.0e+0
1/RATEo (min/M)
y = 6.58e+4 + 40.7x R^2 = 0.784
0
1000
2000
3000
1/[PHENOL]o (1/M)

L-H model applied to phenol irradiated at 350 nm in the presence of TiO2 and O2 in an aqueous media at pH 13.7 (2 N NaOH).

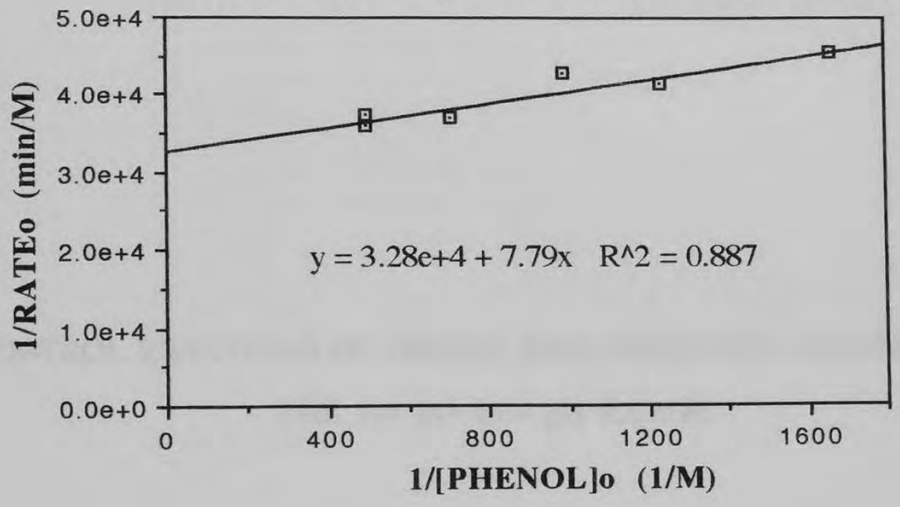

PENDIX IX.

CONTROL REACTIONS OF PHENOL FOLLOWED FOR 4 HOURS OVER THE 1.0 TO 13.7 pH RANGE.

Control reactions of phenol (2.474 mM) at pH 1.0 followed for a period of 4 hours under different experimental conditions.

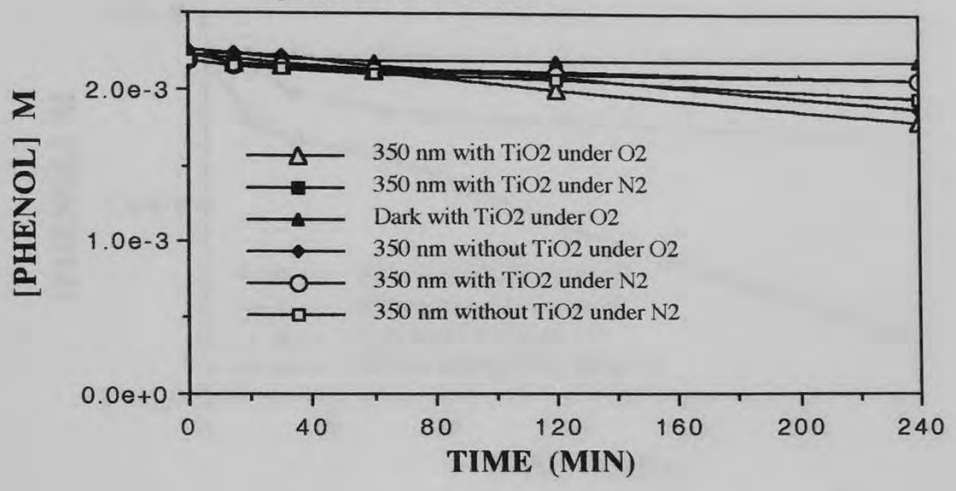

Control reactions of phenol (2.032 mM) at pH 3.0 followed for a period of 4 hours under different experimental conditions.

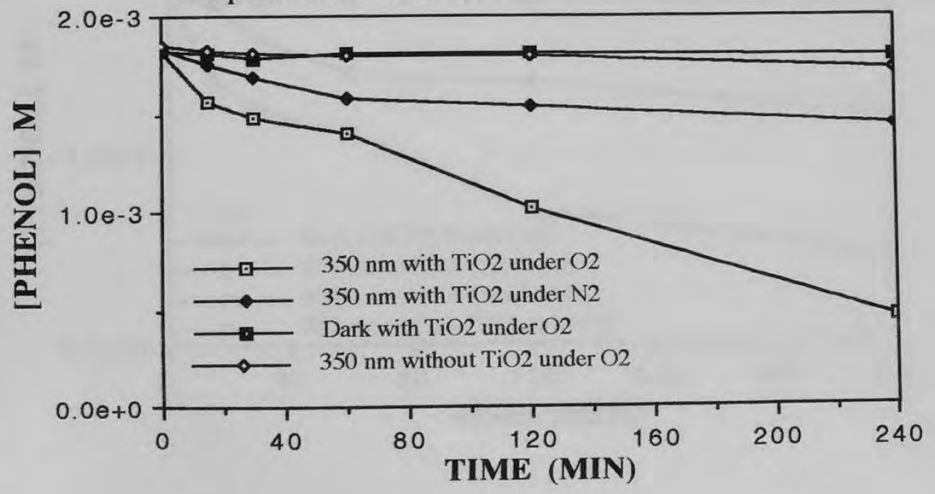

Control reactions of phenol (2.040 mM) at pH 5.0 followed for a period of 4 hours under different experimental conditions.

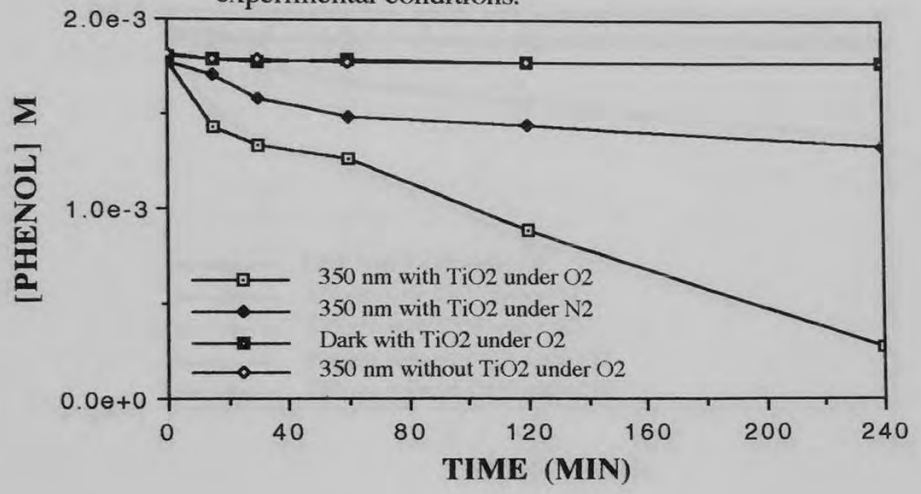

Control reactions of phenol (1.921 mM) at pH 7.0 followed for a period of 4 hours under different experimental conditions.

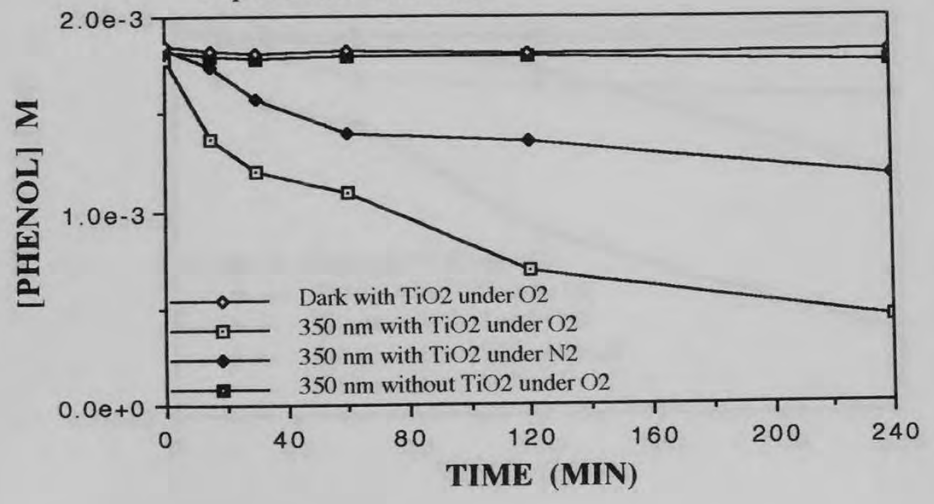

Control reactions of phenol (1.957 mM) at pH 9.0 followed for a period of 4 hours under different experimental conditions.

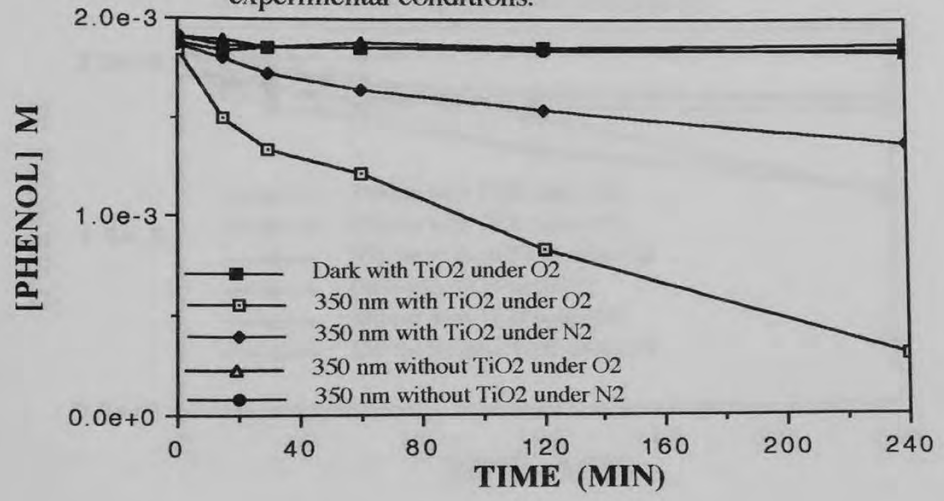

Control recation of phenol (2.040 mM) at pH 11.0 followed for a period of 4 hours under different experimental conditions.

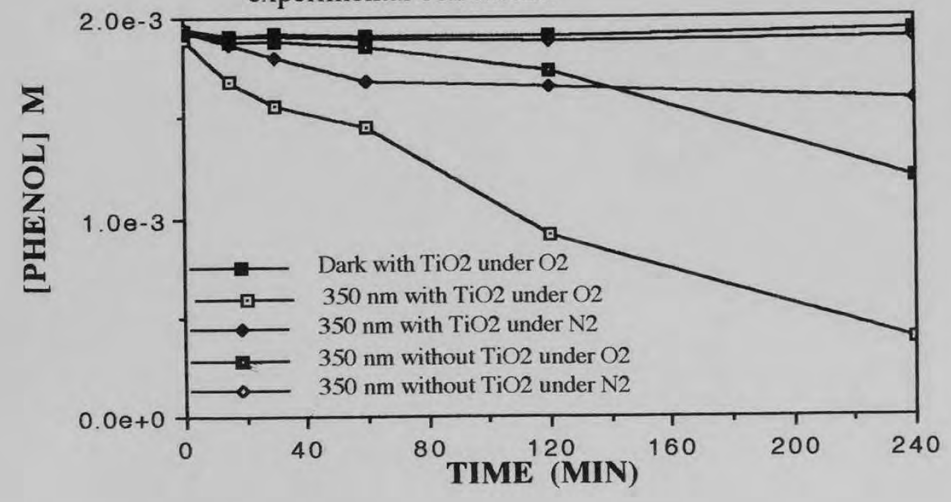

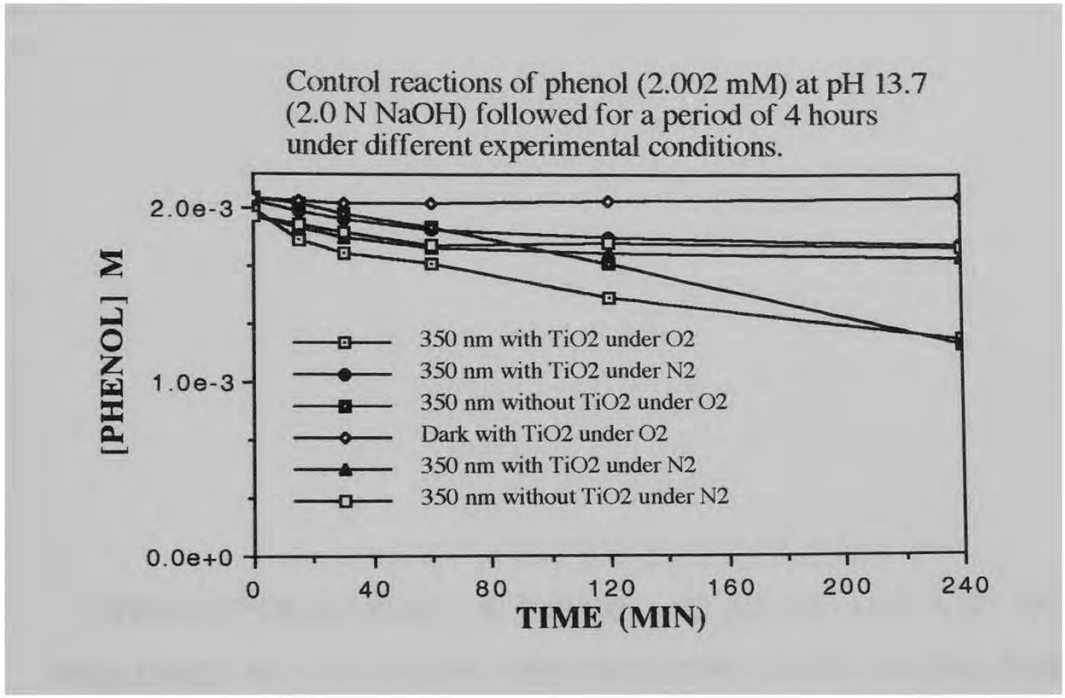
Control reactions of phenol (2.002 mM) at pH 13.7 (2.0 N NaOH) followed for a period of 4 hours under different experimental conditions.
[PHENOL] M
2.0e-3
1.0e-3
0.0e+0
0
40
80
120
160
200
240
TIME (MIN)
350 nm with TiO2 under O2
350 nm with TiO2 under N2
350 nm without TiO2 under O2
Dark with TiO2 under O2
350 nm with TiO2 under N2
350 nm without TiO2 under N2

APPENDIX X.

PHOTODEGRADATION OF PHENOL AT pH 1.0, 11.0, AND 13.7 FOLLOWED BY UV-VISIBLE SPECTROSCOPY OVER A LONG PERIOD OF TIME IN THE PRESENCE AND ABSENCE OF TiO2.

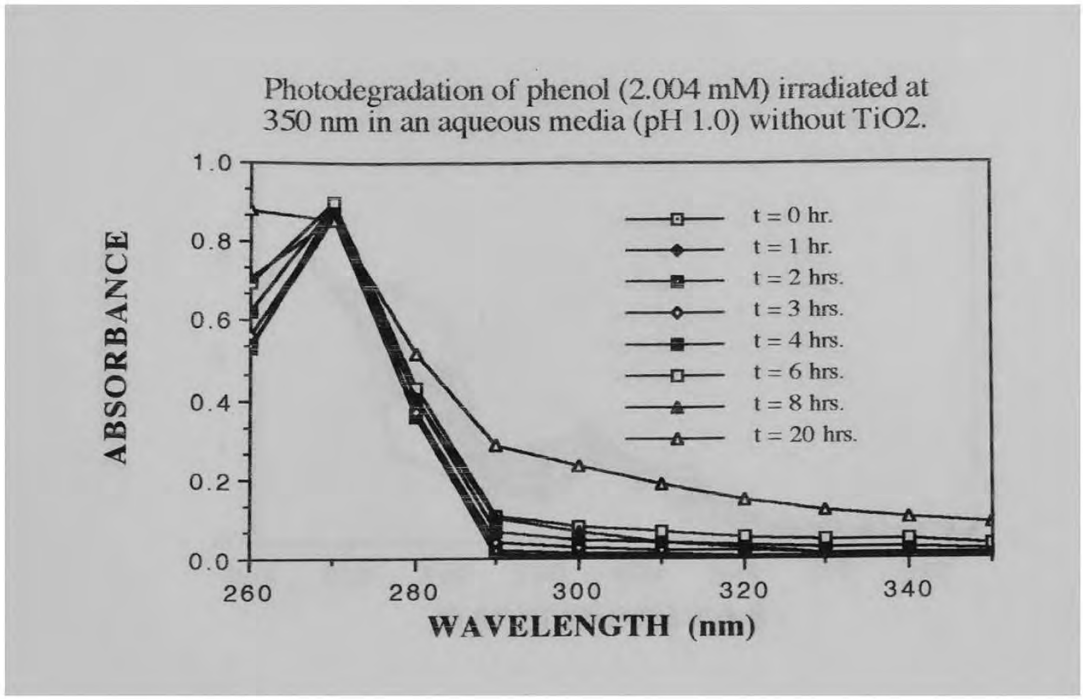
Photodegradation of phenol (2.004 mM) irradiated at 350 nm in an aqueous media (pH 1.0) without TiO2.
ABSORBANCE
1.0
0.8
0.6
0.4
0.2
0.0
260
280
300
320
340
WAVELENGTH (nm)
t = 0 hr.
t = 1 hr.
t = 2 hrs.
t = 3 hrs.
t = 4 hrs.
t = 6 hrs.
t = 8 hrs.
t = 20 hrs.

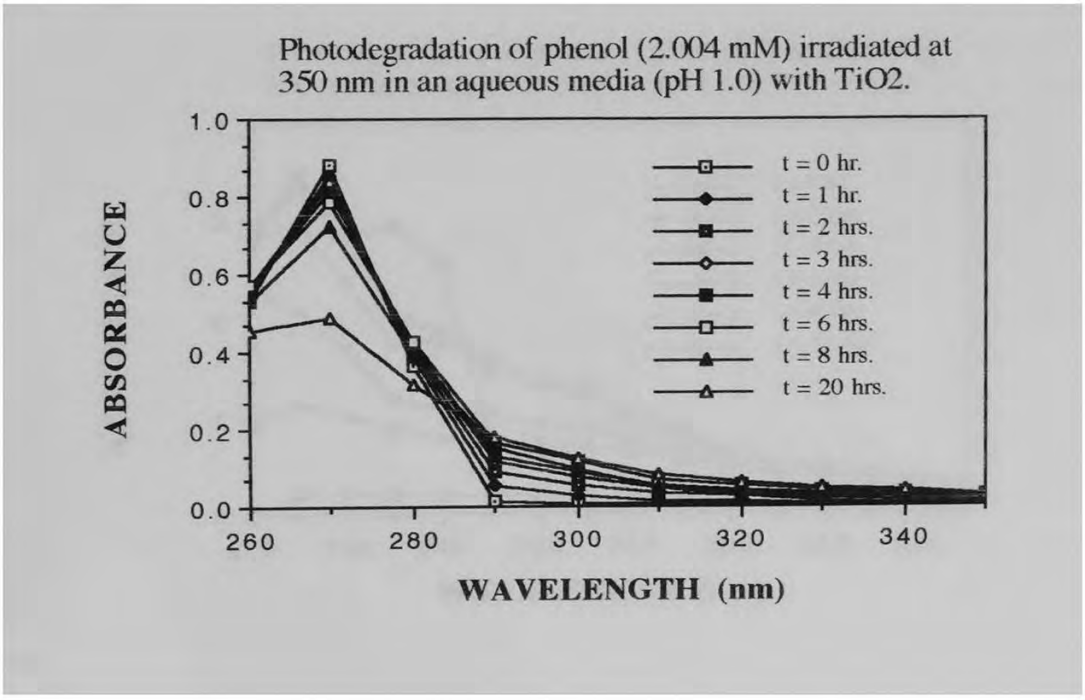
Photodegradation of phenol (2.004 mM) irradiated at 350 nm in an aqueous media (pH 1.0) with TiO2.
ABSORBANCE
1.0
0.8
0.6
0.4
0.2
0.0
260
280
300
320
340
WAVELENGTH (nm)
t = 0 hr.
t = 1 hr.
t = 2 hrs.
t = 3 hrs.
t = 4 hrs.
t = 6 hrs.
t = 8 hrs.
t = 20 hrs.